NTNU
Norwegian University of
Science and Technology

Increased Energy Efficiency in Buildings using Model Predictive Control

Jonas Magnussen

Master of Science in Engineering Cybernetics
Submission date: June 2011
Supervisor: Lars Imsland, ITK

Norwegian University of Science and Technology
Department of Engineering Cybernetics

Increased Energy Efficiency in Buildings using Model Predictive Control

TTK4900 Master Thesis

Author
Jonas Magnussen
June 13, 2011

Supervisor
Professor Lars Imsland

NTNU
Department of Engineering Cybernetics

Summary

The main objective in this thesis is to explore if a model predictive control scheme can increase the energy efficiency in office buildings with waterborne heating systems. The number of office buildings is constantly increasing, which displays the importance of efficient control systems. Since the aim is to decrease the energy consumption, improving the control systems in existing buildings and developing smart control schemes for new buildings are equally important. That is why the vision in this thesis is to design a control scheme that theoretically can be introduced to all new and existing office buildings. The model predictive controller's objective is therefore to minimize the supply water temperature to the heating system, while fulfilling a set of defined indoor temperature demands.

The model is the most important tool when comparing different control schemes. It is derived using an electrical analogy, and includes the most important thermodynamical relations in three rooms, a ventilation system, and a district heating system. To achieve optimal control of the supply-water temperature, a constrained optimization problem is introduced through a model predictive control scheme. Two versions of the model predictive control scheme are compared with a conventional control scheme. The first version is an ordinary formulation with some ad-hoc solutions including time-varying output constraints, while the second version is a robust formulation including slack variables. The energy-consumption analysis imply that a 33 % - 34 % reduction potential is obtainable if a model predictive control scheme is introduced.

Preface

This thesis represents my final work during the degree Master of Science in Engineering Cybernetics at the Norwegian University of Science and Technology (NTNU). Not only does the thesis conclude this degree, it represents the start of a new chapter in my life.

I would like to thank my supervisor professor Lars Imsland at the department of Engineering Cybernetics. His involvement throughout this final year has been essential for the final submitted product. I would also like to thank Natasa Djuric at the department of Energy and Process Engineering. Her ability to help me understand a new discipline has been important.

My fellow students and friends also deserve a big thank you. I really appreciated their different point of views during the work, and especially their camaraderie. I would therefore like to thank Anders, Anne Mai, Eirik, Joakim, Karsten and Øyvind. I am also grateful for the unconditional support my parents have given me during the time as a student. Finally, I would like to thank Hege, who always has been very supportive and kind.

Jonas Magnussen
June 13, 2011

Contents

List of Figures

List of Tables

Chapter 1

Introduction

In industrialized countries, energy usage in buildings represents as much as 40 % of the total energy consumed (Nilsson et al. [2003]), and according to Abel and Elmroth [2007], the building stock is increasing with 1 % to 2 % yearly. Since the number of buildings is continously increasing, it becomes even more important to optimize the energy consumption. The number of buildings in the world is enormous, therefore the energy reduction potential is huge.

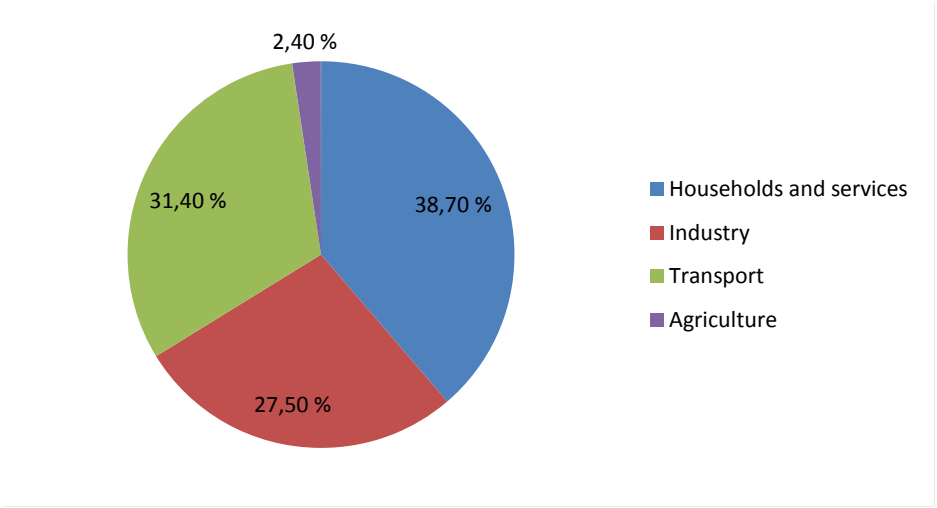

Figure 1.1: Sector-divided energy consumption within the European Union, 2006. Source: Eurostat.

The climate in buildings is controlled by Heating, Ventilation and Air Conditioning (HVAC) systems. An important contribution that will lead to a

reduction in energy consumption, is to control these systems in an optimal manner.

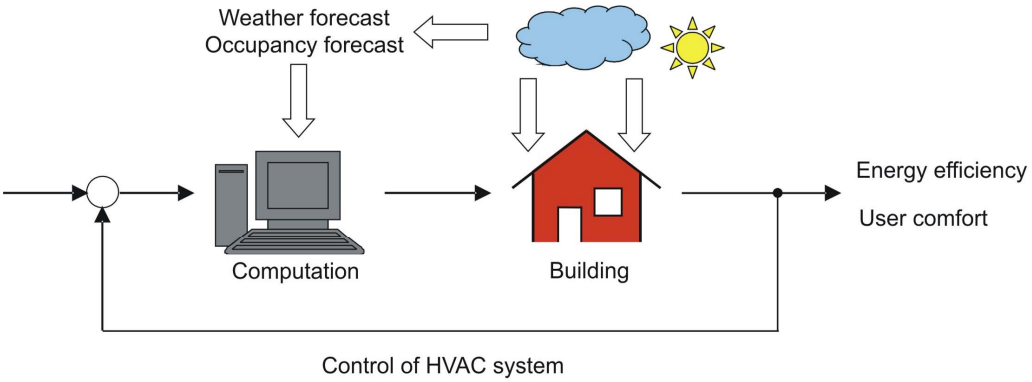

Figure 1.2: The OptiControl MPC control strategy. Source: OptiControl.

Since energy usage in buildings represents a huge energy consumer, the interdisciplinary project OptiControl was launched in 2007. Gyalistras and Gwerder [2009] states that by use of predictive control, the aim of the project is to minimize the energy usage in buildings while maintaining (or even improving) the indoor climate, and reducing peak electricity demand. Gyalistras and Gwerder [2009] focus on predictive control for several reasons.

- Disturbance predictions - in particular weather predictions - can easily be included into the controller.
- Since MPCs include mathematical models of a process, complex dynamical systems with non-linear interactions can be dealt with in a Multi-Input-Multi-Output (MIMO) manner.
- MPC formulations are intuitive (minimize energy usage without violating constraint a and constraint b, for example).

An introduction to MPCs will be given in Chapter 4.

Gyalistras and Gwerder [2009] examine both energy efficiency and control of specific indoor climate aspects, like CO_2 concentration and moisture. Since different types of buildings will have different demands, the control system has to be tailor made for each building. The focus in this thesis will be to minimize the amount of heat supplied to an office building, but still fulfill desired temperature demands. The main idea is that any building (old or new) with a waterborne heating system can deploy such a control system, without having to update all the components in the existing control system.

Figure 1.3: A lot of energy can be saved if the indoor climate is controlled in an optimal manner. Source: `www.zerobuildings.com`.

In Oldewurtel et al. [2009a], the goal is to minimize the energy consumption in a building by controlling the indoor temperature, in addition to the CO_2 and illuminance levels, in a smart manner. The defined comfort demands have to be fulfilled by using a minimal amount of energy. This is done by individual control of each actuator[1] and by feeding weather predictions into the model.

In Oldewurtel et al. [2009b], the focus is yet again to keep the temperature, CO_2 and illuminance levels within a given comfort zone. However, the control strategy differs from the previous case. Oldewurtel et al. [2009b] assume that all the power in the system is given by an electric source, and propose a strategy of how to reduce the peak electricity demand in the building. The proposed strategy includes using an MPC control scheme, and incorporation of real-time electricity prices into the MPC cost function[2]. The internal controllers should then respond with respect to the electricity prices, by responding gently when the prices are high, for example.

The reader should be aware that there are several ongoing projects concerning energy efficiency in buildings using MPC control schemes, and only a few of them are mentioned here. Morosan et al. [2010], Privara et al. [2010] and Siroky et al. [2011] can be of interest in addition to the ones mentioned above. The author of this thesis thinks it is of importance that the control system should be designed in a general and high-leveled manner, such that it can be applied to both old and new buildings by being independent of different

[1] Blind-positioning, ventilation and radiator outputs.

[2] Objective function and other MPC terms will be explained in Chapter 4.

component compositions that exist in different buildings. There are several arguments for choosing an MPC control scheme to increase energy efficiency, and some of them are mentioned in Gyalistras and Gwerder [2009]. It is intuitive to formulate the optimization problem: Minimize a cost function with respect to certain constraints - minimize energy consumption while respecting indoor temperature demands. It it also appealing that disturbances, like the weather, easily can be fed forward and included into the controller. But most importantly, an MPC scheme is employed because of its ability to operate near the system constraints, and thereby obtain the most profitable operation (Maciejowski [2002]). The properties in general seem to make the MPC a useful tool for minimizing the energy consumption in buildings.

Figure 1.4: The vision is to design a control system that is applicable in all existing and new office buildings. Source: OptiControl.

It is important to have in mind that even though new buildings contain state-of-the-art technology and are energy efficient, the total energy consumption will still increase as long as existing buildings remain unchanged (Abel and Elmroth [2007]). It is therefore very important to come up with energy-saving measures that are applicable not only to new buildings, but also to existing buildings. Abel and Elmroth [2007] mention two criteria that must be fulfilled when working with energy efficiency in buildings. First, when coming up with energy-saving measures, it is essential that the indoor-climate properties in the building are maintained. No one is interested in

working in a building where it is freezing cold even though it has a low energy consumption, for example. Second, energy-saving measures and the pertaining technical equipment should not demand more resources than the actual energy-reduction potential. As mentioned above, the vision in this thesis is to develop a high-level control scheme that theoretically is going to be applicable in both existing and new buildings containing a waterborne heating system. And as far as the author is aware of, no one has yet applied a similar control scheme to office buildings. These criteria are the main reasons why the purpose of this thesis is to explore whether an MPC scheme can increase the energy efficiency in office buildings, or not. Details about different control schemes that will be subject for implementation and testing are elaborated in Section 2.6.

The work in this thesis is based on Magnussen [2010]. However, several augmentations and improvements will be carried through. The model will be expanded with several rooms, a ventilation system, and a more realistic heating system. Outdoor temperatures generated from `www.yr.no`, and thermal disturbances from people, equipment and lighting, will also contribute to make the model more realistic. The model is going to be implemented in `Simulink` exclusively, not partially `Simscape` and `Simulink` as in Magnussen [2010]. A Kalman filter is going to be used instead of a Luenberg observer as state estimator, while the MPC formulation will be different by changing the objective function and by adding new constraints. In addition, measures to make the MPC scheme more robust will be carried through. In other words, Magnussen [2010] only forms the basis of this thesis.

1.1 Outline of the report

Chapter 2 concerns the derivation of the model that is going to be used to compare the different control schemes. Initially, different modeling approaches that can be employed to derive thermodynamical models are listed, before the building case that is used in the thesis is presented. Factors that affect the indoor climate, succeeded by the heat balances in the largest room are then elaborated. In this chapter, the reader also gets familiar with some ventilation and district heating schemes, before the control strategies complete the chapter. The conventional control scheme and the corresponding simulations are topics for Chapter 3. Chapter 4 is the main chapter and it starts off with an introduction to MPC control, necessary preparations that have to be made before implementation, and a Kalman filter that must be

included to estimate the system states. Tuning of an MPC controller, simulations of the system, and ad-hoc solutions that has to be implemented are then presented. Approaches for making the control scheme robust and the corresponding simulations complete this chapter. The energy consumption will be explored in Chapter 5, while a discussion is carried out in Chapter 6. A conclusion and proposals for further work complete the thesis in Chapter 7.

Before the control schemes can be compared, a mathematical model of the building has to be derived, and this is the subject for next chapter.

Chapter 2

The Model

In this chapter, a model of a building will be derived. In addition to mathematical descriptions, a short theoretical introduction will be given when presenting new components.

First-principle modeling and black-box modeling[1] are two common modeling approaches and are both suited when deriving building models. Djuric et al. [2007] use a black-box approach when deriving a building model. In their work, heat equations are set up to describe the thermal relations in each zone in the building, and the model is initialized by calibrating it with related measurement data. This method is a good option if the measurements are reliable, since the model gets tailor fit to the specific building. However, instrument failure may lead to incorrect measurements, which may cause model inaccuracy. It is important to develop a model that describes the process in an accurate manner. Moreover, the model should not be more complex than necessary because it is going to be employed in an optimization problem. This will be discussed in more detail in Chapter 6.

Table 2.1 is taken from Table 5.1 in Gyalistras and Gwerder [2009], and it shows a hierarchy of building models. Before choosing a level of control, the purpose of the controller should be defined . Individual control of different indoor climate aspects, like moisture control or CO_2 control, is not going to be subject for examination in this thesis. Therefore, L5 modeling is unnecessary complex. The level of modeling complexity in this thesis will be between L3 and L4. Resistance-Capacitance networks (RC-networks) are used because

[1] Maciejowski [2002] defines these terms in the following way: A black-box model is a model that uses system identification, and the emphasize is on the relationship between input and output. A model of first-principle uses physical laws to derive a model.

the electrical analogy makes it easier to examine all the thermal relations combined together, or individually.

The foundation of the model will be based on Chapter 2.3 in Magnussen [2010]. However, the model presented in Magnussen [2010] is going to be expanded with the purpose of making it more realistic. The building model will consist of 3 rooms and a ventilation system. Radiation noise from people, equipment and lighting, outdoor temperatures, and a district heating system will represent the rest of the model. The specific values in the model (areas, materials, radiation rates) are taken from measurements in Bassengbakken 1 in Trondheim. This building contains a radio station, shops, and office areas. In this thesis, a segment in one of the office floors will be subject for modeling.

Table 2.1: Levels of modeling.

Modeling level	Characteristics	Characteristics - Scope
L1	Verbal model	Easily understandable characterization of a building - communication with non-specialists.
L2	Correlation model	Linear combination between average power use and external temperature, design and rough energy-demand calculations.
L3	Linear dynamical model (thermal RC-network)	Simplest possible representation of a buildings´s thermal dynamics. Design and energy demand calculations of buildings.
L4	Bilinear dynamical model (thermal RC-network)	Representation of a building´s physical processes at intermediate precision and detail. Reliable energy and comfort simulations.
L5	Detailed model based on building simulation software	Best possible representation and detailed simulation of a building´s physical processes.

2.1 Building case

In Grini et al. [2009], information about Bassengbakken 1 in Trondheim can be found. The building was built in 2001 and rehabilitated in 2004, and it is drifted by Trondheim Kommune. The building consists mainly of offices in addition to a business area at the 1st floor. The walls of the building are constructed by bricks, gypsum, insulation (rock wool) and air gaps, and windows account for 25.8 % of the total building area.

District heating supplied from Trondheim Energi AS represents the building´s heating system. The supply water temperature is 95 $°C$, while the return temperature is controlled to 55 $°C$ so that hot tapping water can be ensured. These values will be disregarded this thesis because new supply-water-temperature schemes are going to be introduced. Radiators are placed below the windows in order to fulfill the defined indoor temperature demand at 21 $°C$. A night-time temperature is not defined by Grini et al. [2009], so this is set arbitrarily to 17 $°C$. Fresh air is supplied by a ventilation system where a heat exchanger is used to heat up the supply air to 22 $°C$, which is the desired temperature during winter time. A desired night-time temperature is not defined, and is set to be 15 $°C$.

In order to be able to calculate the building‘s energy consumption, the water flowing through the radiators and the ventilation system has to be determined. 22.15 % of the water runs through radiator A, 22.15 % through radiator B and 26.79 % through radiator C. The flow through radiator C is chosen larger since room C is the biggest[2]. The remaining 28.91 % flows through the ventilation system. These values were decided by determination of pipe dimentions and water flows in the system. The pipe dimentions and water flows are chosen such that the water flow through the ventilation system and the radiators constitutes the total flow through the heating system. The choice of the values are discussed in Chapter 6. Except from radiators and ventilation, important factors that provide heat to the building during working hours are people, lighting, and other equipment like computers and printers.

The building consists of 6 floors including a parking lot in the basement. However, in this thesis only a segment in one of the office floors will be investigated. This is done to prevent the model of becoming too large and complex.

[2]The radiator size in room C is also chosen to be larger than in room A and B for the same reason.

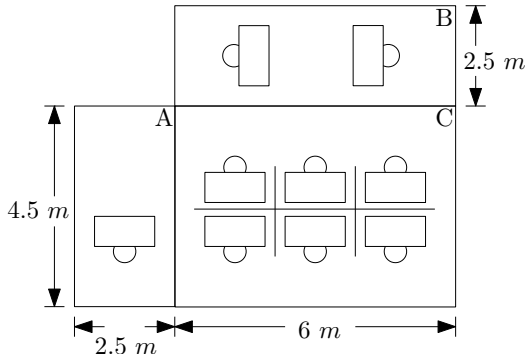

Figure 2.1: A segment of one of the office floors in Bassengbakken 1 that will be subject for simulation in this thesis.

Factors that affect the indoor climate

The heat in a room is determined by the internal heat and heat losses through the building envelope[3], and the internal heat is heat transferred from people, equipment, walls, floor and ceiling (Abel and Elmroth [2007]). The temperature in the room rises if the surface heat on the surroundings is higher than the room temperature, and vice versa. Solar radiation leads to heat storage in the building structure, which also affects the temperature in the room (Abel and Elmroth [2007]).

Table 2.2: Notation in modeling.

Example	Subscript 1 (Location)	Subscript 2 (Identity)	Subscript 3 (Room)	Explanation
θ_{36C}	Wall surface temp.	Towards outdoor air	Room C	Wall surface temp. towards outdoor air in room C
θ_{1BC} $(= \theta_{1CB})$	Wall (mass center) temp.	Towards room B	Room C	Wall (mass center) temp. between room B and room C
θ_{2B}	Air temp.		Room B	Air temp. in room B

Initially, the thermal relations in a room will be studied. Except from a

[3]A building envelope is the separation between the interior and the exterior environment.

different notation (see Table 2.2), these calculations will be the same as in Magnussen [2010]. A complete overview of the variables can be found in the nomenclature.

2.2 The thermal relations in a room

The thermal relations in a building include heat storage in the building structure (only walls in this model), inventory, and room air. In addition to this, thermal radiation from radiators, window surface, people, equipment and lighting constitute the thermal relations. Solar radiation will be left out because this is very hard to model accurately. It is impossible to know how long the sun will affect the building, and how long it will be obstructed by clouds during a day. If this was to be included, additional sensors would have been needed to measure whether the sun radiates the building or not. The author of this thesis is of the comprehension that including the affection from the sun will contribute to a larger source of error, rather than making the model more accurate.

Four simplifications are made to prevent the model of being too complex (the third and fourth are from (Novakovic [1995])).

1. There are two sorts of walls. Walls towards outdoor air, and walls towards other rooms.
2. Floor and ceiling will not be included in the model.
3. There is no heat accumulation in the windows.
4. The equipment in the room does not transfer heat to each other.

The only thing that separates the thermal relations in the rooms from each other, is the number of walls towards other rooms and outdoor air. Therefore, the calculations will only be derived for room C, since it faces both room A, room B, and the outdoor air.

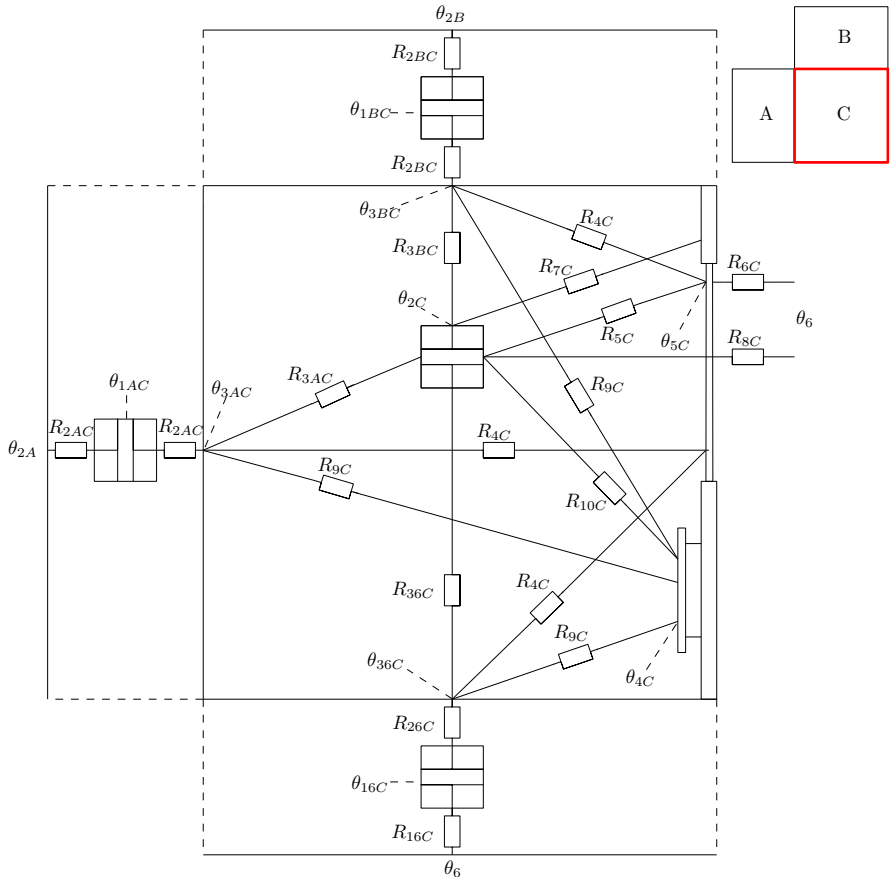

Figure 2.2: Thermal relations in a room (room C). The figure is inspired by Figure 19.1 in Novakovic [1995].

2.2.1 Heat balance of the wall (towards outdoor)

The heat balance of the wall towards the outdoor air is given by studying Figure 2.2.

$$\frac{d}{dt}(C_{6C}\theta_{16C}) = \frac{1}{R_{16C}}(\theta_6 - \theta_{16C}) + \frac{1}{R_{26C}}(\theta_{36C} - \theta_{16C}) \tag{2.1}$$

$$C_{6C}\frac{d\theta_{16C}}{dt} = \frac{1}{R_{16C}}(\theta_6 - \theta_{16C}) + \frac{1}{R_{26C}}(\theta_{36C} - \theta_{16C}) \tag{2.2}$$

$$C_{6C}\frac{d\theta_{16C}}{dt} + (\frac{1}{R_{16C}} + \frac{1}{R_{26C}})\theta_{16C} = \frac{1}{R_{16C}}\theta_6 + \frac{1}{R_{26C}}\theta_{36C}, \tag{2.3}$$

where C_{6C} is constant. By defining

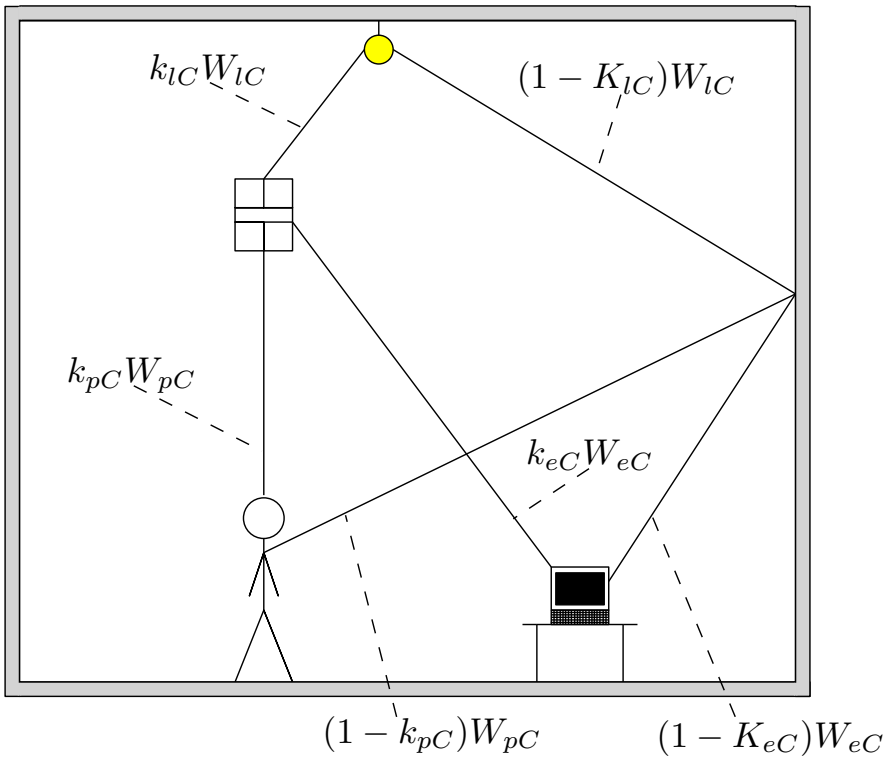

Figure 2.3: Thermal disturbances in a room (room C). The figure is inspired by Figure 19.2 in Novakovic [1995].

$$R_{1tC} = \frac{1}{\frac{1}{R_{16C}} + \frac{1}{R_{26C}}}, \tag{2.4}$$

$$T_{1C} = C_{6C} R_{1tC}, \tag{2.5}$$

equation (2.3) can be written as

$$T_{1C}\frac{d\theta_{16C}}{dt} + \theta_{16C} = \frac{R_{1tC}}{R_{26C}}\theta_{36C} + \frac{R_{1tC}}{R_{16C}}\theta_6. \tag{2.6}$$

Then (2.6) is Laplace transformed, so that the transfer functions can be obtained:

$$\mathcal{L}(\cdots) \Rightarrow \tag{2.7}$$

$$T_{1C}\theta_{16C}s + \theta_{16C} = \frac{R_{1tC}}{R_{26C}}\theta_{36C} + \frac{R_{1tC}}{R_{16C}}\theta_6. \tag{2.8}$$

If the principle of super position is applied, the transfer functions become

$$\frac{\theta_{16C}}{\theta_{36C}}(s) = \frac{\frac{R_{1tC}}{R_{26C}}}{1 + T_{1C}s}, \tag{2.9}$$

$$\frac{\theta_{16C}}{\theta_{6}}(s) = \frac{\frac{R_{1tC}}{R_{16C}}}{1 + T_{1C}s}. \tag{2.10}$$

2.2.2 Heat balance of the wall (towards room A)

The heat balance of the wall towards room A is found in the same manner as the previous case.

$$\frac{d}{dt}(C_{AC}\theta_{1AC}) = \frac{1}{R_{2AC}}(\theta_{3AC} - \theta_{1AC}) + \frac{1}{R_{2AC}}(\theta_{3CA} - \theta_{1AC}) \tag{2.11}$$

$$\Downarrow$$

$$C_{AC}\frac{d\theta_{1AC}}{dt} + (\frac{1}{R_{2AC}} + \frac{1}{R_{2AC}})\theta_{2AC} = \frac{1}{R_{2AC}}\theta_{3AC} + \frac{1}{R_{2AC}}\theta_{3CA}. \tag{2.12}$$

The equation is then multiplied with R_{3tAC} and Laplace-transformed. This yields

$$T_{3C}\theta_{1AC}s + \theta_{1AC} = \frac{R_{3tAC}}{R_{2AC}}(\theta_{3AC} + \theta_{3CA}), \tag{2.13}$$

where

$$R_{3tAC} = \frac{1}{\frac{1}{R_{2AC}} + \frac{1}{R_{2AC}}}, \tag{2.14}$$

$$T_{3C} = C_{AC}R_{3tAC}. \tag{2.15}$$

By applying the principle of super position, this results in

$$\frac{\theta_{1AC}}{\theta_{3AC}}(s) = \frac{\frac{R_{3tAC}}{R_{2AC}}}{1 + T_{3C}s}, \tag{2.16}$$

$$\frac{\theta_{1AC}}{\theta_{3CA}}(s) = \frac{\frac{R_{3tAC}}{R_{2AC}}}{1 + T_{3C}s}. \tag{2.17}$$

2.2.3 Heat balance of the wall (towards room B)

The heat balance of the wall towards room B is identical to the one towards room A:

$$\frac{d}{dt}(C_{BC}\theta_{1BC}) = \frac{1}{R_{2BC}}(\theta_{3BC} - \theta_{1BC}) + \frac{1}{R_{2BC}}(\theta_{3CB} - \theta_{1BC}) \tag{2.18}$$

$$\Downarrow$$

$$C_{BC}\frac{d\theta_{1BC}}{dt} + (\frac{1}{R_{2BC}} + \frac{1}{R_{2BC}})\theta_{2BC} = \frac{1}{R_{2BC}}\theta_{3BC} + \frac{1}{R_{2BC}}\theta_{3CB}. \tag{2.19}$$

The Laplace-transformation leads to

$$T_{4C}\theta_{1BC}s + \theta_{1BC} = \frac{R_{3tBC}}{R_{2BC}}(\theta_{3BC} + \theta_{3CB}), \tag{2.20}$$

where

$$R_{3tBC} = \frac{1}{\frac{1}{R_{2BC}} + \frac{1}{R_{2BC}}}, \tag{2.21}$$

$$T_{4C} = C_{BC}R_{3tBC}. \tag{2.22}$$

Once again the principle of super position is employed, which yields

$$\frac{\theta_{1BC}}{\theta_{3BC}}(s) = \frac{\frac{R_{3tBC}}{R_{2BC}}}{1 + T_{4C}s}, \tag{2.23}$$

$$\frac{\theta_{1BC}}{\theta_{3CB}}(s) = \frac{\frac{R_{3tBC}}{R_{2BC}}}{1 + T_{4C}s}. \tag{2.24}$$

2.2.4 Heat balance of the room air

The room air model is found in the same manner as the wall model, by studying Figure 2.2 and Figure 2.3 and extracting the corresponding equations.

$$\begin{aligned}\frac{d}{dt}(C_{2C}\theta_{2C}) = &\frac{1}{R_{36C}}(\theta_{36C}-\theta_{2C}) + \frac{1}{R_{3AC}}(\theta_{3AC}-\theta_{2C}) + \frac{1}{R_{3BC}}(\theta_{3BC}-\theta_{2C})\\ &+ \frac{1}{R_{5C}}(\theta_{5C}-\theta_{2C}) + \frac{1}{R_{7C}}(\theta_{7C}-\theta_{2C}) + \frac{1}{R_{8C}}(\theta_{6}-\theta_{2C})\\ &+ \frac{1}{R_{10C}}(\theta_{4C}-\theta_{2C}) + k_{eC}W_{eC} + k_{lC}W_{lC} + k_{pC}W_{pC}\end{aligned} \tag{2.25}$$

$$\Downarrow$$

$$\begin{aligned}C_{2C}\frac{d\theta_{2C}}{dt} + (&\frac{1}{R_{36C}} + \frac{1}{R_{3AC}} + \frac{1}{R_{3BC}} + \frac{1}{R_{5C}} + \frac{1}{R_{7C}} + \frac{1}{R_{8C}} + \frac{1}{R_{10C}})\theta_{2C}\\ &= \frac{1}{R_{36C}}\theta_{36C} + \frac{1}{R_{3AC}}\theta_{3AC} + \frac{1}{R_{3BC}}\theta_{3BC} + \frac{1}{R_{5C}}\theta_{5C} + \frac{1}{R_{7C}}\theta_{7C}\\ &+ \frac{1}{R_{8C}}\theta_{6} + \frac{1}{R_{10C}}\theta_{4C} + k_{eC}W_{eC} + k_{lC}W_{lC} + k_{pC}W_{pC}.\end{aligned} \tag{2.26}$$

The equation is multiplied by R_{2tC} and Laplace-transformed. This yields

$$\begin{aligned}(T_{2C}s+1)\theta_{2C} = &\frac{R_{2tC}}{R_{36C}}\theta_{36C} + \frac{R_{2tC}}{R_{3AC}}\theta_{3AC} + \frac{R_{2tC}}{R_{3BC}}\theta_{3BC} + \frac{R_{2tC}}{R_{5C}}\theta_{5C}\\ &+ \frac{R_{2tC}}{R_{7C}}\theta_{7C} + \frac{R_{2tC}}{R_{8C}}\theta_{6} + \frac{R_{2tC}}{R_{10C}}\theta_{4C}\\ &+ R_{2tC}(k_{eC}W_{eC} + k_{lC}W_{lC} + k_{pC}W_{pC}),\end{aligned} \tag{2.27}$$

where

$$R_{2tC} = \frac{1}{\frac{1}{R_{36C}} + \frac{1}{R_{3AC}} + \frac{1}{R_{3BC}} + \frac{1}{R_{5C}} + \frac{1}{R_{7C}} + \frac{1}{R_{8C}} + \frac{1}{R_{10C}}}, \tag{2.28}$$

$$T_{2C} = C_{2C}R_{2tC}. \tag{2.29}$$

This leads to the following transfer functions:

$$\frac{\theta_{2C}}{\theta_{36C}}(s) = \frac{\frac{R_{2tC}}{R_{36C}}}{1 + T_{2C}s}, \tag{2.30}$$

$$\frac{\theta_{2C}}{\theta_{3AC}}(s) = \frac{\frac{R_{2tC}}{R_{3AC}}}{1 + T_{2C}s}, \tag{2.31}$$

$$\frac{\theta_{2C}}{\theta_{3BC}}(s) = \frac{\frac{R_{2tC}}{R_{3BC}}}{1 + T_{2C}s}, \tag{2.32}$$

$$\frac{\theta_{2C}}{\theta_{5C}}(s) = \frac{\frac{R_{2tC}}{R_{5C}}}{1 + T_{2C}s}, \tag{2.33}$$

$$\frac{\theta_{2C}}{\theta_{6}}(s) = \frac{\frac{R_{2tC}}{R_{8C}}}{1 + T_{2C}s}, \tag{2.34}$$

$$\frac{\theta_{2C}}{\theta_{7C}}(s) = \frac{\frac{R_{2tC}}{R_{7C}}}{1 + T_{2C}s}, \tag{2.35}$$

$$\frac{\theta_{2C}}{\theta_{4C}}(s) = \frac{\frac{R_{2tC}}{R_{10C}}}{1 + T_{2C}s}, \tag{2.36}$$

$$\frac{\theta_{2C}}{W_{eC}}(s) = \frac{R_{2tC}k_{eC}}{1 + T_{2C}s}, \tag{2.37}$$

$$\frac{\theta_{2C}}{W_{lC}}(s) = \frac{R_{2tC}k_{lC}}{1 + T_{2C}s}, \tag{2.38}$$

$$\frac{\theta_{2C}}{W_{pC}}(s) = \frac{R_{2tC}k_{pC}}{1 + T_{2C}s}. \tag{2.39}$$

2.2.5 Heat balance of the wall surface (towards outdoor)

When the heat balance of the wall surface is explored, it is assumed that all the heat in this point (see θ_{36C} in Figure 2.2) is directly transfered to the thermal mass inside the wall, i.e. this point does not have a thermal mass. The heat balance in this point is therefore static, thus $\frac{d\theta_{36C}}{dt} \equiv 0$.

$$
\begin{aligned}
0 = &\frac{1}{R_{26C}}(\theta_{16C} - \theta_{36C}) + \frac{1}{R_{36C}}(\theta_{2C} - \theta_{36C}) + \frac{1}{R_{4C}}(\theta_{5C} - \theta_{36C}) \\
&+ \frac{1}{R_{9C}}(\theta_{4C} - \theta_{36C}) + (1 - k_{eC})W_{eC} + (1 - k_{lC})W_{lC} \\
&+ (1 - k_{pC})W_{pC}
\end{aligned} \tag{2.40}
$$

$$\Downarrow$$

$$
\begin{aligned}
&(\frac{1}{R_{26C}} + \frac{1}{R_{36C}} + \frac{1}{R_{4C}} + \frac{1}{R_{9C}})\theta_{36C} = \frac{1}{R_{26C}}\theta_{16C} + \frac{1}{R_{36C}}\theta_{2C} \\
&+ \frac{1}{R_{4C}}\theta_{5C} + \frac{1}{R_{9C}}\theta_{4C} + (1 - k_{eC})W_{eC} + (1 - k_{lC})W_{lC} \\
&+ (1 - k_{pC})W_{pC}.
\end{aligned} \tag{2.41}
$$

The equation is then multiplied with R_{4tC} and Laplace-transformed.

$$
\begin{aligned}
\theta_{36C} = &\frac{R_{4tC}}{R_{26C}}\theta_{16C} + \frac{R_{4tC}}{R_{36C}}\theta_{2C} + \frac{R_{4tC}}{R_{4C}}\theta_{5C} + \frac{R_{4tC}}{R_{9C}}\theta_{4C} \\
&+ R_{4tC}((1 - k_{eC})W_{eC} + (1 - k_{lC})W_{lC} + (1 - k_{pC})W_{pC}),
\end{aligned} \tag{2.42}
$$

where

$$R_{4tC} = \frac{1}{R_{26C}} + \frac{1}{R_{36C}} + \frac{1}{R_{4C}} + \frac{1}{R_{9C}}. \tag{2.43}$$

The following transfer functions are static since there are no derivatives in the heat balance.

$$\frac{\theta_{36C}}{\theta_{16C}}(s) = \frac{R_{4tC}}{R_{26C}}, \tag{2.44}$$

$$\frac{\theta_{36C}}{\theta_{2C}}(s) = \frac{R_{4tC}}{R_{36C}}, \tag{2.45}$$

$$\frac{\theta_{36C}}{\theta_{5C}}(s) = \frac{R_{4tC}}{R_{4C}}, \tag{2.46}$$

$$\frac{\theta_{36C}}{\theta_{4C}}(s) = \frac{R_{4tC}}{R_{9C}}, \tag{2.47}$$

$$\frac{\theta_{36C}}{W_{eC}}(s) = R_{4tC}(1 - k_{eC}), \tag{2.48}$$

$$\frac{\theta_{36C}}{W_{lC}}(s) = R_{4tC}(1 - k_{lC}), \tag{2.49}$$

$$\frac{\theta_{36C}}{W_{pC}}(s) = R_{4tC}(1 - k_{pC}). \tag{2.50}$$

2.2.6 Heat balance of the wall surface (towards room A)

The heat balance of the wall surface towards room A is found in the same manner as in the previous case.

$$\begin{aligned} 0 &= \frac{1}{R_{2AC}}(\theta_{1AC} - \theta_{3AC}) + \frac{1}{R_{3AC}}(\theta_{2C} - \theta_{3AC}) + \frac{1}{R_{4C}}(\theta_{5C} - \theta_{3AC}) \\ &+ \frac{1}{R_{9C}}(\theta_{4C} - \theta_{3AC}) + (1 - k_{eC})W_{eC} + (1 - k_{lC})W_{lC} \\ &+ (1 - k_{pC})W_{pC} \end{aligned} \tag{2.51}$$

$$\Downarrow$$

$$\begin{aligned} &(\frac{1}{R_{2AC}} + \frac{1}{R_{3AC}} + \frac{1}{R_{4C}} + \frac{1}{R_{9C}})\theta_{3AC} = \frac{1}{R_{2AC}}\theta_{1AC} + \frac{1}{R_{3AC}}\theta_{2C} \\ &+ \frac{1}{R_{4C}}\theta_{5C} + \frac{1}{R_{9C}}\theta_{4C} + (1 - k_{eC})W_{eC} + (1 - k_{lC})W_{lC} \\ &+ (1 - k_{pC})W_{pC}. \end{aligned} \tag{2.52}$$

The equation is multiplied with R_{5tAC} and Laplace-transformed.

$$\begin{aligned} \theta_{3AC} = &\frac{R_{5tAC}}{R_{2AC}}\theta_{1AC} + \frac{R_{5tAC}}{R_{3AC}}\theta_{2C} + \frac{R_{5tAC}}{R_{4C}}\theta_{5C} + \frac{R_{5tAC}}{R_{9C}}\theta_{4C} \\ &+ R_{5tAC}((1 - k_{eC})W_{eC} + (1 - k_{lC})W_{lC} + (1 - k_{pC})W_{pC}), \end{aligned} \tag{2.53}$$

where

$$R_{5tAC} = \frac{1}{R_{2AC}} + \frac{1}{R_{3AC}} + \frac{1}{R_{4C}} + \frac{1}{R_{9C}}. \tag{2.54}$$

The transfer functions become

$$\frac{\theta_{3AC}}{\theta_{1AC}}(s) = \frac{R_{5tAC}}{R_{2AC}}, \tag{2.55}$$
$$\frac{\theta_{3AC}}{\theta_{2C}}(s) = \frac{R_{5tAC}}{R_{3AC}}, \tag{2.56}$$
$$\frac{\theta_{3AC}}{\theta_{5C}}(s) = \frac{R_{5tAC}}{R_{4C}}, \tag{2.57}$$
$$\frac{\theta_{3AC}}{\theta_{4C}}(s) = \frac{R_{5tAC}}{R_{9C}}, \tag{2.58}$$
$$\frac{\theta_{3AC}}{W_{eC}}(s) = R_{5tAC}(1 - k_{eC}), \tag{2.59}$$
$$\frac{\theta_{3AC}}{W_{lC}}(s) = R_{5tAC}(1 - k_{lC}), \tag{2.60}$$
$$\frac{\theta_{3AC}}{W_{pC}}(s) = R_{5tAC}(1 - k_{pC}). \tag{2.61}$$

2.2.7 Heat balance of the wall surface (towards room B)

The wall-surface transfer functions towards room B are presented without derivation, since they are the same as towards room A.

$$\frac{\theta_{3AC}}{\theta_{1AC}}(s) = \frac{R_{5tAC}}{R_{2AC}}, \tag{2.62}$$
$$\frac{\theta_{3AC}}{\theta_{2C}}(s) = \frac{R_{5tAC}}{R_{3AC}}, \tag{2.63}$$
$$\frac{\theta_{3AC}}{\theta_{5C}}(s) = \frac{R_{5tAC}}{R_{4C}}, \tag{2.64}$$
$$\frac{\theta_{3AC}}{\theta_{4C}}(s) = \frac{R_{5tAC}}{R_{9C}}, \tag{2.65}$$
$$\frac{\theta_{3AC}}{W_{eC}}(s) = R_{5tAC}(1 - k_{eC}), \tag{2.66}$$
$$\frac{\theta_{3AC}}{W_{lC}}(s) = R_{5tAC}(1 - k_{lC}), \tag{2.67}$$
$$\frac{\theta_{3AC}}{W_{pC}}(s) = R_{5tAC}(1 - k_{pC}). \tag{2.68}$$

2.2.8 Heat balance of the window surface

According to Assumption 3, there is no heat accumulation in the windows. All the heat passing the windows is transfered either inside (air/wall) or outside. This leads to a static heat balance.

$$\begin{aligned} 0 = &\frac{1}{R_{4C}}(\theta_{3AC} - \theta_{5C}) + \frac{1}{R_{4C}}(\theta_{3CA} - \theta_{5C}) + \frac{1}{R_{4C}}(\theta_{36C} - \theta_{5C}) \\ &+ \frac{1}{R_{5C}}(\theta_{2C} - \theta_{5C}) + \frac{1}{R_{6C}}(\theta_6 - \theta_{5C}) \end{aligned} \tag{2.69}$$

$$\Downarrow$$

$$\theta_{5C} = \frac{R_{6tC}}{R_{4C}}(\theta_{36C} + \theta_{3AC} + \theta_{3CA}) + \frac{R_{6tC}}{R_{5C}}\theta_{2C} + \frac{R_{6tC}}{R_{6C}}\theta_6, \tag{2.70}$$

where

$$R_{6tC} = \frac{1}{\frac{3}{R_{4C}} + \frac{1}{R_{5C}} + \frac{1}{R_{6C}}}. \tag{2.71}$$

The static transfer functions yield:

$$\frac{\theta_{5C}}{\theta_{36C}}(s) = \frac{R_{6tC}}{R_{4C}}, \tag{2.72}$$

$$\frac{\theta_{5C}}{\theta_{3AC}}(s) = \frac{R_{6tC}}{R_{4C}}, \tag{2.73}$$

$$\frac{\theta_{5C}}{\theta_{3CA}}(s) = \frac{R_{6tC}}{R_{4C}}, \tag{2.74}$$

$$\frac{\theta_{5C}}{\theta_{2C}}(s) = \frac{R_{6tC}}{R_{5C}}, \tag{2.75}$$

$$\frac{\theta_{5C}}{\theta_{6}}(s) = \frac{R_{6tC}}{R_{6C}}. \tag{2.76}$$

2.3 Ventilation systems

Introduction

The introduction of ventilation systems are taken partly from Magnussen [2010], and is based on Abel and Elmroth [2007]. The indoor climate in a building will always have certain requirements, whether it is a hospital, a school, or an office building. Generally, ventilation means that clean air is supplied to a room, and the pollutants generated there are removed. However, in addition to the removal of pollutants, ventilation systems can remove surplus heat from a building. This is especially the case in places like Scandinavia, where the outdoor temperature most often is lower than the indoor temperature. The air in the room is set in motion when air is supplied into the room. This air flow speed can be high, low or varying, depending on how sophisticated the system is (Figure 2.4). If warm air is supplied at ceiling level, it may not mix with the polluted air, and the air quality will remain poor. However, if cold air is supplied at high speed, this may be perceived as unpleasant for the occupants. Depending on where the supply air is supplied, what temperature it has, and at which speed, the air mixture in the room will vary. For example, if cold air is supplied with low speed at floor level, it will lead to a stratified air distribution, where the cold air displaces the the pollutant and warm air (see Figure 2.4).

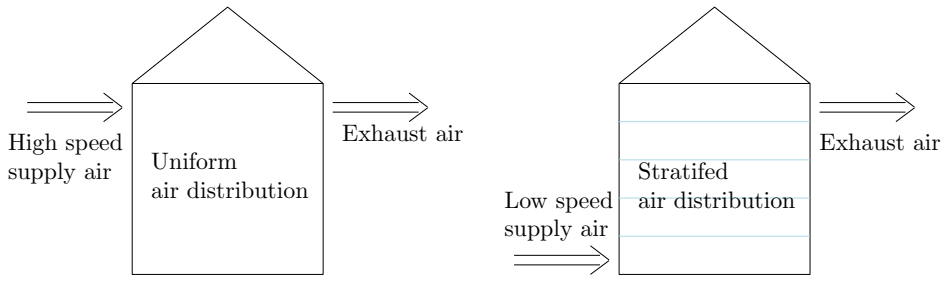

Figure 2.4: Two common ventilation schemes. The figure is taken from Magnussen [2010].

In order to save energy when heating the supply air, the air can be routed through a duct buried in the ground, or by using a heat recovery unit [4].

Intelligent buildings may have variable air volume (VAV) ventilation, such that different zones in a building (even in a room) can have different air flows.

[4] A heat recovery unit utilizes the heat from the exhaust air.

During a day there may be unoccupied zones in open-planed offices, and it is unnecessary to provide a constant air volume to these areas. It is desirable to only provide supply air to occupied zones, and this can be achieved by additional sensors and a VAV ventilation system. This will have a larger initial cost than a conventional ventilation system, but it may be worth it from a long-term point of view.

VAV and heat recovery units will increase the complexity level when modeling. Therefore, a constant air volume (CAV) system will be used in this thesis, and the supplied air will be heated by including a heat exchanger.

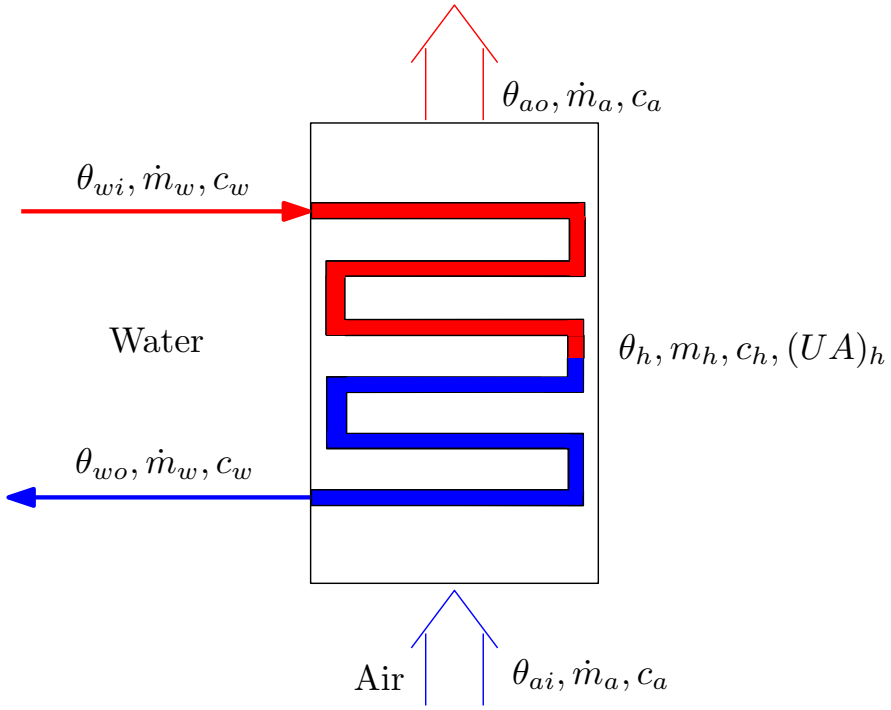

Figure 2.5: The heat exchanger in the ventilation system. The figure is inspired by Figure 13.1 in Novakovic [1995].

The air in the ventilation system is heated when it passes through a heat exchanger (see Figure 2.5). The input air has to maintain a certain temperature to prevent it of being uncomfortable for the occupants. Since the outdoor temperature fluctuates from day to day, this leads to a varying energy demand that is necessary to heat the input air. The water in the heat exchanger circuit (Figure 2.5) is a mixture of water from the main supply line, and outgoing water from the heat exchanger. A three-point valve (shunt connection) ensures that the water in the heat exchanger circuit is sufficiently

warm. In order to be able to study the ventilation system, a heat exchanger and a shunt connection have to be modeled.

2.3.1 Heat exchanger

The derivation of the heat exchanger model is based on the calculations in Chapter 13 in Novakovic [1995]. It consists of a dynamical heat balance on the water side, and a static heat equation on the air side. Novakovic [1995] makes 5 assumptions to simplify the derivation.

1. Constant amount of water through the heat exchanger ($\dot{m}_w = const$).
2. Constant amount of air through the heat exchanger ($\dot{m}_a = const$).
3. No heat loss to the surroundings.
4. Direct connection between metal temperature in the heat exchanger (θ_h) and the temperature of the incoming air (θ_{ai}).
5. The metal temperature in the heat exchanger is equal to the outgoing water temperature ($\theta_h = \theta_{wo}$).

The heat balance on the water side yields

$$\frac{d}{dt}(m_h c_h \theta_h) = \dot{m}_w c_w(\theta_{wi} - \theta_{wo}) - (UA)_h(\theta_{wo} - \theta_{ai}). \tag{2.77}$$

According to Assumtion 5, $\theta_h = \theta_{wo}$, so the equation is written as

$$m_h c_h \frac{d\theta_{wo}}{dt} = \dot{m}_w c_w(\theta_{wi} - \theta_{wo}) - (UA)_h(\theta_{wo} - \theta_{ai}), \tag{2.78}$$

where $(UA)_h$ is the heat exchanger´s unknown heat-transmission number. The heat equation on the air side is given by

$$\dot{m}_a c_a(\theta_{ao} - \theta_{ai}) = (UA)_h(\theta_{wo} - \theta_{ai}), \tag{2.79}$$

where the received heat is equal to the produced heat (Assumption 3).

The water in Figure 2.5 is cooled by the incoming air, while the incoming air gains heat from the water. These reactions are captured in the following coefficients:

$$\epsilon_w = \frac{\theta_{wi} - \theta_{wo}}{\theta_{wi} - \theta_{ai}} \tag{2.80}$$

is relative water cooling, while

$$\epsilon_a = \frac{\theta_{ao} - \theta_{ai}}{\theta_{wi} - \theta_{ai}} \tag{2.81}$$

is relative air heating. Equations (2.80) and (2.81) are evaluated at the heat exchanger´s nominal conditions, i.e. design temperatures (see Appendix A.2).

By combining (2.79), (2.80) and (2.81), $(UA)_h$ can be written as

$$(UA)_h = \frac{\epsilon_a}{1 - \epsilon_w} \dot{m}_a c_a. \tag{2.82}$$

The air coefficients can be replaced by the corresponding water coefficients because the static heat balance is equal on the water side and air side (Novakovic [1995]),

$$(UA)_h = \frac{\epsilon_w}{1 - \epsilon_w} \dot{m}_w c_w. \tag{2.83}$$

If (2.83) is inserted into (2.78), the unknown heat-transmission term is eliminated.

$$m_h c_h \frac{d\theta_{wo}}{dt} = \dot{m}_w c_w (\theta_{wi} - \theta_{wo}) - \dot{m}_w c_w \frac{\epsilon_w}{1 - \epsilon_w} (\theta_{wi} - \theta_{ai}) \tag{2.84}$$

$$\Downarrow$$

$$\frac{m_h c_h}{\dot{m}_w c_w}(1 - \epsilon_w)\frac{d\theta_{wo}}{dt} + \theta_{wo}(1 - \epsilon_w + \epsilon_w) = (1 - \epsilon_w)\theta_{wi} + \epsilon_w \theta_{ai} \tag{2.85}$$

$$\Downarrow$$

$$T_h \frac{d\theta_{wo}}{dt} + \theta_{wo} = (1 - \epsilon_w)\theta_{wi} + \epsilon_w \theta_{ai}, \tag{2.86}$$

where

$$T_h = \frac{m_h c_h}{\dot{m}_w c_w}(1 - \epsilon_w). \tag{2.87}$$

Equation (2.86) does not include information about the air going out of the heat exchanger. By combining (2.80) and (2.81), this yields

$$\theta_{wo} = \frac{1 - \epsilon_w}{\epsilon_a}\theta_{ao} + \frac{1 - \epsilon_w - \epsilon_a}{\epsilon_a}\theta_{ai}. \tag{2.88}$$

If this is inserted into (2.86), θ_{ao} is included in the model.

$$T_h \frac{d}{dt}\left(\frac{1-\epsilon_w}{\epsilon_a}\theta_{ao} + \frac{1-\epsilon_w-\epsilon_a}{\epsilon_a}\theta_{ai}\right) + \frac{1-\epsilon_w}{\epsilon_a}\theta_{ao} + \frac{1-\epsilon_w-\epsilon_a}{\epsilon_a}\theta_{ai}$$
$$= (1-\epsilon_w)\theta_{wi} + \epsilon_w\theta_{ai} \tag{2.89}$$
$$T_h\frac{d\theta_{ao}}{dt} + \theta_{ao} = \frac{1-\epsilon_w-\epsilon_a}{\epsilon_a}\left(T_h\frac{d\theta_{ai}}{dt} + \theta_{ai}\right) + \epsilon_a\theta_{wi} + \frac{\epsilon_w\epsilon_a}{1-\epsilon_w}\theta_{ai} \tag{2.90}$$
$$\Downarrow$$
$$T_h\frac{d\theta_{ao}}{dt} + \theta_{ao} = K_h\frac{d\theta_{ai}}{dt} + (1-\epsilon_a)\theta_{ai} + \epsilon_a\theta_{wi}, \tag{2.91}$$

where

$$K_h = T_h\frac{1-\epsilon_w-\epsilon_a}{1-\epsilon_w}. \tag{2.92}$$

Equation (2.86) and (2.91) are then Laplace-transformed, before the principle of super position is applied. This results in

$$\frac{\theta_{wo}}{\theta_{wi}}(s) = \frac{1-\epsilon_w}{1+T_hs}, \tag{2.93}$$
$$\frac{\theta_{wo}}{\theta_{ai}}(s) = \frac{\epsilon_w}{1+T_hs}, \tag{2.94}$$
$$\frac{\theta_{ao}}{\theta_{wi}}(s) = \frac{\epsilon_a}{1+T_hs}, \tag{2.95}$$
$$\frac{\theta_{ao}}{\theta_{ai}}(s) = \frac{1-\epsilon_a+K_hs}{1+T_hs}. \tag{2.96}$$

2.3.2 Shunt connection

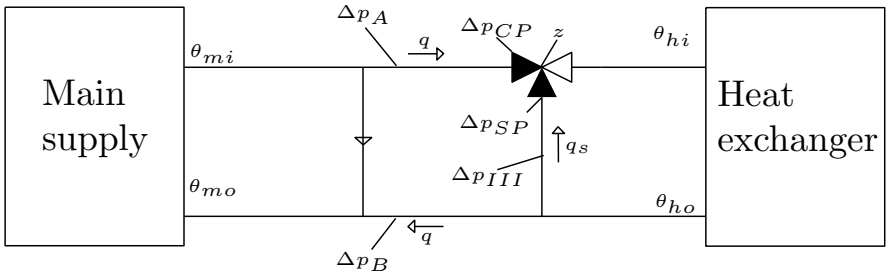

Figure 2.6: The shunt connection in the ventilation system. The figure is inspired by Figure 10.1 in Novakovic [1995].

The following assumptions are made when the model is derived (Novakovic [1995])

1. Constant pressure drop and therefore constant water amount in the heat exchanger circuit.
2. Turbulent flow.
3. No heat loss to the surroundings.

The constant pressure over the shunt connection is given by

$$\Delta p_{CPz} + \Delta p_{IIz} = \Delta p_{SPz} + \Delta p_{IIIz} = const, \tag{2.97}$$

where

$$\Delta p_{IIz} = \Delta p_A + \Delta p_B. \tag{2.98}$$

The z subscripts indicate that the pressures vary with respect to the valve position. The water amount through the control port, depending on the pressure drop and capacity number (k_{vs}), is defined by Novakovic [1995] to be

$$\dot{Q}_{CP} = k_{vs} f_{CP}(z) \sqrt{\Delta p_{CPz}} = \dot{Q}_{max} f_{CP}(z) \sqrt{\frac{\Delta p_{CPz}}{\Delta p_{CP}}}. \tag{2.99}$$

If (2.97) is solved with respect to varying pressure, this yields

$$\Delta p_{CPz} = \Delta p_{CP} \frac{q^2}{f_{CP}(z)^2}, \tag{2.100}$$

where $f_{CP}(z)$ is the control-valve characteristic. The same equation applies for the shunt connection,

$$\Delta p_{SPz} = \Delta p_{SP} \frac{q_s^2}{f_{SP}(z)^2}. \tag{2.101}$$

If (2.100) and (2.101) are inserted into (2.97), the relation between the shunt valve and control valve appears:

$$\Delta p_{CP} \frac{q^2}{f_{CP}(z)^2} + \Delta p_{II} = \Delta p_{SP} \frac{q_s^2}{f_{SP}(z)^2} + \Delta p_{III}. \tag{2.102}$$

Since the water flow in the heat-exchanger circuit is assumed to be constant,

$$q_s = 1 - q. \tag{2.103}$$

Finally, by inserting (2.103) into (2.102), this results in an expression for the relative water flow through the control valve,

$$q = \frac{1}{1 + \sqrt{\Psi}} \tag{2.104}$$

$$\Psi = \frac{\frac{\Delta p_{CP}}{f_{CP}(z)^2} + \Delta p_{II}}{\frac{\Delta p_{SP}}{f_{SP}(z)^2} + \Delta p_{III}}. \tag{2.105}$$

The relative water flow through the shunt port is found by replacing z with $1 - z$ in (2.105). The valve characteristics in this thesis are chosen to be the same as in Section 23.5 in Novakovic [1995]. That is exponential control-port characteristic and linear shunt-port characteristic.

$$f_{CP}(z) = R_{CP}^{z-1} \tag{2.106}$$

$$f_{SP}(z) = (1 - \frac{1}{R_{SP}})(1 - z) + \frac{1}{R_{SP}}. \tag{2.107}$$

R denotes the relationship between volume flow at $z = 1$ and a fictive leakage through the port at $z = 0$, $R = \frac{Q_{max}}{Q_{min}}$. The heat balance in the shunt

connection is trivial to set up by studying Figure 2.6.

$$\theta_{mo} = (1 - q)\theta_{mi} + q\theta_{ho} \tag{2.108}$$
$$\theta_{ho} = q\theta_{mi} + (1 - q)\theta_{ho}. \tag{2.109}$$

Because of (2.105), the shunt connection model is nonlinear. In Chapter 4, a linear MPC scheme will be introduced, and because this control scheme demands a linear model, the shunt-connection model has to be linearized. However, the linearization will not be derived explicitly here. When the total model has been derived and implemented in `Simulink`, it will be linearized using the `MATLAB` function `linmod(system)`. This is explained in detail in Chapter 4.

2.4 Heating systems

Introduction

The introduction to heating systems will be based on Abel and Elmroth [2007]. A heating system has to be able to meet the demands of the building it is installed in. Residential buildings, warehouses, and office building have different demands when it comes to indoor climate, and the building owner should choose a system which fulfills these demands in the best possible way. The running costs should be kept low, but still guarantee a satisfying indoor climate. There is a large number of different heating- and distributing systems installed in buildings nowadays, but they will not be listed here. Since a waterborne district heating system is used in Bassengbakken 1, this will be the focus in this section. A district heating system (Figure 2.7) consists of a few, but large heat generator plants, which are connected to a distribution system. These distribution systems supply households and buildings nearby with heat in form of water or steam. The fluid flow varies with the load of the system. Control valves open when the system load increases, so that the fluid flow is increased. The initial costs are large when a district heating system is introduced, because of the construction of large generation plants and comprehensive distribution systems. In other words, district heating is a long-term investment that would fit poorly if a building owner wishes to obtain a short-term profit. However, on a long-term basis, such systems are efficient in both financial and environmental terms. It is common to combine ordinary boiling and furnace systems with alternative

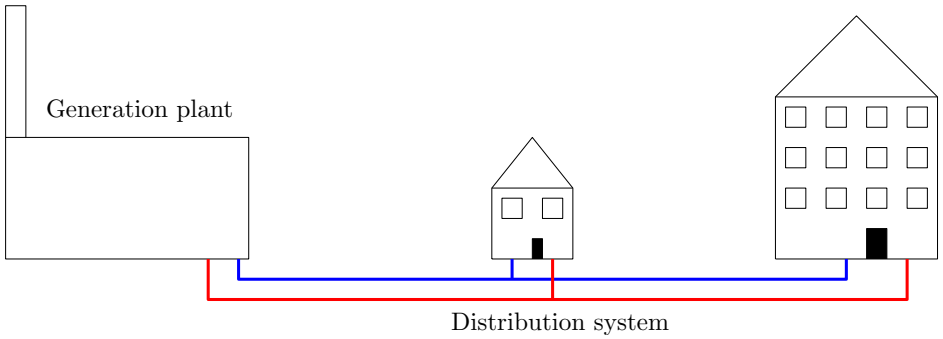

Figure 2.7: A district heating system. This figure is taken from Magnussen [2010].

heating, and this is easier utilized in district heating systems, compared to local plants.

In a district heating system, a heat exchanger is used to transfer energy from one fluid to another. These fluids are normally separated from each other by a solid medium (Kreider et al. [2002]). As one fluid is heated, the other one is cooled down. The supply water varies with outdoor temperature, but is usually not lower than 60 $°C$. This is done to provide hot tapping water. As mentioned before, tapping water is not taken into account in this thesis. This will be elaborated in Chapter 6

2.4.1 Room heating

In buildings with waterborne heating systems, radiators are used to provide heating to each room in the building, and they are placed below the windows (Abel and Elmroth [2007]). Cold air penetrates windows more easily than walls since windows are thinner and have higher U-values than walls (Appendix A). Because particles in warm air are more separated than in cold air, cold air is heavier than warm air. This can lead to increased air movement and to a stratified air distribution with cold air at floor level and warm air at ceiling level. By placing the radiators below the windows, this unpleasant effect is avoided because of the warm air emitted from the radiators.

Hot water is sent through a radiator to heat it up, and when the desired indoor temperature has been reached, the supply water is bypassed (Figure 2.8). In order to be able to study how the radiator temperature varies during the room heating, the radiator dynamics has to be described. This is not done in Novakovic [1995], but the principle intuitive. The radiator gains heat

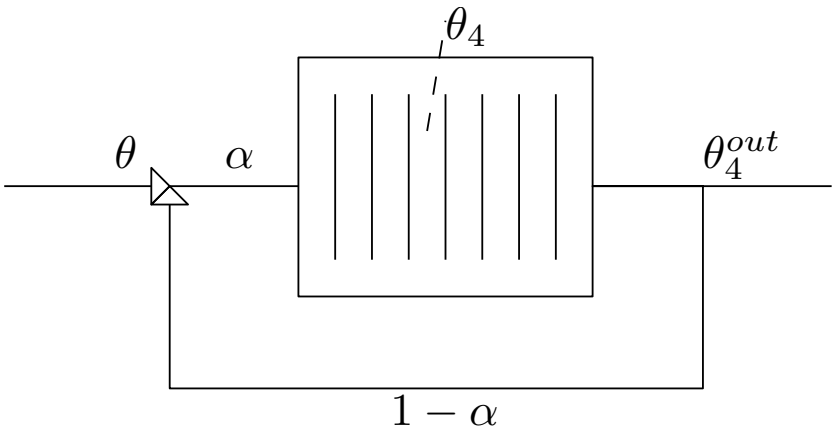

Figure 2.8: Illustration of a radiator.

from the water flowing into it, while it dissipates heat when water is flowing out. In addition to this, the radiator dissipates heat to the surrounding walls and room air. If this is taken into account, the heat balance of the radiator becomes

$$\frac{d}{dt}(C_{4C}\theta_{4C}) = \alpha w_w \rho_w c_w(\theta - \theta_{4C}) - Q_{4C}, \tag{2.110}$$

where $0 \leq \alpha \leq 1$ is the amount of supplied water that is sent through the radiator. Q_{4C} is the heat dissipation from the radiator to the surroundings, and is given by

$$Q_{4C} = \frac{1}{R_{10C}}(\theta_{4C}-\theta_{2C})+\frac{1}{R_{9C}}(\theta_{4C}-\theta_{36C})+\frac{1}{R_{9C}}(\theta_{4C}-\theta_{3AC})+\frac{1}{R_{9C}}(\theta_{4C}-\theta_{3BC}). \tag{2.111}$$

(2.110) and (2.111) is combined and Laplace transformed in the same manner as earlier, and this yields

$$(C_{4C}s+\alpha\rho_w c_w w_w+\frac{1}{R_{10C}}+\frac{3}{R_{9C}})\theta_{4C} = \frac{1}{R_{10C}}\theta+\frac{1}{R_{9C}}\theta_{36C}+\frac{1}{R_{9C}}\theta_{3AC}+\frac{1}{R_{9C}}\theta_{3BC}. \tag{2.112}$$

The transfer functions become

$$\frac{\theta_{4C}}{\theta}(s) = \frac{\frac{\kappa_C}{R_{10C}}}{1 + T_{5C}s}, \tag{2.113}$$

$$\frac{\theta_{4C}}{\theta_{36C}}(s) = \frac{\frac{\kappa_C}{R_{9C}}}{1 + T_{5C}s}, \tag{2.114}$$

$$\frac{\theta_{4C}}{\theta_{3AC}}(s) = \frac{\frac{\kappa_C}{R_{9C}}}{1 + T_{5C}s}, \tag{2.115}$$

$$\frac{\theta_{4C}}{\theta_{3BC}}(s) = \frac{\frac{\kappa_C}{R_{9C}}}{1 + T_{5C}s}, \tag{2.116}$$

where

$$\kappa_C = \frac{1}{\alpha\rho_w c_w w_w + \frac{3}{R_{9C}} + \frac{1}{R_{10C}}}, \tag{2.117}$$

and

$$T_{5C} = \frac{C_{4C}}{\kappa}. \tag{2.118}$$

2.4.2 Heat exchanger

The district heating system consists of a heat exchanger and a shunt connection, and is therefore modeled in the same manner as the ventilation system.

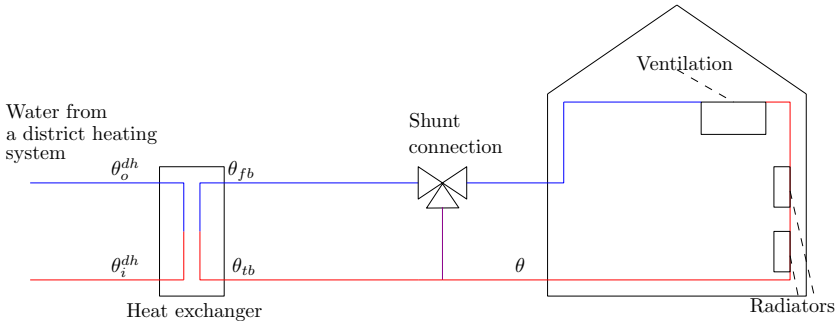

Figure 2.9: A simplified building structure that illustrates the heating system. The figure is taken from Magnussen [2010].

Since the derivation of the heat exchanger dynamics is identical to the one

in Section 2.3, the transfer functions are written directly.

$$\frac{\theta_o^{dh}}{\theta_i^{dh}}(s) = \frac{1-\epsilon_w^{dh}}{1+T^{dh}s}, \tag{2.119}$$

$$\frac{\theta_o^{dh}}{\theta_{fb}}(s) = \frac{\epsilon_w^{dh}}{1+T^{dh}s}, \tag{2.120}$$

$$\frac{\theta_{tb}}{\theta_i^{dh}}(s) = \frac{\epsilon_w^{b}}{1+T^{dh}s}, \tag{2.121}$$

$$\frac{\theta_{tb}}{\theta_{fb}}(s) = \frac{1-\epsilon_w^{b}+K^{dh}s}{1+T^{dh}s}. \tag{2.122}$$

The water flowing out of the building (see θ_{fb} Figure 2.9) is dependent of how much heat that is used by the 3 radiators and by the ventilation system. The temperature of the water flowing out of a radiator can be found by studying Figure 2.8

$$\theta_4^{out} = (1-\alpha)\theta + \alpha\theta_4, \tag{2.123}$$

and the temperature of the water flowing out of the ventilation system is found by using (2.109). θ_{fb} is then calculated by multiplying the outgoing temperatures with the percentage of water flowing through the different components. These values and other building-specific information are found in Section 2.1 and in Appendix A.

2.4.3 Shunt connection

The valve characteristics for the shunt port and controller port, and the heat balances over the shunt connection are also identical to those given in Section 2.3.

$$f_{CP}^{dh}(z) = {R_{CP}^{dh}}^{z^{dh}-1} \tag{2.124}$$

$$f_{SP}^{dh}(z) = (1-\frac{1}{R_{CP}^{dh}})(1-z^{dh}) + \frac{1}{R_{CP}^{dh}}, \tag{2.125}$$

$$\theta_{mo}^{dh} = (1-q^{dh})\theta_{mi}^{dh} + q^{dh}\theta_{ho}^{dh} \tag{2.126}$$

$$\theta_{ho}^{dh} = q^{dh}\theta_{mi}^{dh} + (1-q^{dh})\theta_{ho}^{dh}. \tag{2.127}$$

2.5 Disturbances

As mentioned in Chapter 2, disturbances acting on the system from inside the building include radiation from people, equipment, and lightning. The outdoor temperature is the only disturbance from outside the building, since solar radiation is left out.

Thermal radiation

In Grini et al. [2009], information concerning radiation from the different sources can be found. Radiation from people (W_p) is 4.8 W/m^2, radiation from equipment (W_e) is 14 W/m^2, and radiation from lighting (W_l) is 11.6 W/m^2. These values are valid during working hours. Their values after working hours are not measured in Grini et al. [2009], but they will be smaller since the workers shut down their computers, turn of their lights, and go home. The radiation values after working hours are given arbitrarily values around 0 W/m^2 - 3 W/m^2. In addition to this, random white noise is added to the disturbances because the mentioned values will fluctuate from day to day (absence of workers and broken down equipment).

Weather

In order to get sensible results when comparing the conventional control strategy with the sophisticated ones, it is desirable that the outdoor temperature affecting the system is equal in all the cases. Therefore, hourly weather data from `www.yr.no` over 4 days are used. If the simulation time exceeds 4 days, the values are repeated. Since the temperatures are given hourly, they are interpolated such that the system behavior can be studied minute by minute.

The interpolation algorithm is linear, and it also contains a restart function when the simulation time exceeds 4 days. The outdoor temperatures are found by using the principle of similitude. $weather_{forecast}$ is an array containing hourly outdoor temperatures for Trondheim between Monday February 14 through Thursday February 18.

Algorithm 1 Outdoor temperature (θ_6) interpolated from hourly weather data.

$k = second - \frac{mod(second,hour)}{hour}$
$e_1 = mod(k+1, length(weather_{forecast}) - 1) + 1$
$e_2 = mod(e_1, length(weather_{forecast}))$

if $e_2 = e_1$ **then**
  $e_2 = e_1 + 1$
end if

$\theta_{6,i} = weather_{forecast}(e_1)$
$\theta_{6,i+1} = weather_{forecast}(e_2)$
$\Delta\theta_6 = \theta_{6,i+1} - \theta_{6,i}$

$\theta_6 = \theta_{6,i} + \Delta\theta_6 \frac{mod(second,hour)}{hour}$

2.6 Control strategy

As emphasized above, the objective in this thesis is to minimize the energy consumption in an office building, but still maintain set indoor temperature demands. And as mentioned in Chapter 1, there are numerous different projects concerning energy efficiency in buildings, and they use various strategies when it comes to control. There are several different approaches to ensure increased energy efficiency, and these different control strategies have to be chosen carefully with respect to certain priorities.

- Is the control strategy supposed to be tailor fit to one specific building, or should it be compatible with several buildings?
- Should the controller be low-leveled with careful control of indoor climate aspects, or should it be high-leveled by determination of set-points?

It is the heat dissipated from the water that represents the actual energy consumption in a building with a waterborne heating system. If the aim is to reduce the energy consumption, i.e. decrease the amount of used water, the radiators and ventilation systems have to be controlled individually. It is common that both blind-positioning and radiators are controlled manually in each office in a building, but if a low-leveled control strategy is going to be applicable, all components have to support automatic control. This could make it problematic to fulfill all the occupants desires when it comes to indoor temperature and lightness in the office, and at the same time it will probably lead to more expensive components. This will vary from building to building, which implies that a low-leveled control strategy will have to be tailor made for each building. Even though it is implied that a low-leveled control strategy will lead to a large initial investment, it could be economically beneficial in a long-term point of view.

2.6.1 Conventional control strategy

As mentioned in Chapter 1, the author of this thesis wants to keep the control strategy high-leveled, such that the control system potentially can be applied to all buildings with waterborne heating systems. Therefore, the focus in this thesis will be to provide the system with smart set-points. The control variable will therefore be the reference temperature of the supplied water (θ_{ref} in Figure 2.10 and Figure 2.11).

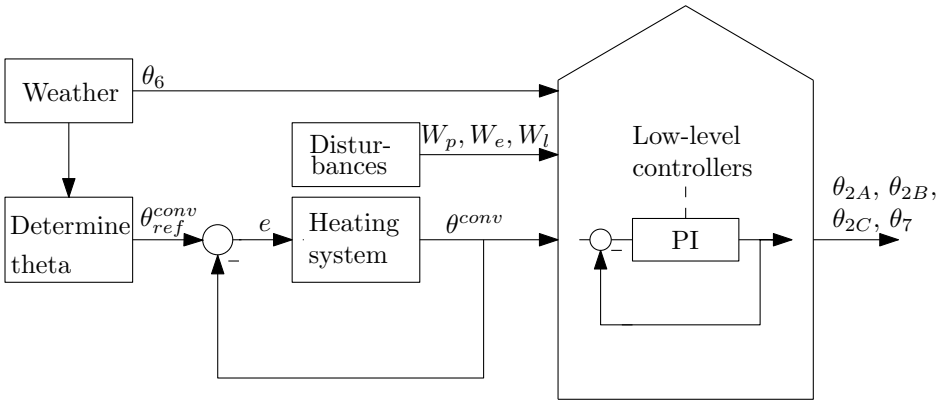

Figure 2.10: A conventional control strategy.

Figure 2.10 presents a conventional control strategy. The determination of θ_{ref} is only dependent on the outdoor temperature (θ_6), which means that an algorithm decides various values for θ_{ref} when θ_6 varies. The running costs of the system will depend on the amount of and the temperature of the supplied water. An example of a conventional set-point regime is that θ_{ref} is 70 $^\circ C$ when θ_6 lies between -5 $^\circ C$ and 0 $^\circ C$, while θ_{ref} is 65 $^\circ C$ when θ_6 lies between 0 $^\circ C$ and 5 $^\circ C$, and so on. Details of conventional control strategies will be given in Chapter 3.

2.6.2 MPC strategy

The actual energy consumption is dependent on how much heat that dissipates when the hot water passes the ventilation system and the radiators in the building (Figure 2.9). However, if θ_{ref} is minimized, potential heat losses will be minimized, since there will be less energy available. The actual consumption will not be subject for minimization in this thesis, but the focus will be to ensure that the system contains the smallest sufficient amount of energy.

When using an MPC scheme, a weather forecast and measurements of indoor temperatures will be used when θ_{ref} gets decided by solving a constrained optimization problem (see Chapter 4). The purpose of this strategy is to minimize θ_{ref} without affecting the indoor climate negatively.

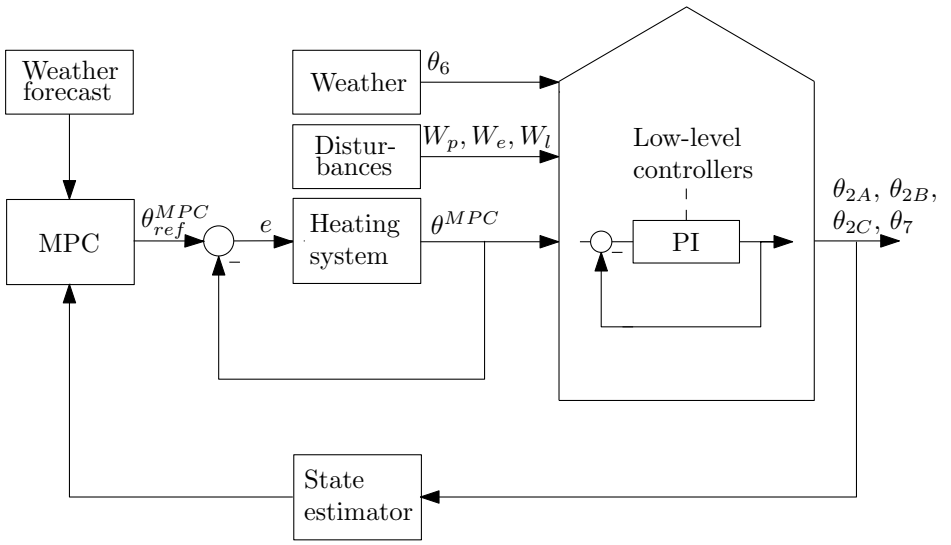

Figure 2.11: An MPC strategy.

2.7 Implementation

The building model presented in this chapter is implemented in `Simulink`, and this is done by using the transfer functions derived above. The electrical elements in Figure 2.2 and Figure 2.3 are given values based on a set of rules in Chapter 19 in Novakovic [1995], and these calculations can be studied in detail in Appendix A. The top-level `Simulink` diagram of the building model with a conventional control scheme can be seen in Figure C.1. The walls of the building are divided into two different types when implementing the model, and they are walls facing outdoor air and walls facing other rooms. The walls, in addition to the floor and the ceiling, could have been described by one heat balance each to make the model as accurate as possible. However, to prevent the model of being to complex, only two types of walls are included. The floor and the ceiling are left out, which is the same as setting their U-values equal to 0 (Appendix A).

As mentioned in Section 2.6, the control goal in this thesis is to keep the water-supply temperature as low as possible, but at the same time maintain a desired indoor climate. In order to do the latter part, internal controllers have to be included to control the radiators and the ventilation system. PI controllers are used when implementing these low-level controllers. The P-term provides a desired gain while the I-term removes stationary deviation. The controllers are given their proportional and integral gains by trail and error. This can be done in a more sophisticated manner, but as stressed above, low level control is not the main purpose in this thesis, which makes trail and error sufficiently accurate.

In the next chapter, the conventional control scheme is introduced.

Chapter 3

Introducing Conventional Set-Point Determination

In order to have a foundation of comparison when examining the energy consumption, the system will initially be implemented and simulated with a conventional control strategy (Figure 2.10). This means that the determination of θ_{ref} only will depend on the outdoor temperature.

According to Djuric et al. [2007], it is common that the supply-water temperature varies in an approximately linear manner with respect to the outdoor temperature. As Figure 3.1 implies, one is guaranteed hot supply water when it is cold outside if θ_{ref} is determined in the suggested manner. A similar method is the square-pulse strategy suggested in Magnussen [2010]. It is important that the water supplied to the building contains enough energy such that the ventilation system and the radiators can fulfill the set temperature demands. The simulations in this chapter will examine the correlation between the supplied energy and the system´s internal behavior. θ_{ref}´s set-points will be decided according to Figure 3.1.

3.1 Indoor temperature behavior

As mentioned in Section 2.1, the desired indoor temperature is 21 $^{\circ}C$ during the day and 17 $^{\circ}C$ during the night. Day time is defined as working hours and include the first 12 hours of the day. Even though a normal working day in Norway is 8 hours, working hours is set to 12 to cover flexible working hours time and over time. Figure 3.3 shows the indoor temperature behavior

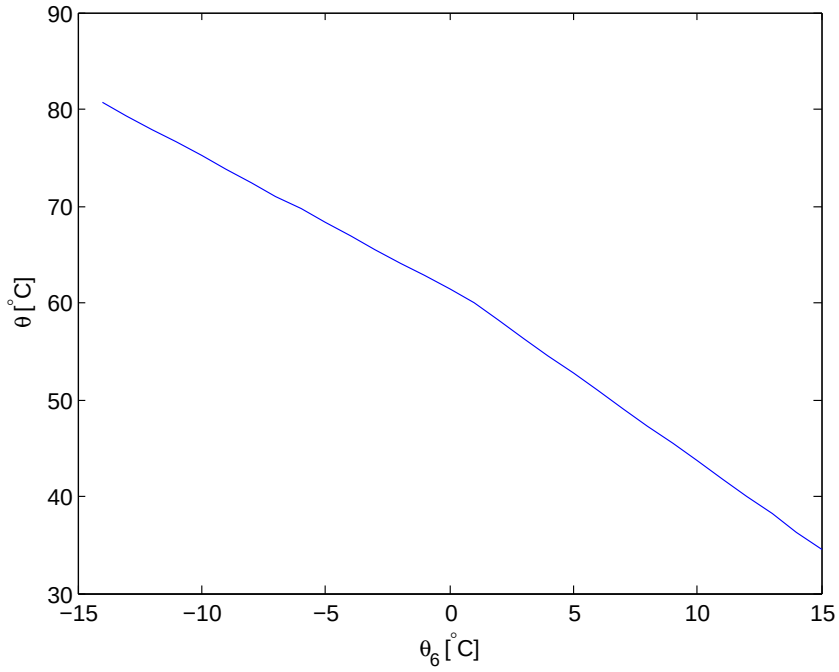

Figure 3.1: The supply-water temperature (θ) varies with respect to the outdoor temperature (θ_6). This figure is similar to Figure 3 in Djuric et al. [2007].

when the system switches from night mode to day mode in room A, B and C, respectively. Note the starting time. The night-to-day behavior is studied when the system has simulated for 1 day. This is to avoid that the initial values in `Simulink` affect the temperature responses. It is more natural to study the temperature responses when the system starts at its night-time values. Therefore, all the night-to-day temperature responses in this thesis will start after 1435 - 1440 minutes.

From night to day

If Figure 3.3a is examined, it is seen that θ_{2A} goes from 17 $^{\circ}C$ to 21 $^{\circ}C$ in about 26 minutes. θ_{4A} increases at maximum rate from 23 $^{\circ}C$ until it is saturated at 61.6 $^{\circ}C$, which is actually lower than the supply-water temperature. θ_{4A} is saturated for 15 minutes before it settles at 32.9 $^{\circ}C$ while θ_{2A} reaches its desired value 21 $^{\circ}C$. The temperature response is slightly underdamped, and this is probably because the radiator is in saturation when the desired temperature is reached. Figure 3.3b and Figure 3.3c present the same temperature responses in room B and room C, but the response times

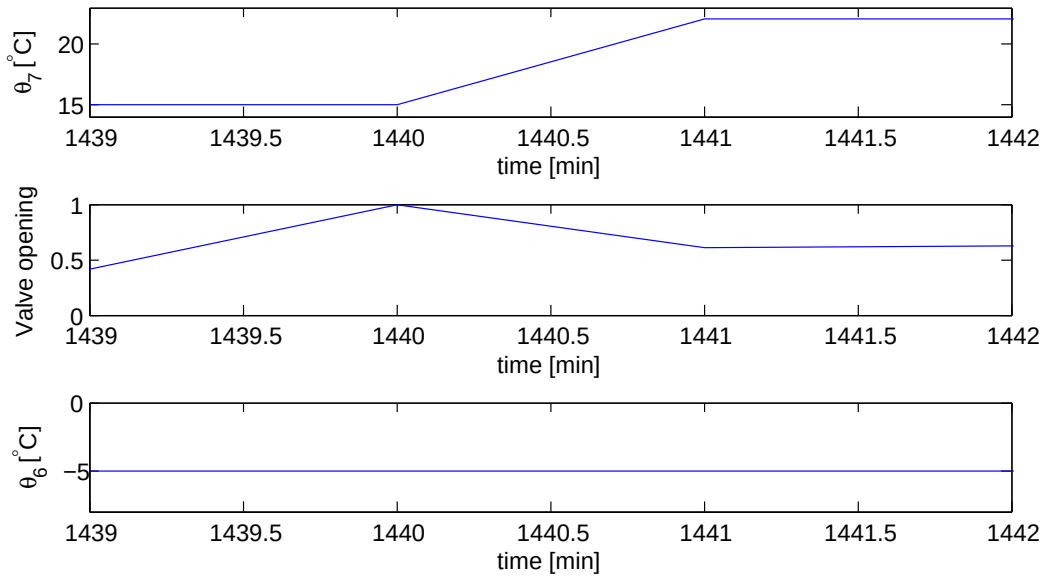

Figure 3.2: Ventilation-air temperature (θ_7), control-valve opening, and outdoor temperature (θ_6) (from night to day).

are different. θ_{4B} remains saturated for 30 minutes before θ_{2B} reaches 21 $°C$ after 48 minutes. The responses are even slower for room C, θ_{4C} is saturated for about 70 minutes before θ_{2C} reaches 21 $°C$ after 88 minutes. These results are reasonable considering the room areas. The heating process gets slower as the rooms get larger, thus since room C is the largest one and room A is the smallest (see Figure 2.1), these results make sense.

In Figure 3.2, it is seen that the ventilation-air temperature is heated from the desired night-time temperature 15 $°C$ to desired day-time temperature 22 $°C$ in 1 minute. This quick response is reasonable because of the second assumption made in Section 2.3.1, namely that there is a direct connection between the heat exchanger's metal temperature and the incoming air, and that there is no heat loss to the surroundings. The valve in the ventilation system is saturated only for a few seconds during the heating. Except when the radiators are saturated during the heating, the supply-water temperature (θ) remains to be 30 $°C$ - 40 $°C$ higher than the respective radiator temperatures. Intuitively, the more heat supplied to the system, the larger energy consumption and energy losses will be the case. After examination of Figure 3.2 and Figure 3.3, it seems unnecessary to keep the supply temperature at such high levels. Even though most of the unused heat is sent back into the building (see θ_{fb} in Figure 2.9), the heat losses to the surroundings in a real application will vary proportionally with the supply temperature.

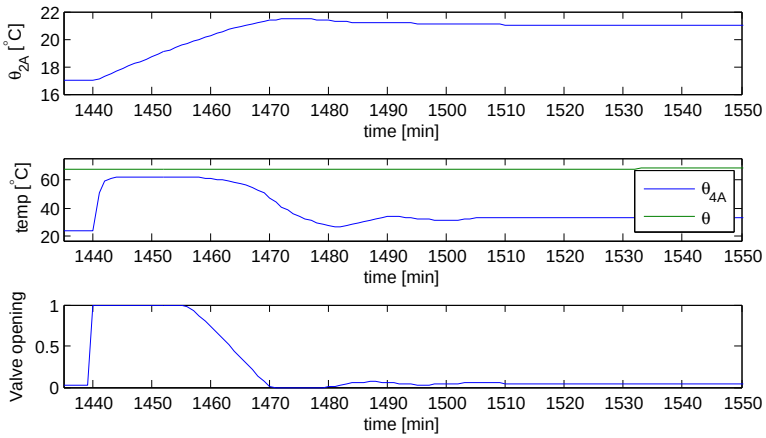

(a) Room A.

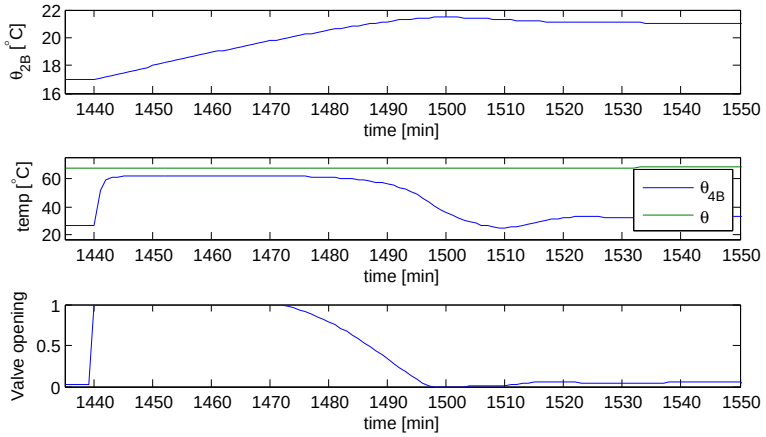

(b) Room B.

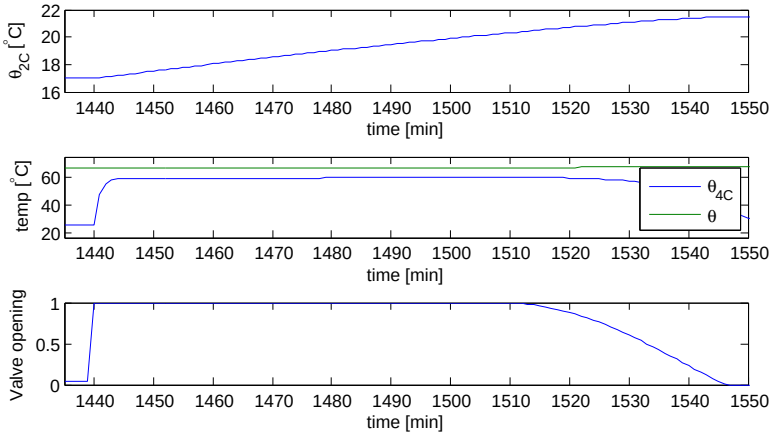

(c) Room C.

Figure 3.3: Indoor temperature (θ_2), radiator temperature (θ_4), supply-water temperature (θ), and control-valve opening of the radiator (from night to day).

From day to night

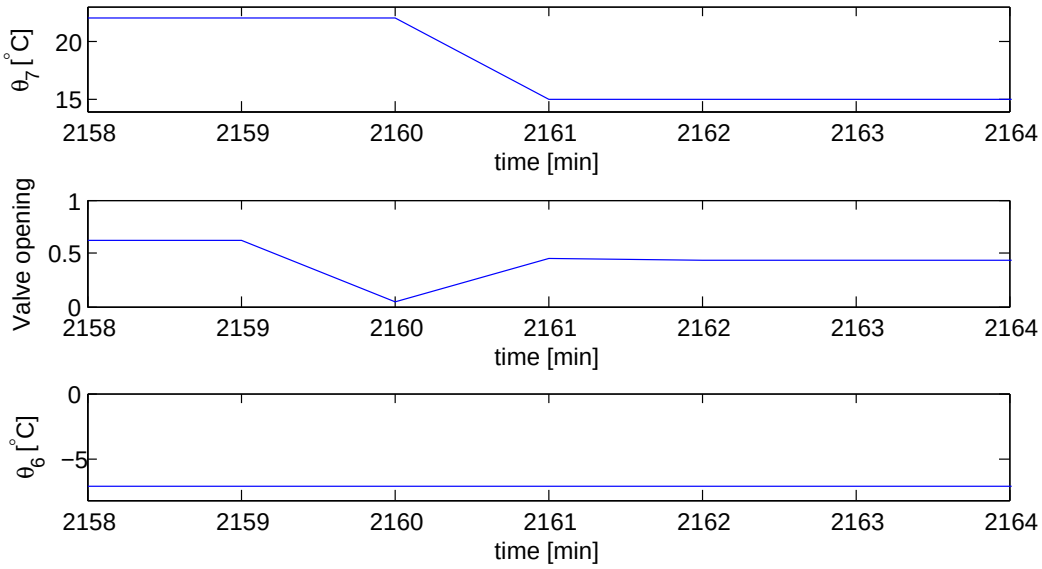

Figure 3.4: Ventilation-air temperature (θ_7), control-valve opening, and outdoor temperature (θ_6) (from day to night).

Figure 3.5 presents the corresponding temperature responses when the system switches from day mode to night mode. In room A, the indoor temperature drops from 21 $°C$ to 17 $°C$ in about 128 minutes. As mentioned in Section 2.4.1, the radiator does not participate actively when the room is cooled, it drops to 17 $°C$ and does not get any lower. The supply air from the ventilation system is 15 $°C$ during the night (Figure 3.4), thus it takes explicit part in the cooling of the room. However, since the supply air is not colder than 15 $°C$ and because the building is well insulated, the cooling process is slower than the heating process. As seen during the heating process, the cooling process is slower for room B and room C than it is for room A. Again, this is because of the different sizes of the 3 rooms. θ_{2B} settles at 17 $°C$ after approximately 160 minutes, while θ_{2C} settles at 17 $°C$ after about 300 minutes.

During night mode it is even more evident that the supply temperature seem higher than necessary. θ is about 50 $°C$ higher than the radiator temperatures, nor the ventilation system is dependent of such a high supply temperature. The supply water is studied in more detail in the following section.

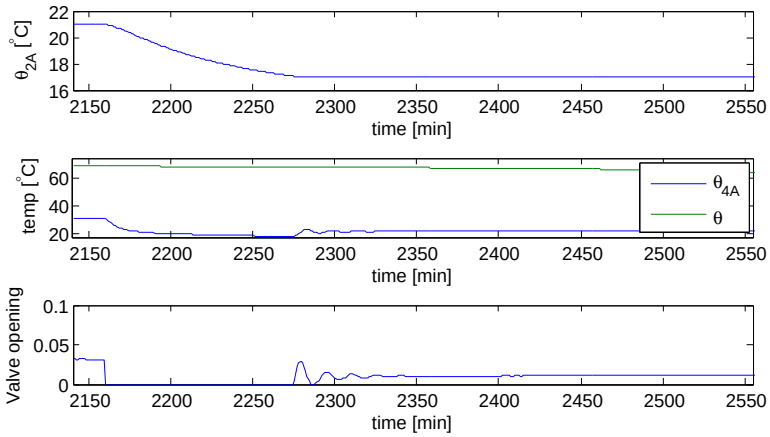

(a) Room A.

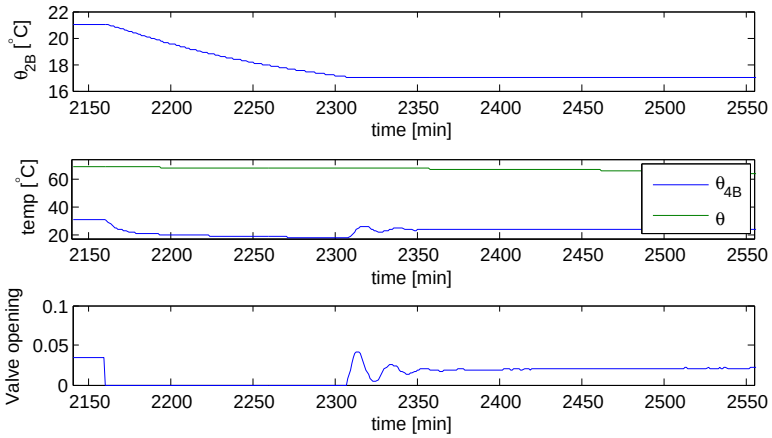

(b) Room B.

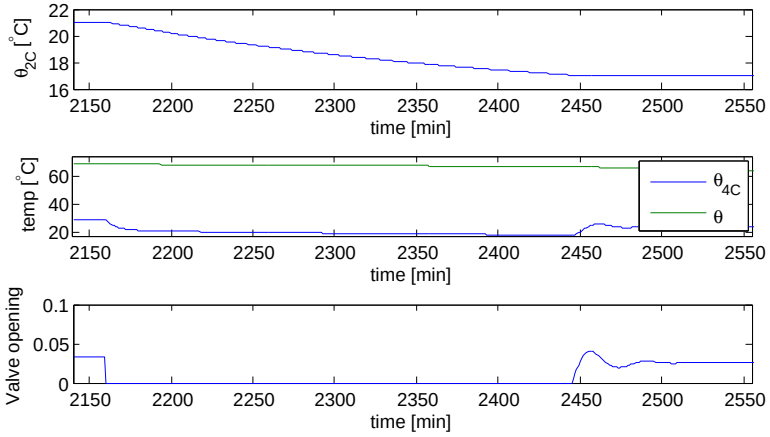

(c) Room C.

Figure 3.5: Indoor temperature (θ_2), radiator temperature (θ_4), supply-water temperature (θ), and control-valve opening of the radiator (from day to night).

Supply water

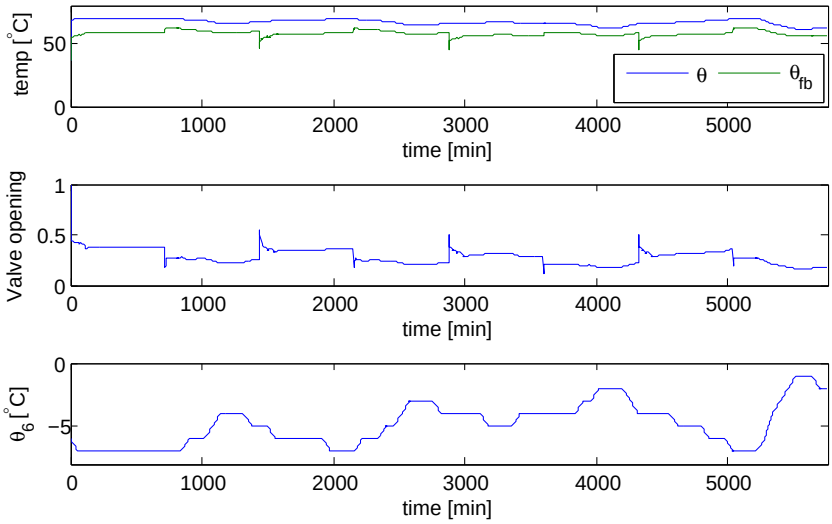

Figure 3.6: Supply-water temperature (θ), water temperature returned from the building (θ_{fb}), control-valve opening in the heat exchanger (%), and outdoor temperature (θ_6) (during 4 days).

As seen in Figure 3.6, a lot of the supplied heat (θ) is returned and sent back into the heat exchanger (θ_{fb}). Therefore, the actual energy consumption is not as high as the supplied heat alone may convey. The supply-water temperature is strictly dependent of the outdoor temperature (θ_6) as mentioned above (see Figure 3.1), and the supply-water temperature varies between 61 $^{\circ}C$ and 70 $^{\circ}C$ during 4 days. θ_{fb} has a larger dynamic area and fluctuates between 62 $^{\circ}C$ and 45 $^{\circ}C$. This makes sense because θ_{fb} depends on how much energy that is used in the system, and this energy amount differs during heating and cooling processes. The energy consumption will be studied in more detail in Chapter 5 after the MPC set-point determination has been introduced.

Chapter 4

Model Predictive Control

The focus until now has been to model a segment of an office building with a waterborne heating system. The system has been simulated with internal temperature controllers and a conventional control regime of the supply water temperature. This conventional strategy determines set-point temperatures on the basis of the outdoor temperature. However, if Figure 3.5 and Figure 3.3 are examined, the reader should be able to see that the radiators do not exploit all the available energy in the water. To obtain an optimal value for θ_{ref}, a Model Predictive Control (MPC) scheme will be introduced. This introduction is taken partly from Magnussen [2010], and it is based on Maciejowski [2002] and Imsland [2007].

4.1 Introduction to MPC

MPCs are becoming increasingly common nowadays, and the control scheme is preferred because

- it uses a process model (may be multivariable and nonlinear) to predict the future behavior,
- it handles constraints on input variables (manipulated variables) and states,
- and it uses mathematical programming to optimize future behavior.

Being able to place constraints on the manipulated variables and states makes it possible to find the most profitable operation, or in this case, minimize the energy consumption. The optimal solution is often found on a constraint.

Constraints on the manipulated variables involve adjustment limits on valves, and staying within given flow rates in pipes.

Depending on the complexity of the process, both linear and nonlinear MPCs may be implemented. Nonlinear MPCs are more complex and time consuming than linear MPCs when it comes to both the modeling and calculation complexity. Nevertheless, they are necessary if e.g. the process has several operating points (Imsland [2007]). The model derived in Chapter 2 consists mainly of first-order transfer functions, except from the shunt connections in the ventilation and district-heating system. Before implementing the controller, the total `Simulink` model will be linearized, such that a linear MPC can be used. Accurate valve dynamics in the shunt connections is not important in this thesis, which implies that the nonlinear version is not necessary to implement.

In linear MPCs, linear state-space models are used, and they are written in a discrete form

$$\boldsymbol{x}(k+1) = \boldsymbol{A_d}\boldsymbol{x}(k) + \boldsymbol{B_d}\boldsymbol{u}(k), \tag{4.1}$$
$$\boldsymbol{y}(k) = \boldsymbol{C_{dy}}\boldsymbol{x}(k), \tag{4.2}$$
$$\boldsymbol{z}(k) = \boldsymbol{C_{dz}}\boldsymbol{x}(k), \tag{4.3}$$

where $\boldsymbol{x}$ is a n-dimentional state vector, $\boldsymbol{u}$ is an l-dimentional input vector, $\boldsymbol{y}$ is an m_y-dimentional vector of measured outputs, and $\boldsymbol{z}$ is an m_z-dimentional vector of outputs which are to be controlled. In this thesis, all the measured outputs in the system are going to be controlled, $\boldsymbol{C_{dy}} = \boldsymbol{C_{dz}} = \boldsymbol{C_d}$.

The objective function (also called the cost function) penalizes deviations between the predicted controlled outputs, and a reference trajectory (desired value). This is done at every time-step, k. The objective function may be defined as

$$\boldsymbol{V}(k) = \sum_{i=H_w}^{H_p} \|\hat{z}(k+i|k) - r(k+i)\|^2_{\boldsymbol{Q}(i)} + \sum_{i=0}^{H_u-1} \|\Delta\hat{u}(k+i|k)\|^2_{\boldsymbol{R}(i)}.^{1} \tag{4.4}$$

H_w, H_p and H_u are the Window Horizon (WH), Prediction Horizon (PH) and Control Horizon (CH), respectively. The optimization starts at WH. The behavior of the system is predicted until PH, while optimal inputs are calculated until CH. It is assumed that $H_u \leq H_p$ and $H_w \leq i \leq H_p$. $\hat{\boldsymbol{z}}(k+i|k)$ denotes the predicted controlled outputs, $r(k+i)$ the reference trajectory, and $\Delta\hat{u}(k+i|k)$ the change of the controlled inputs.

[1] The norm that is used here is defined by Khalil [2002]: $\|v\|_2 = [\sum_i \sigma_i]^{1/2}$.

The objective function has a form that leads to penalization of the error vector $(\hat{z}(k+i|k) - r(k+i))$ and penalization of the change of control input $(\Delta\hat{u}(k+i|k))$ at each time-step, k. The penalties are determined by the weight matrices, $\boldsymbol{Q}$ and $\boldsymbol{R}$, which are

$$\boldsymbol{Q} = diag\left[Q_{11}, Q_{22}, \cdots, Q_{H_p}\right] \tag{4.5}$$

$$\boldsymbol{R} = diag\left[R_{11}, R_{22}, \cdots, R_{H_u-1}\right]. \tag{4.6}$$

$\boldsymbol{Q} \geq 0$ and $\boldsymbol{R} \geq 0$. Values of H_w, H_p, H_u, $\boldsymbol{Q}$ and $\boldsymbol{R}$ are tuning parameters since they all affect the closed-loop behavior of the plant (Maciejowski [2002]).

The objective function (4.4) can be rewritten in the following manner:

$$\boldsymbol{V}(k) = \left[\boldsymbol{Z}(k) - \boldsymbol{T}(k)\right]^T \boldsymbol{Q}\left[\boldsymbol{Z}(k) - \boldsymbol{T}(k)\right] + \boldsymbol{\Delta U}(k)^T \boldsymbol{R}\boldsymbol{\Delta U}(k), \tag{4.7}$$

where

$$\boldsymbol{Z}(k) = \begin{bmatrix} \hat{z}(k+H_w|k) \\ \vdots \\ \hat{z}(k+H_p|k) \end{bmatrix}, \tag{4.8}$$

$$\boldsymbol{T}(k) = \begin{bmatrix} \hat{r}(k+H_w|k) \\ \vdots \\ \hat{r}(k+H_p|k) \end{bmatrix}, \tag{4.9}$$

$$\boldsymbol{\Delta U(k)} = \begin{bmatrix} \Delta\hat{u}(k|k) \\ \vdots \\ \Delta\hat{u}(k+H_u-1|k) \end{bmatrix}. \tag{4.10}$$

If $\boldsymbol{Z}(k)$ is written on a compact form

$$\boldsymbol{Z}(k) = \boldsymbol{\Psi}\hat{\boldsymbol{x}}(k) + \boldsymbol{\Upsilon}\boldsymbol{u}(k-1) + \boldsymbol{\Theta\Delta U(k)}, \tag{4.11}$$

$\boldsymbol{\Psi}$, $\boldsymbol{\Upsilon}$ and $\boldsymbol{\Theta}$ are found by using (2.66) and (2.70) in Maciejowski [2002]. They become

$$\boldsymbol{\Psi} = \begin{bmatrix} \boldsymbol{C_d} & 0 & \cdots & 0 \\ 0 & \boldsymbol{C_d} & \cdots & 0 \\ \vdots & \vdots & \ddots & \vdots \\ 0 & 0 & \cdots & \boldsymbol{C_d} \end{bmatrix} \begin{bmatrix} \boldsymbol{A_d} \\ \vdots \\ \boldsymbol{A_d}^{H_u} \\ \vdots \\ \boldsymbol{A_d}^{H_p} \end{bmatrix}, \tag{4.12}$$

$$\boldsymbol{\Upsilon} = \begin{bmatrix} \boldsymbol{C_d} & 0 & \cdots & 0 \\ 0 & \boldsymbol{C_d} & \cdots & 0 \\ \vdots & \vdots & \ddots & \vdots \\ 0 & 0 & \cdots & \boldsymbol{C_d} \end{bmatrix} \begin{bmatrix} \boldsymbol{B_d} \\ \vdots \\ \sum_{i=0}^{H_u-1} \boldsymbol{A_d}^i \boldsymbol{B_d} \\ \vdots \\ \sum_{i=0}^{H_p-1} \boldsymbol{A_d}^i \boldsymbol{B_d} \end{bmatrix}, \tag{4.13}$$

and

$$\boldsymbol{\Theta} = \begin{bmatrix} \boldsymbol{C_d} & 0 & \cdots & 0 \\ 0 & \boldsymbol{C_d} & \cdots & 0 \\ \vdots & \vdots & \ddots & \vdots \\ 0 & 0 & \cdots & \boldsymbol{C_d} \end{bmatrix} \begin{bmatrix} \boldsymbol{B_d} & \cdots & 0 \\ \boldsymbol{A_d B_d} + \boldsymbol{B_d} & \cdots & 0 \\ \vdots & \ddots & \vdots \\ \sum_{i=0}^{H_u-1} \boldsymbol{A_d}^i \boldsymbol{B_d} & \cdots & \boldsymbol{B_d} \\ \vdots & \vdots & \vdots \\ \sum_{i=0}^{H_p-1} \boldsymbol{A_d}^i \boldsymbol{B_d} & \cdots & \sum_{i=0}^{H_p-H_u} \boldsymbol{A_d}^i \boldsymbol{B_d} \end{bmatrix}. \quad (4.14)$$

The tracking error matrix ($\boldsymbol{\varepsilon}$) is defined as

$$\boldsymbol{\varepsilon}(k) = \boldsymbol{T}(k) - \boldsymbol{\Psi}\hat{\boldsymbol{x}}(k) - \boldsymbol{\Upsilon}u(k-1). \quad (4.15)$$

This tracking error is the difference between the future target trajectory, and the free response of the system[2]. However, the purpose of the MPC in this thesis is to minimize θ_{ref}. This means that all the diagonal elements in $\boldsymbol{Q}$ will be set to 0 because there is no desired trajectory to follow. As the reader should be aware of, the system input $u(k)$ is not present in the objective function (4.7). If the input-minimization objective is taken into account and if the system input is included, the objective function can be rewritten as

$$\boldsymbol{V}(k) = \boldsymbol{\Delta U}(k)^T \boldsymbol{R} \boldsymbol{\Delta U}(k) + \tilde{\boldsymbol{Z}}(k)^T \boldsymbol{S} \tilde{\boldsymbol{Z}}(k), \quad (4.16)$$

where

$$\boldsymbol{S} = diag\left[S_{11}, S_{22}, \cdots, S_{H_p}\right] \quad (4.17)$$

is an additional tuning parameter. $\tilde{\boldsymbol{Z}}$ is introduced such that u can be included in the objective function.

Example 4.1 Decide $\tilde{\boldsymbol{Z}}$

From Maciejowski [2002], $\hat{u}$ can be written as

$$\hat{u}(k+i-1|k) = u(k-1) + \sum_{j=0}^{i-1} \Delta\hat{u}(k+j|k). \quad (4.18)$$

If this sum is written out for $i = 1, 2, \cdots, H_u$, a pattern evolves. This pattern will result in matrices that are going to be used in the objective function. For $i = 1$,

$$\hat{u}(k|k) = u(k-1) + \Delta\hat{u}(k|k) \quad (4.19)$$

[2]The free response is the response over PH if no input changes are made $\Rightarrow \boldsymbol{\Delta U}(k) = 0$.

and for $i = 2$

$$\hat{u}(k+1|k) = u(k-1) + \Delta\hat{u}(k|k) + \Delta\hat{u}(k+1|k). \tag{4.20}$$

This should be done until $i = H_u$*, but it is not necessary to include more terms to see the pattern.*

$$\hat{u}(k) = \begin{bmatrix} 1 & 0 & \cdots & 0 \\ 1 & 1 & \cdots & 0 \\ \vdots & \vdots & \ddots & \vdots \\ 1 & 1 & \cdots & 1 \end{bmatrix} \begin{bmatrix} \Delta\hat{u}(k|k) \\ \Delta\hat{u}(k+1|k) \\ \vdots \\ \Delta\hat{u}(k+H_u-1|k) \end{bmatrix} + \begin{bmatrix} 1 \\ 1 \\ \vdots \\ 1 \end{bmatrix} u(k-1) \tag{4.21}$$

$\hat{u}(k|k)$ *can then be included in the objective function by defining*

$$\tilde{\boldsymbol{Z}}(k) = \hat{u}(k|k) = \vartheta\Delta u(k) + \chi u(k-1). \tag{4.22}$$

4.1.1 Feedforward - anticipate and cancel the disturbances

It is common with anticipation and removal of certain disturbances when designing control systems. Feedforward control can actually be more efficient than feedback control, because it is not necessary to wait until the disturbance has affected the system before it can be removed (as is the case in feedback control). In order for this to be possible, measurements have to be made, or a model of the disturbance must be available. Examples of disturbances that can be removed by feedforward control are wind in dynamic positioning systems on boats, or outdoor temperature in building-control systems. The reader should be aware of the demands that have to be fulfilled in order for feedforward control to be possible:

- A reliable measurement, or a reliable model of the disturbance has to exist,
- and the measurement has to be processed fast enough.

If one were to cancel the disturbances totally, the performance from disturbances to outputs would have to be known perfectly. Since this is rarely the case in industrial systems, feedforward control is most often combined

with feedback control. The feedback part then removes the part of the disturbance that is not taken care of by the feedforward, in addition to unmeasured disturbances that affect the system.

Including feedforward into the MPC formulation is straightforward. The only thing that has to be done is to include the effects of the disturbances into the predictions (4.3). In this thesis, a weather forecast from `www.yr.no` is used in the feedforward instead of measured disturbances. It is assumed that the weather predictions are perfect, such that the weather presented in Section 2.5 is used to generate the feedforward in the MPC formulation. Recall that the outdoor temperatures acting on the system always are generated by Algorithm 1.

$$\boldsymbol{x}(k+1) = \boldsymbol{A_d}\boldsymbol{x}(k) + \boldsymbol{B_d}\boldsymbol{u}(k) + \boldsymbol{B_d^d}\boldsymbol{d}(k) \tag{4.23}$$

shows how feedforward is included into the model. The disturbance term in (4.23) leads to an expansion of (4.11)

$$\boldsymbol{Z}(k) = \boldsymbol{\Psi}\hat{\boldsymbol{x}}(k) + \boldsymbol{\Upsilon}\boldsymbol{u}(k-1) + \boldsymbol{\Theta}\boldsymbol{\Delta U(k)} + \boldsymbol{\Xi}\boldsymbol{D_m}(k), \tag{4.24}$$

where

$$\boldsymbol{D_m}(k) = \begin{bmatrix} \boldsymbol{d}(k) \\ \hat{\boldsymbol{d}}(k+1|k) \\ \vdots \\ \hat{\boldsymbol{d}}(k+H_p-1|k) \end{bmatrix} \tag{4.25}$$

and

$$\boldsymbol{\Xi} = \begin{bmatrix} \boldsymbol{C_d}\boldsymbol{B_d^d} & 0 & \cdots & 0 \\ \boldsymbol{C_d}\boldsymbol{A_d}\boldsymbol{B_d^d} & \boldsymbol{C_d}\boldsymbol{B_d^d} & \cdots & 0 \\ \vdots & \vdots & \ddots & \vdots \\ \boldsymbol{C_d}\boldsymbol{A_d}^{H_p-1}\boldsymbol{B_d^d} & \boldsymbol{C_d}\boldsymbol{A_d}^{H_p-2}\boldsymbol{B_d^d} & \cdots & \boldsymbol{C_d}\boldsymbol{B_d^d} \end{bmatrix}. \tag{4.26}$$

The matrices $\boldsymbol{\Psi}$, $\boldsymbol{\Upsilon}$ and $\boldsymbol{\Theta}$ remain unchanged. The output predictions will be affected by the designer's assumptions about the future disturbance behavior. If the disturbance is measured, the most common thing to do is to assume that the disturbance remains constant after the last measurement. That is $\boldsymbol{d}(k) = \hat{\boldsymbol{d}}(k+1|k) = \cdots = \hat{\boldsymbol{d}}(k+H_p-1|k)$. However, since Algorithm 1 is used to generate a perfect weather forecast, equation (4.25) is filled with H_p temperature predictions.

4.1.2 Defining the constraints

To complete the MPC definition, the constraints have to be included. They can be written as

$$\boldsymbol{E}\begin{bmatrix}\boldsymbol{\Delta U}(k)\\1\end{bmatrix} \leq 0 \Leftrightarrow -\Delta u_{min} \leq \Delta u \leq \Delta u_{max}, \tag{4.27}$$

$$\boldsymbol{F}\begin{bmatrix}\boldsymbol{U}(k)\\1\end{bmatrix} \leq 0 \Leftrightarrow u_{min} \leq u \leq u_{max}, \tag{4.28}$$

$$\boldsymbol{Z}\begin{bmatrix}\boldsymbol{Z}(k)\\1\end{bmatrix} \leq 0 \Leftrightarrow z_{min} \leq z \leq z_{max}. \tag{4.29}$$

These inequalities are rewritten as

$$\begin{bmatrix}\boldsymbol{F}\\ \boldsymbol{\Gamma\Theta}\\ \boldsymbol{W}\end{bmatrix}\boldsymbol{\Delta U}(k) \leq \begin{bmatrix}-\boldsymbol{F_1}u(k-1)-\boldsymbol{f}\\ -\boldsymbol{\Gamma}\left(\boldsymbol{\Psi}\hat{\boldsymbol{x}}(k)+\boldsymbol{\Upsilon}u(k-1)+\boldsymbol{\Xi D_m}(k)\right)-\boldsymbol{g}\\ \boldsymbol{w}\end{bmatrix}. \tag{4.30}$$

See Section 3.2.1 in Maciejowski [2002] for details.

Example 4.2 How to decide the input-constraint matrices $\boldsymbol{F}$, $\boldsymbol{f}$ and $\boldsymbol{F_1}$

It is desirable to have the constraints on the form given in (4.30). In order to achieve this, $\hat{u}(k)$ is written as in Example 4.1

$$\hat{u}(k+i-1|k) = u(k-1) + \sum_{j=0}^{i-1}\Delta\hat{u}(k+j|k). \tag{4.31}$$

The system input in this MPC scheme is θ_{ref}, and since the conventional strategy introduced in Chapter 3 is no longer going to be used, θ_{ref} is given a maximum value of 80 °C and a minimum value of 20 °C. When these values are included, the reader should be able to recognize a pattern.

$$20 \leq \hat{u}(k|k) \Rightarrow 20 \leq u(k-1)+\Delta\hat{u}(k|k) \Rightarrow -\Delta\hat{u}(k|k) \leq u(k-1)-20 \tag{4.32}$$

$$\hat{u}(k|k) \leq 80 \Rightarrow u(k-1)+\Delta\hat{u}(k|k) \leq 80 \Rightarrow \Delta\hat{u}(k|k) \leq -u(k-1)+80 \tag{4.33}$$

for $i = 1$,

$$20 \leq \hat{u}(k+1|k) \Rightarrow 20 \leq u(k-1) + \Delta\hat{u}(k|k) + \Delta\hat{u}(k+1|k) \quad (4.34)$$
$$\Rightarrow -\Delta\hat{u}(k|k) - \Delta\hat{u}(k+1|k) \leq u(k-1) - 20 \quad (4.35)$$
$$\hat{u}(k+1|k) \leq 80 \Rightarrow u(k-1) + \Delta\hat{u}(k|k) + \Delta\hat{u}(k+1|k) \leq 80 \quad (4.36)$$
$$\Rightarrow \Delta\hat{u}(k|k) + \Delta\hat{u}(k+1|k) \leq -u(k-1) + 80 \quad (4.37)$$

for $i = 2$. *The constraints on* $\hat{u}(k)$ *can now be written on the desired form.*

$$\begin{bmatrix} -1 & 0 & 0 & \cdots & 0 \\ 1 & 0 & 0 & \cdots & 0 \\ -1 & -1 & 0 & \cdots & 0 \\ 1 & 1 & 0 & \cdots & 0 \\ \vdots & \vdots & \vdots & \ddots & \vdots \\ -1 & -1 & -1 & \cdots & -1 \\ 1 & 1 & 1 & \cdots & 1 \end{bmatrix} \begin{bmatrix} \Delta\hat{u}(k|k) \\ \Delta\hat{u}(k+1|k) \\ \vdots \\ \Delta\hat{u}(k+H_u-1|k) \end{bmatrix} \leq \begin{bmatrix} 1 \\ -1 \\ 1 \\ -1 \\ \vdots \\ 1 \\ -1 \end{bmatrix} u(k-1) + \begin{bmatrix} -20 \\ 80 \\ -20 \\ 80 \\ \vdots \\ -20 \\ 80 \end{bmatrix} \quad (4.38)$$

The change of input is also penalized and $\boldsymbol{W}$ and $\boldsymbol{w}$ are derived in the same manner as the example above. The input is constrained so that the MPC cannot impress input changes larger than 5 and smaller than -5, $-5 \leq \Delta u(k) \leq 5$.

Example 4.3 How to decide the output-constraint matrices $\boldsymbol{\Gamma}$ and $\boldsymbol{g}$

There are four system outputs in the system that need to get constrained, and these are $\theta_{2A}, \theta_{2B}, \theta_{2C}$ *and* θ_7. *Their desired values are defined in Section 2.1. Since the temperatures have two different desired values during a day, two optimization problems have to be solved to fulfill these demands.*

$$\boldsymbol{z}_1^{min} \leq \boldsymbol{Z} \quad (4.39)$$
$$[21, 21, 21, 22]^T \leq \boldsymbol{Z} \quad (4.40)$$

the first 12 *hours and*

$$\boldsymbol{z}_2^{min} \leq \boldsymbol{Z} \quad (4.41)$$
$$[17, 17, 17, 15]^T \leq \boldsymbol{Z} \quad (4.42)$$

the last 12 *hours during a day.* $\boldsymbol{Z}$ *is given by (4.24). Together, (4.40), (4.42) and (4.24) result in constraints on the correct form*

$$\boldsymbol{\Gamma\Theta\Delta U}(k) \leq -\boldsymbol{\Gamma}\left(\boldsymbol{\Psi}\hat{\boldsymbol{x}}(k) + \boldsymbol{\Upsilon}u(k-1) + \boldsymbol{\Xi D_m}(k)\right) - \boldsymbol{g}. \tag{4.43}$$

If (4.40) is written out as in Example 4.2, a pattern evolves such that $\boldsymbol{\Gamma}$ *and* $\boldsymbol{g}$ *can be found.*

$$\begin{aligned}
\boldsymbol{z}_1^{min} &\leq \boldsymbol{Z}(k|k) && (4.44)\\
\boldsymbol{z}_1^{min} &\leq \boldsymbol{\Psi}\hat{\boldsymbol{x}}(k|k) + \boldsymbol{\Upsilon u}(k-1) \\
&\quad + \boldsymbol{\Theta\Delta U}(k|k) + \boldsymbol{\Xi D_m}(k) && (4.45)\\
-\boldsymbol{\Theta\Delta U}(k|k) &\leq \boldsymbol{\Psi}\hat{\boldsymbol{x}}(k|k) + \boldsymbol{\Upsilon u}(k-1) + \boldsymbol{\Xi D_m}(k) - \boldsymbol{z}_1^{min} && (4.46)
\end{aligned}$$

for $i = 1$.

$$\begin{aligned}
\boldsymbol{z}_1^{min} &\leq \boldsymbol{Z}(k+1|k) && (4.47)\\
\boldsymbol{z}_1^{min} &\leq \boldsymbol{\Psi}\hat{\boldsymbol{x}}(k+1|k) + \boldsymbol{\Upsilon u}(k-1) \\
&\quad + \boldsymbol{\Theta\Delta U}(k+1|k) + \boldsymbol{\Xi D_m}(k+1) && (4.48)\\
-\boldsymbol{\Theta\Delta U}(k+1|k) &\leq \boldsymbol{\Psi}\hat{\boldsymbol{x}}(k+1|k) + \boldsymbol{\Upsilon u}(k-1) \\
&\quad + \boldsymbol{\Xi D_m}(k+1) - \boldsymbol{z}_1^{min} && (4.49)
\end{aligned}$$

for $i = 2$.

The pattern reveals itself clearly, and the matrices can be written out

$$\boldsymbol{\Gamma} = \begin{bmatrix} -I & 0 & \cdots & 0 \\ 0 & -I & \cdots & 0 \\ \vdots & \vdots & \ddots & \vdots \\ 0 & 0 & \cdots & -I \end{bmatrix}, \tag{4.50}$$

and

$$\boldsymbol{g} = \begin{bmatrix} [21 & 21 & 21 & 22], & \cdots, & \boldsymbol{z_1^{min}} \end{bmatrix}^T. \tag{4.51}$$

When 12 *hours have past, the constraint changes from* $\boldsymbol{z}_1^{min}$ *to* $\boldsymbol{z}_2^{min}$. *Except from this, the calculations are identical.*

Algorithm

Before defining the optimization algorithm, the objective function (4.7) is written out (recall that $diag\left[Q_{11}, Q_{22}, \cdots, Q_{H_p}\right] = 0$)

$$\begin{aligned}
\boldsymbol{V}(k) &= \boldsymbol{Z}(k)^T \boldsymbol{Q} \boldsymbol{Z}(k) + \boldsymbol{\Delta U}(k)^T \boldsymbol{R} \boldsymbol{\Delta U}(k) + \tilde{\boldsymbol{Z}}(k)^T \boldsymbol{S} \tilde{\boldsymbol{Z}}(k) && (4.52)\\
&= \boldsymbol{\Delta U}(k)^T \boldsymbol{R} \boldsymbol{\Delta U}(k) \\
&\quad + \left[\boldsymbol{\vartheta} \boldsymbol{\Delta U}(k) + \boldsymbol{\chi} u(k-1)\right]^T \boldsymbol{S} \left[\boldsymbol{\vartheta} \boldsymbol{\Delta U}(k) + \boldsymbol{\chi} u(k-1)\right] && (4.53)\\
&= \boldsymbol{\Delta U}(k)^T \boldsymbol{\vartheta}^T \boldsymbol{S} \boldsymbol{\vartheta} \boldsymbol{\Delta U}(k) + 2 \boldsymbol{\Delta U}(k)^T \boldsymbol{\vartheta}^T \boldsymbol{S} \boldsymbol{\chi} u(k-1) \\
&\quad + u(k-1)^T \boldsymbol{\chi}^T \boldsymbol{S} \boldsymbol{\chi} u(k-1) && (4.54)\\
&= \boldsymbol{\Delta U}(k)^T \left[\boldsymbol{R} + \boldsymbol{\vartheta}^T \boldsymbol{S} \boldsymbol{\vartheta}\right] \boldsymbol{\Delta U}(k) + 2 \boldsymbol{\Delta U}(k)^T \boldsymbol{\vartheta}^T \boldsymbol{S} \boldsymbol{\chi} u(k-1) \\
&\quad + u(k-1)^T \boldsymbol{\chi}^T \boldsymbol{S} \boldsymbol{\chi} u(k-1) && (4.55)
\end{aligned}$$

which is on the form

$$\boldsymbol{V}(k) = const \cdot \boldsymbol{I} + \boldsymbol{\Delta U}(k)^T \boldsymbol{G} + \boldsymbol{\Delta U}(k)^T \boldsymbol{H} \boldsymbol{\Delta U}(k), \tag{4.56}$$

where $\boldsymbol{G}$ can be defined as

$$\boldsymbol{G} = 2 \boldsymbol{\vartheta}^T \boldsymbol{S} \boldsymbol{\chi} u(k-1), \tag{4.57}$$

and $\boldsymbol{H}$ can be defined as

$$\boldsymbol{H} = 2 \left[\boldsymbol{R} + \boldsymbol{\vartheta}^T \boldsymbol{S} \boldsymbol{\vartheta}\right]. \tag{4.58}$$

With these definitions, the form of the optimization problem becomes equal to a regular quadratic programming problem (Maciejowski [2002]):

$$\min \frac{1}{2} \boldsymbol{\Delta U}(k)^T \boldsymbol{H} \boldsymbol{\Delta U}(k) + \boldsymbol{\Delta U}(k)^T \boldsymbol{G} \tag{4.59}$$

subject to

$$\begin{bmatrix} \boldsymbol{F} \\ \boldsymbol{\Gamma\Theta} \\ \boldsymbol{W} \end{bmatrix} \boldsymbol{\Delta U}(k) \leq \begin{bmatrix} -F_1 u(k-1) - \boldsymbol{f} \\ -\boldsymbol{\Gamma} \left[\boldsymbol{\Psi} \hat{\boldsymbol{x}}(k) + \boldsymbol{\Upsilon} u(k-1) + \boldsymbol{\Xi} \boldsymbol{D_m}(k)\right] - \boldsymbol{g} \\ \boldsymbol{w} \end{bmatrix} \tag{4.60}$$

This is clearly a quadratic programming (QP) problem. Imsland [2007] states the key elements in the optimization.

1. Solve the QP problem at time-step (k) to obtain an optimal, feasible input sequence.
2. Apply the first input in the input sequence ($u(1)$, $u(2)$, $\cdots u(H_u - 1)$) to the process.
3. Set $k = k + 1$, and go to step 1.

4.2 Necessary preparations

Before running the system with an MPC controller, there are some preparations that have to be done. The first step is to obtain a discrete linear representation of the system. The MPC controller needs the model to be able to predict the future behavior of the plant (Qin and Badgwell [2003]). However, it should be noticed that discrete time models are not necessary, a continuous model can also be used. According to Maciejowski [2002], all that is needed is to know the step-responses in the coincidence points[3], and it is necessary to be able to compute the free response at the coincidence points. Nevertheless, a discrete time model is used in this thesis. Before discretizing the model, it has to be linearized.

4.2.1 Linearization

The model derived in Chapter 2 is nonlinear, and in order to implement an MPC control scheme, the system has to be linearized[4]. Egeland and Gravdahl [2002] define a nonlinear system as

$$\boldsymbol{x}(k+1) = \boldsymbol{f}(\boldsymbol{x}, \boldsymbol{u}, k) \tag{4.61}$$
$$\boldsymbol{y}(k) = \boldsymbol{h}(\boldsymbol{x}, \boldsymbol{u}, k), \tag{4.62}$$

given that $\boldsymbol{f}$ and (or) $\boldsymbol{h}$ is nonlinear. Linearization is done around a solution of the system, often referred to as an operating point (Egeland and Gravdahl [2002]). This operating point is a solution of the system $(\boldsymbol{x}_0(k), \boldsymbol{u}_0(k))$ that satisfy

$$\boldsymbol{x}_0(k+1) = \boldsymbol{f}[\boldsymbol{x}_0, \boldsymbol{u}_0, k], \tag{4.63}$$

which is the system equation (Egeland and Gravdahl [2002]). If the perturbations $\boldsymbol{\Delta x}, \boldsymbol{\Delta u}$ and $\boldsymbol{\Delta y}$ are defined from the operating point

$$\boldsymbol{x}(k) = \boldsymbol{x}_0(k) + \boldsymbol{\Delta x}(k) \tag{4.64}$$
$$\boldsymbol{u}(k) = \boldsymbol{u}_0(k) + \boldsymbol{\Delta u}(k) \tag{4.65}$$
$$\boldsymbol{y}(k) = \boldsymbol{h}[\boldsymbol{x}_0(k), \boldsymbol{u}_0(k), k] + \boldsymbol{\Delta y}(k), \tag{4.66}$$

[3] At a coincidence point, the process output should be equal to a desired value.

[4] This is not the case for nonlinear MPC (NMPC), but this will not be elaborated in this thesis.

standard Taylor-series linearization around the operating point yield (Egeland and Gravdahl [2002])

$$\boldsymbol{x}(k+1) = \boldsymbol{f}[\boldsymbol{x}_0(k), \boldsymbol{u}_0(k), k] + \left.\frac{\partial \boldsymbol{f}}{\partial \boldsymbol{x}}\right|_{\boldsymbol{x}_0(k),\boldsymbol{u}_0(k)} \boldsymbol{\Delta x} + \left.\frac{\partial \boldsymbol{f}}{\partial \boldsymbol{u}}\right|_{\boldsymbol{x}_0(k),\boldsymbol{u}_0(k)} \boldsymbol{\Delta u}, \tag{4.67}$$

$$\boldsymbol{y}(k) = \boldsymbol{h}[\boldsymbol{x}_0(k), \boldsymbol{u}_0(k), k] + \left.\frac{\partial \boldsymbol{h}}{\partial \boldsymbol{x}}\right|_{\boldsymbol{x}_0(k),\boldsymbol{u}_0(k)} \boldsymbol{\Delta x} + \left.\frac{\partial \boldsymbol{h}}{\partial \boldsymbol{u}}\right|_{\boldsymbol{x}_0(k),\boldsymbol{u}_0(k)} \boldsymbol{\Delta u}. \tag{4.68}$$

The linearized state-space system is then defined as (citemodsim)

$$\boldsymbol{\Delta x}(k+1) = \overbrace{\left.\frac{\partial \boldsymbol{f}}{\partial \boldsymbol{x}}\right|_{\boldsymbol{x}_0(k),\boldsymbol{u}_0(k)}}^{\boldsymbol{A_d}} \boldsymbol{\Delta x} + \overbrace{\left.\frac{\partial \boldsymbol{f}}{\partial \boldsymbol{u}}\right|_{\boldsymbol{x}_0(k),\boldsymbol{u}_0(k)}}^{\boldsymbol{B_d}} \boldsymbol{\Delta u}, \tag{4.69}$$

$$\boldsymbol{\Delta y}(k) = \overbrace{\left.\frac{\partial \boldsymbol{h}}{\partial \boldsymbol{x}}\right|_{\boldsymbol{x}_0(k),\boldsymbol{u}_0(k)}}^{\boldsymbol{C_d}} \boldsymbol{\Delta x} + \overbrace{\left.\frac{\partial \boldsymbol{h}}{\partial \boldsymbol{u}}\right|_{\boldsymbol{x}_0(k),\boldsymbol{u}_0(k)}}^{\boldsymbol{D_d}} \boldsymbol{\Delta u}. \tag{4.70}$$

The linearization can easily be performed 'by hand' if the system is small and does not contain a large number of states. However, the system in this thesis is complex and contains 26 states. Fortunately, there exist `MATLAB` functions that can perform linearization. The system matrices are obtained by using `linmod(Simulink model)`. During the linearization, the nonlinearities should not get excited more than necessary, and therefore strongly discontinuous and nonlinear terms should be considered removed (Imsland [2011]). The operating point has to be chosen wisely in order for the linearized model to be accurate.

The heat exchanger and shunt connection in the district-heating part of the model is left out during the linearization, and there are two reasons why this can be done. (1) It is the behavior from θ to $\theta_{2A}, \theta_{2B}, \theta_{2C}, \theta_7$ (see Figure 2.11) that describes how different water temperatures affect the system outputs. The behavior from θ_{ref} to θ only describes the portion of main supply water and the portion of return water from the building that constitute the water that is sent into the building. The latter part is not necessary to describe the behavior from input to output sufficiently accurate. (2) The district-heating dynamics is removed because the `MATLAB` function that calculates θ_{fb} (Figure 2.9) contains logic that makes it discontinuous, and discontinuities are very hard to linearize (Imsland [2011]).

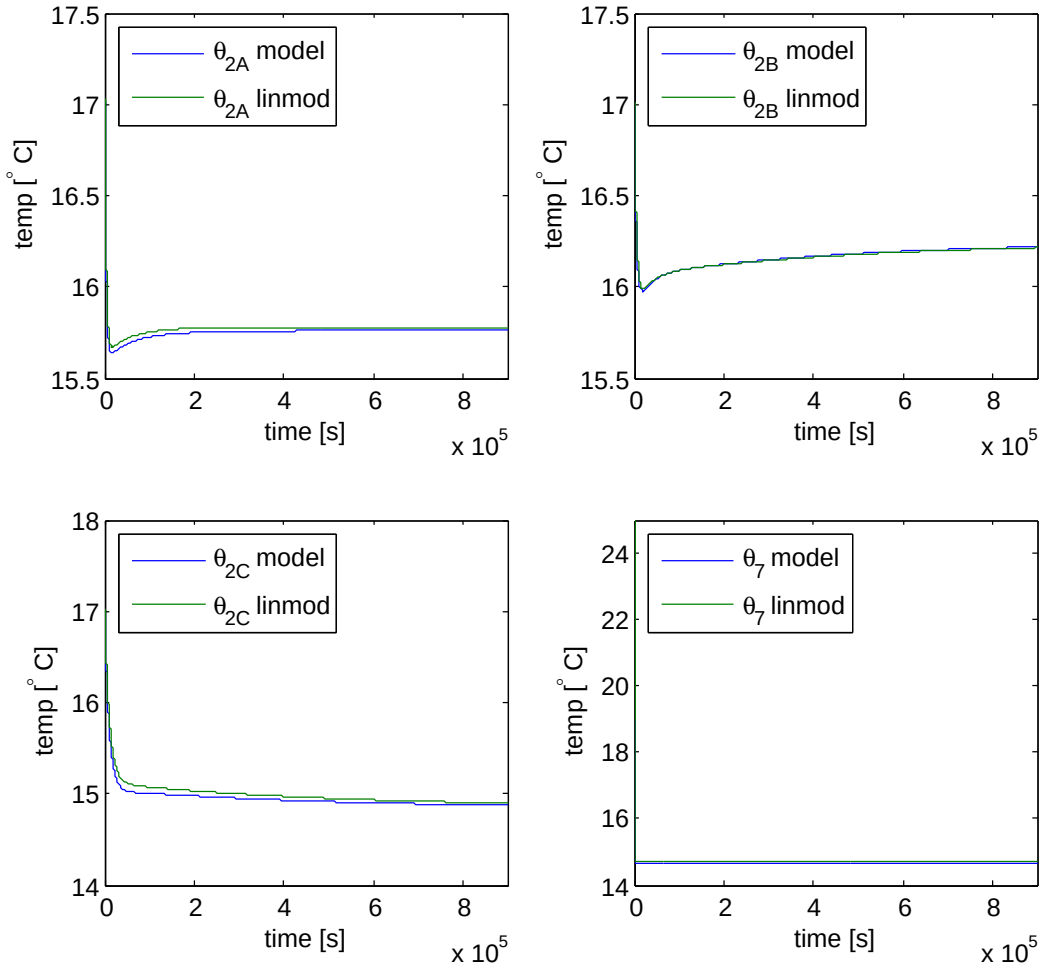

Figure 4.1: Behavior of $\theta_{2A}, \theta_{2B}, \theta_{2C}$ and θ_7 simulated with the Simulink model and the linmod() model.

In addition to the removal of the district-heating dynamics, the thermal radiation disturbances are removed and the internal controllers are chosen to be P controllers with small proportional gains, when linearizing the system. Again, this is done in order to not excite the nonlinearities in the system simultaneously as the number of states in the model is limited. The number of states in the linearized system is 17. The responses in Figure 4.1 do not coincide with the specified desired temperatures (see Section 2.1). However, they show that the system outputs respond equally to a given system input in both the linearized system and in the `Simulink` system. This indicates that the linearized model is accurate enough and can therefore be used further when implementing the MPC.

After the linearization, the system is discretized using the `MATLAB` function `c2d(sys, time step)`. The time step should be chosen small enough such that the faster dynamics also is described accurately in the discrete model. Since different time steps will be used in the state estimator and in the MPC, they will be presented and explained later.

4.2.2 Scaling

The matrices found during the linearization may have elements that differ greatly in magnitude, which makes them badly scaled (Nocedal and Wrigth [2006]). For example, $f(x) = x_1 + 10^7 x_2$ will be very sensitive to changes in x_2 compared to x_1, which makes it badly scaled. Since the performance of optimization algorithms is dependent on how the problem is formulated, scaling is an important issue (Nocedal and Wrigth [2006]). According to Skogestad and Postlethwaite [2008], a system can be scaled by making assumptions about expected disturbances, reference changes, allowed input variations and allowed output deviations in the system. The unscaled system can be formulated as in (4.3),

$$\boldsymbol{x}(k+1) = \boldsymbol{A_d}\boldsymbol{x}(k) + \boldsymbol{B_d}\boldsymbol{u}(k), \tag{4.71}$$

$$\boldsymbol{y}(k) = \boldsymbol{C_d}\boldsymbol{x}(k), \tag{4.72}$$

where $\boldsymbol{B_d}$ can be divided into one disturbance part and one input part

$$\boldsymbol{B_d}\boldsymbol{u}(k) = \boldsymbol{B_{du}}\boldsymbol{u}(k) + \boldsymbol{B_{dd}}\boldsymbol{d}(k). \tag{4.73}$$

$\boldsymbol{d}(k)$ contains the disturbances in the system.

A normal scaling approach is to make the variables less than 1 in magnitude, which is done by dividing each variable by its maximum expected or allowed value (Skogestad and Postlethwaite [2008]),

$$\boldsymbol{D_u^s} = u_{max}, \tag{4.74}$$

$$\boldsymbol{D_d^s} = diag\left(d_{1max}, \cdots, d_{nmax}\right)^T, \tag{4.75}$$

$$\boldsymbol{D_e^s} = diag\left(e_{1max}, \cdots, e_{4max}\right)^T. \tag{4.76}$$

u_{max} is the largest allowed input change, $d_{1max}, \cdots, d_{nmax}$ are the largest expected changes in disturbances, and $e_{1max}, \cdots, e_{4max}$ are the largest allowed control errors. The system in this thesis has 1 input (θ_{ref}) and 4 outputs ($\theta_{2A}, \theta_{2B}, \theta_{2C}$ and θ_7). That is a Single-Input-Multiple-Output (SIMO) system, which is a special case of a Multiple-Input-Multiple-Output (MIMO) system.

The scaled variables then become

$$\boldsymbol{u}^s = (\boldsymbol{D}_u^s)^{-1}\boldsymbol{u}, \tag{4.77}$$
$$\boldsymbol{d}^s = (\boldsymbol{D}_d^s)^{-1}\boldsymbol{d}, \tag{4.78}$$
$$\boldsymbol{y}^s = (\boldsymbol{D}_e^s)^{-1}\boldsymbol{y}, \tag{4.79}$$

and if this is inserted into (4.72), the scaled system becomes

$$\boldsymbol{x}(k+1) = \boldsymbol{A}_d\boldsymbol{x}(k) + \boldsymbol{B}_{du}\boldsymbol{D}_u^s\boldsymbol{u}^s(k) + \boldsymbol{B}_{dd}\boldsymbol{D}_d^s\boldsymbol{d}^s(k), \tag{4.80}$$
$$\boldsymbol{y}^s(k) = (\boldsymbol{D}_e^s)^{-1}\boldsymbol{C}_d\boldsymbol{x}(k). \tag{4.81}$$

As mentioned above, the number of states system in the linearized system is 17, and only 4 of them are being measured during simulation. In order for the MPC to work, all the states have to be included. This is done by using a state estimator. There are several different state estimators and among them are Luenberger observers, Wiener filters and Kalman filters. According to Simon [2006], the Kalman filter is the optimal estimator when the noise is Gaussian, and it is the optimal linear estimator if the noise is not Gaussion. A Kalman filter will therefore be implemented such that an estimate of the entire state vector can be included in the MPC.

4.3 Kalman Filter

This section will be based on Brown and Hwang [1997] and Simon [2006]. In the 1960s, R.E. Kalman formed an alternative solution of how to formulate a Minimum Mean-Square Error (MMSE) filtering problem using state-space methods, and his work was a contribution[5] to the Wiener filter that was formulated in the 1940s. One of the main features of the Kalman filter, the one that separates it from the Wiener filter, is that it is recursive (see Figure 4.2). The results from the previous step is used to obtain the desired results in the current step. Both the process noise and measurement noise have to be modeled as vectors such that the recursive estimation formulation is possible, and this denotes another important feature about the Kalman filter.

The filter can be defined both continuously and discrete. A discrete process may arise if several events occur naturally in discrete steps, or that a continuous signal is sampled at discrete steps. Nevertheless, most Kalman filters

[5]Kalman's work is not based on Wiener's, but it is an important contribution to MMSE filters.

are implemented in a discrete manner (Imsland [2011]). Process noise and measurement noise are added to the formulation in (4.3) when the Kalman filter equations are to be derived.

$$\boldsymbol{x}(k) = \boldsymbol{A_d}\boldsymbol{x}(k-1) + \boldsymbol{B_d}\boldsymbol{u}(k-1) + \boldsymbol{w}(k-1), \tag{4.82}$$
$$\boldsymbol{y}(k) = \boldsymbol{A_d}\boldsymbol{x}(k) + \boldsymbol{v}(k), \tag{4.83}$$

where the process noise and measurement noise ($\boldsymbol{w}$ and $\boldsymbol{v}$) are white, zero mean, uncorrelated, and have known covariance matrices $\boldsymbol{M}(k)$ and $\boldsymbol{N}(k)$.

$$\boldsymbol{w}(k) \sim (0, \boldsymbol{M}(k)), \tag{4.84}$$
$$\boldsymbol{v}(k) \sim (0, \boldsymbol{N}(k)), \tag{4.85}$$
$$E[\boldsymbol{w}(k)\boldsymbol{w}(j)^T] = \boldsymbol{M}(k)\delta_{k-j}, \tag{4.86}$$
$$E[\boldsymbol{v}(k)\boldsymbol{v}(j)^T] = \boldsymbol{N}(k)\delta_{k-j}, \tag{4.87}$$
$$E[\boldsymbol{v}(k)\boldsymbol{w}(j)^T] = 0, \tag{4.88}$$

where δ_{k-j} is the Kronecker delta function[6]. The goal is to estimate the state vector $\boldsymbol{x}(k)$ based on knowledge about the system and availability of the measurements $\boldsymbol{y}(k)$. The state vector estimate is divided into two parts when formulating the Kalman filter equations, namely $\boldsymbol{x}(k)^+$ and $\boldsymbol{x}(k)^-$. The + and − superscripts denote that the estimate is a posteriori or a priori, respectively. A posteriori indicates that all the measurements including the one in the current time step is used in the estimation, while a priori estimate includes all the measurements excluding the measurement at the current time step. It is important to notice that both the posteriori and the priori are estimates of the same time step.

$\boldsymbol{P}(k)$ is used to denote the covariance of the estimation error. The covariance matrix is also divided into a posteriori and a priori part, and these denote the covariance of the estimation error of the posteriori and priori estimates, respectively. The Kalman-filter gain $\boldsymbol{K}(k)$ is the last variable that has to be introduced before the filter equations can be presented. The reader should be aware of the numerous different representations of the Kalman-filter that occur in literature, and even though these may seem different, they are mathematically equivalent (Simon [2006]).

The filter is initialized by setting

$$\boldsymbol{x}(0)^+ = E(\boldsymbol{x}(0)), \tag{4.89}$$
$$\boldsymbol{P}(0)^+ = E[(\boldsymbol{x}(0) - \boldsymbol{x}(0)^+)(\boldsymbol{x}(0) - \boldsymbol{x}(0)^+)^T]. \tag{4.90}$$

[6] $\delta_{k-j} = 1$ if $k = j$ and $\delta_{k-j} = 0$ if $k \neq j$.

The Kalman filter is given by the following equations that have to be calculated at each time step $k = 1, 2, \cdots$.

$$\boldsymbol{P}(k)^- = \boldsymbol{A_d}\boldsymbol{P}(k-1)^+\boldsymbol{A_d}^T + \boldsymbol{M}(k-1) \tag{4.91}$$

$$\boldsymbol{K}(k) = \boldsymbol{P}(k)^-\boldsymbol{C_d}^T\left(\boldsymbol{C_d}\boldsymbol{P}(k)^-\boldsymbol{C_d}^T + \boldsymbol{N}(k)\right)^{-1} \tag{4.92}$$

$$= \boldsymbol{P}(k)^+\boldsymbol{C_d}^T\boldsymbol{N}(k)^{-1} \tag{4.93}$$

$$\hat{\boldsymbol{x}}(k)^- = \boldsymbol{A_d}\hat{\boldsymbol{x}}(k-1)^+ + \boldsymbol{B_d}\boldsymbol{u}(k-1) \tag{4.94}$$

$$\hat{\boldsymbol{x}}(k)^+ = \hat{\boldsymbol{x}}(k)^- + \boldsymbol{K}(k)\left(\boldsymbol{y}(k) - \boldsymbol{C_d}\hat{\boldsymbol{x}}(k)^-\right) \tag{4.95}$$

$$\begin{aligned}\boldsymbol{P}(k)^+ &= \left(\boldsymbol{I} - \boldsymbol{K}(k)\boldsymbol{C_d}\right)\boldsymbol{P}(k)^-\left(\boldsymbol{I} - \boldsymbol{K}(k)\boldsymbol{C_d}\right)^T \\ &\quad + \boldsymbol{K}(k)\boldsymbol{M}(k)\boldsymbol{K}(k)^T \end{aligned}\tag{4.96}$$

$$= \left((\boldsymbol{P}(k)^-)^{-1} - \boldsymbol{C_d}^T\boldsymbol{M}(k)\boldsymbol{C_d}\right)^{-1} \tag{4.97}$$

$$= \left(\boldsymbol{I} - \boldsymbol{K}(k)\boldsymbol{C_d}\right)\boldsymbol{P}(k)^-. \tag{4.98}$$

Even though there are several expressions explaining the same variables, they must be chosen wisely. For example, the first expression of $\boldsymbol{P}(k)^+$ is called the Joseph version of the covariance and it is known that this is the most robust and stable one (Simon [2006]). It is most common to use the first expression of both $\boldsymbol{P}(k)^+$ and $\boldsymbol{K}(k)$. The time step in the Kalman filter is set to be 1 minute. This value is chosen such that the estimates of the fast ventilation dynamics become accurate. As with other state estimators, the Kalman filter also has to be tuned. This is done by choosing the values of the diagonal covariance matrices $\boldsymbol{M}(k)$ and $\boldsymbol{N}(k)$. $\boldsymbol{N}(k)$ is given low values compared to the ones in $\boldsymbol{M}(k)$ if the system measurements are reliable, and high values if the measurements are not reliable. In the same manner, $\boldsymbol{M}(k)$ is given high values if the designer do not trust the model, and given low values if the model is to be trusted. However, it is not necessarily the case that the model is assumed to be good if $\boldsymbol{M}(k)$ is given low values. If the designer for any reason do not want to emphasize certain state estimates, $\boldsymbol{M}(k)$ is given low values at these points. A reason to provide these low values can be that the system contains unobservable elements and therefore lacks information about certain states. It is better not to do anything with unobservable states than trying to estimate them with little or no information (Imsland [2011]). Because of this it is common to give one of the matrices high values and give the other one low values. If the measurements are considered reliable, this may imply that the measurements are more reliable than the model, hence provide lower values in $\boldsymbol{N}(k)$ compared with $\boldsymbol{M}(k)$. On the other hand, if the measurements are unreliable it could be equally important to trust the model.

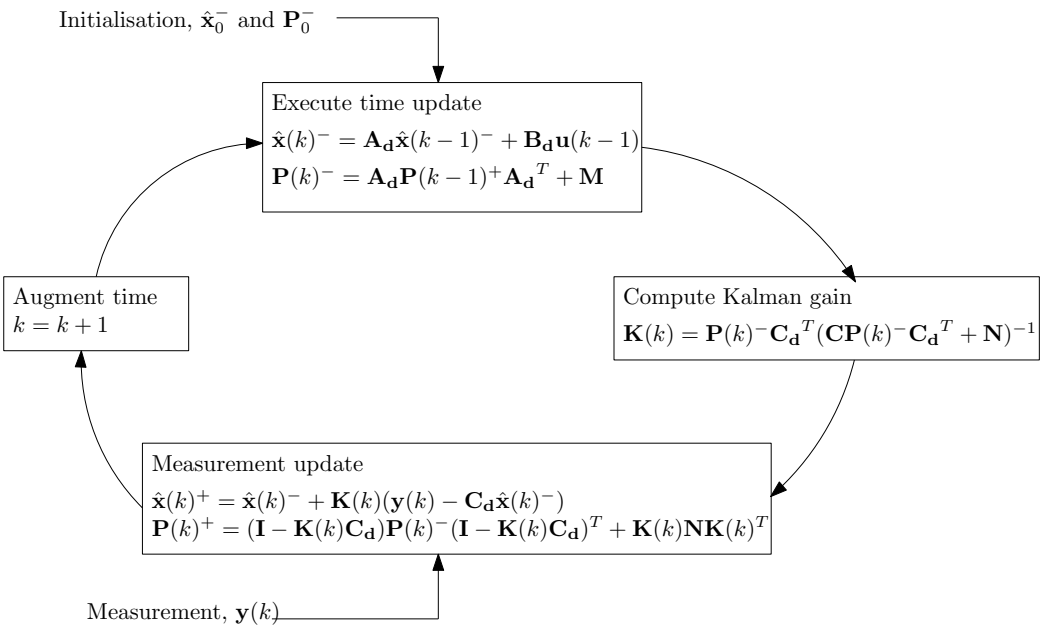

Figure 4.2: The Kalman-filter cycle (Ersdal [2011]).

The values of $\boldsymbol{x}(0)^+$ are taken from the `Simulink` model. If the initial states are known perfectly, $\boldsymbol{P}(0)^+$ is set to $diag(0, \cdots, 0)$ (Simon [2006]). Since the initial states are taken directly from `Simulink`, they are known perfectly. However, since some of the dynamics was left out when obtaining the linearized model, $\boldsymbol{P}(0)^+$ is set to $diag(10, \cdots, 10)$ instead of $diag(0, \cdots, 0)$ because the initial values are not assumed to be perfect. As mentioned above, the system's observability has to be examined in order to find out whether some of the elements in $\boldsymbol{M}(k)$) should be set to 0. The observability of the system can be found by examination of the observability gramian. The observability gramian is defined as

$$\boldsymbol{W_o}(t) = \int_0^t e^{\boldsymbol{A_d}^T\tau}\boldsymbol{C_d}^T\boldsymbol{C_d}e^{\boldsymbol{A_d}\tau}d\tau, \tag{4.99}$$

and the system is observable if and only if (4.99) is nonsingular[7] for $t > 0$ (Chen [1999]). The `MATLAB` function `gram(sys, 'o')` returns the observability gramian, which has the rank $rank(\boldsymbol{W_o}) = 15 < 17 = n$, i.e. there are two unobservable states in the system. The most common approach when exploring the system's observability is to check the rank of the observability matrix (Equation (6.29) in Chen [1999]). However, the reader should be aware that when this is calculated in `MATLAB`, numerical problems are likely to arise

[7](4.99) is nonsingular if it has full rank.

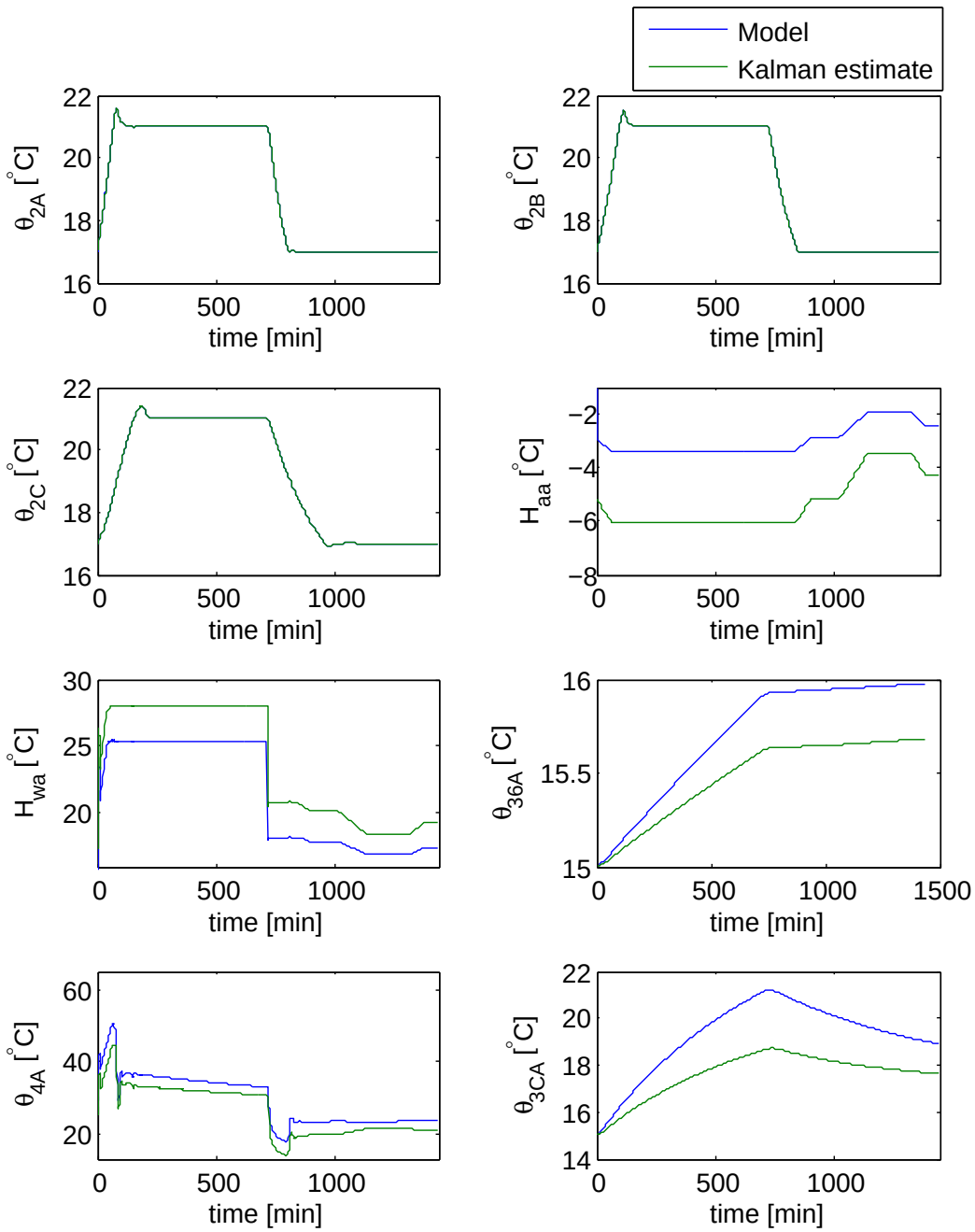

Figure 4.3: The Kalman-filter estimates $(1-8)$.

for large systems. Actually, MathWorks [2011] states that the `obsv(A, C)` function is intended for educational purposes and is not recommended for observability testing in real applications, because it is likely to be numeri-

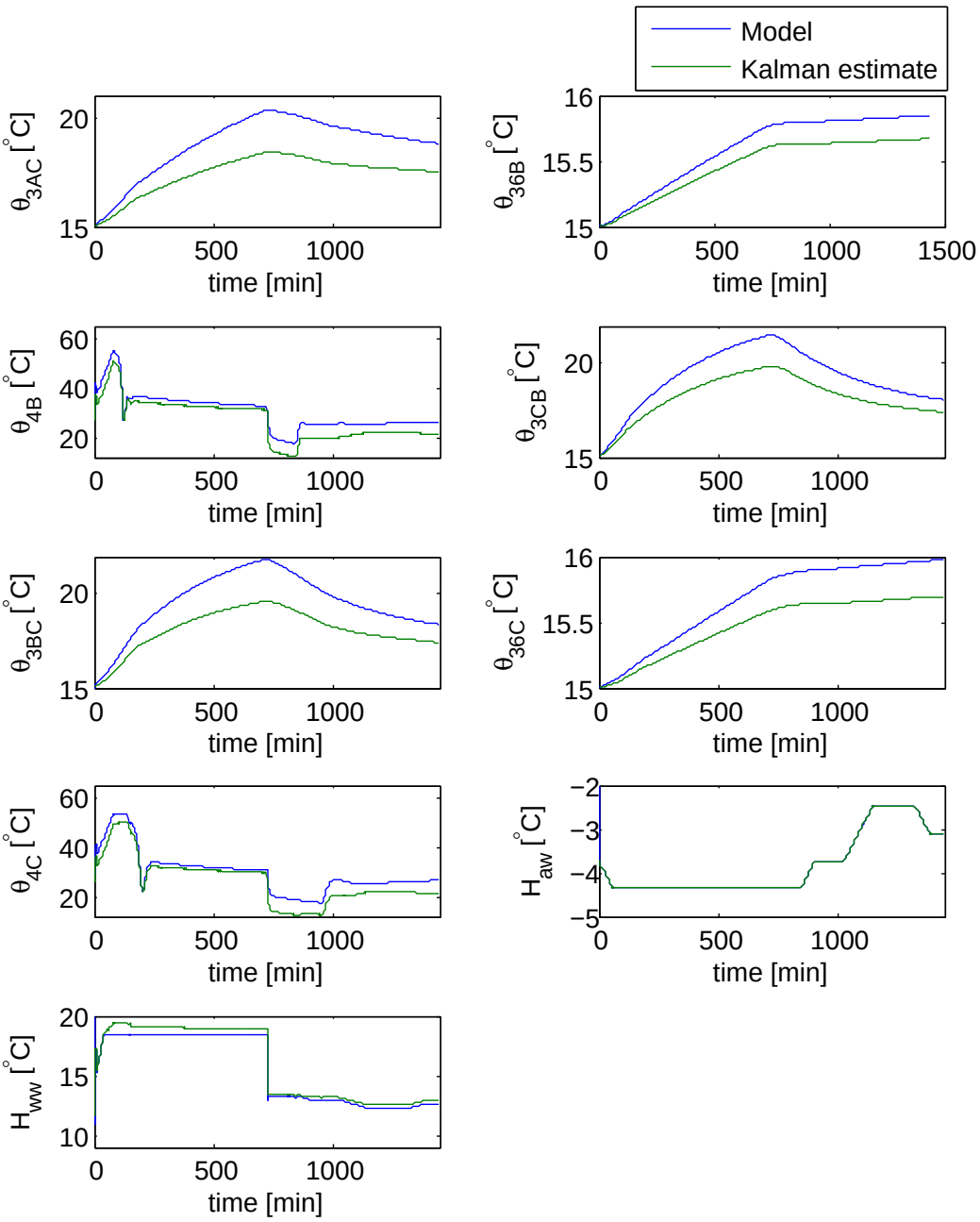

Figure 4.4: The Kalman-filter estimates $(9-17)$.

cally singular for most systems with more than a handful of states. Anyway, the observability gramian implies that two of the elements in $\boldsymbol{M}(k)$ should be set to 0. By following this and the other advises listed above, the values in $\boldsymbol{M}(k)$ are found by trail and error. Since the district-heating dynamics is

left out of the linearized model, this leads to a certain degree of uncertainty. Therefore, the elements in $\boldsymbol{M}(k)$ are generally given high values because the author does not trust the model. Similarly, the values in $\boldsymbol{N}(k)$ are given low values because the author trusts and want to emphasize the measurements (there is no measurement noise) in the system.

Figure 4.3 and 4.4 indicate that the estimates are fairly good. Almost everyone have similar movement pattern as their corresponding states even though they deviate to a greater or lesser degree when it comes to amplitude. As long they have similar responses and are close to each other, the estimates are suited to be used in an MPC scheme (Imsland [2011]). However, the consequences of inaccurate estimates are more severe for two of the states. The ventilation temperature (θ_7) is a sum of two states, namely state 4 and 5. It can be seen in Figure 4.3 that these estimates differ from their corresponding states. However, if they are added they become equal to the measured ventilation temperature. Since the measured value is trusted in the Kalman filter and the model is not, the filter is of the opinion that it has estimated the states correctly when the sum of the estimates is equal to the measured value. It is known that the system is not observable, which means that there exists a linear dependence in (4.99). It is likely that this linear dependence consists of state 4 and 5, thus it is not enough information available to allow both of them to be estimated correctly. This can be a problem because of the defined constraints on the ventilation temperature. The optimizer may not be able to fulfill these particular constraints if the estimates are wrong.

4.4 Optimization

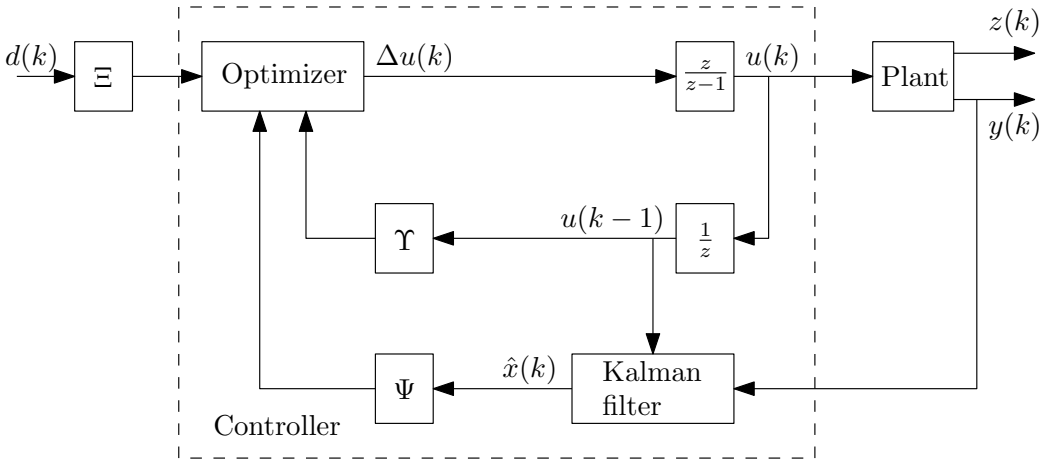

Figure 4.5: The structure of an MPC controller, inspired by Figure 3.3 in Maciejowski [2002].

After having obtained satisfying state estimates using a Kalman filter, the MPC controller shown in Figure 4.5 is implemented. The last thing that has to be done before running the system, is to make an algorithm that solves the optimization problem. Since the optimization problem (4.59) is a quadratic programming problem, it can be solved by using the `MATLAB` function `quadprog(H, G, Omega, omega)`, where $\boldsymbol{H}$ and $\boldsymbol{G}$ are given by (4.58) and (4.57), respectively. $\boldsymbol{\Omega}$ and $\boldsymbol{\omega}$ contain the constraints, and are given by Example 4.2 and 4.3

$$\boldsymbol{\Omega} = \begin{bmatrix} \boldsymbol{F_1} \\ \boldsymbol{\Gamma\Theta} \\ \boldsymbol{W} \end{bmatrix}, \tag{4.100}$$

$$\boldsymbol{\omega} = \begin{bmatrix} -\boldsymbol{F_1}u(k-1) - \boldsymbol{f} \\ -\boldsymbol{\Gamma}\left(\boldsymbol{\Psi}\hat{\boldsymbol{x}}(k) + \boldsymbol{\Upsilon}u(k-1) + \boldsymbol{\Xi}\boldsymbol{D_m}(k)\right) - \boldsymbol{g} \\ \boldsymbol{w} \end{bmatrix}. \tag{4.101}$$

The optimization problem has to be solved every time step. The time step used in the MPC has to be equal to the time step that is used when the system is discretized(Maciejowski [2002]). The MPC time step is set to 5 minutes because the author finds it unnecessary to calculate a new reference supply-water temperature every minute. Beware that if different time steps

are used in the Kalman filter and in the MPC, two separate discretized models are necessary (Imsland [2011]). Since the filter and the MPC examine the system at different rates, the system matrices have to reflect this. Implementation of the MPC controller in `Simulink` is not straightforward (see Figure C.3). Since the `mux` block in `Simulink` does not handle matrices, all of them have to be transformed into vectors, and then transformed back again at the `Optimize` block (see Figure C.4). `MATLAB` functions are written to take care of this. The total `Simulink` diagram of the building with an MPC control scheme can be studied in Figure C.2.

4.5 Tuning

After having implemented the MPC controller, the tuning parameters have to be chosen wisely for the controller to work in an optimal manner. Recall that the available tuning parameters are H_w, H_p, H_u, $\boldsymbol{R}$ and $\boldsymbol{S}$. There is some literature that deals with MPC tuning. Shah and Engell [2010] for example, present a systematic tuning approach such that a desired closed-loop performance for SISO systems is obtained. However, MPC tuning is mostly a matter of experience (Maciejowski [2002]).

H_w decides when the defined constraints are going to be included into the optimization problem (Maciejowski [2002]). The constraints on the system input are hard constraints, which means that they can not be violated because of physically limitations[8]. The constraints on the system outputs are pursuant to the defined indoor temperature demands. However, the margin of error (the permitted deviation from set point) is not likely to be stricter than plus minus 0.5 $^\circ C$ from the desired value, such that the output constraints do not have to be hard. Nevertheless, it is important that climate demands are fulfilled at all times, which implies that H_w should be set to 1. H_u should be chosen sufficiently large such that no additional inputs to the system are necessary. That is, when the system responds in the same manner even though H_u is increased. θ_{ref} (the system input) is especially important when the system switches from night-to-day mode, and from day-to-night mode. This is because the required water temperature varies when the desired indoor temperature varies. By studying the slower transient temperature responses in Chapter 3, this gives a pointer when choosing H_u.

[8]The The system is dimensioned to handle a supply water temperature between 20 $^\circ C$ and 80 $^\circ C$.

$H_u = 35$ provides a good basis for the control horizon[9]. When it comes to H_p, a rule of thumb is that the prediction horizon should be equal to or larger than the largest time constant in the system. This is because the controller ought to be able to predict the system behavior also nearby large transients. However, the largest time constant the building model is 79 hours, which seems like an unnecessarily long prediction horizon. H_p is therefore initially set to 50. It should be noted that de Jager [2004] explores strategies of how to reduce the prediction horizon, and presents predictions over infinite horizons as unreliable and unrealistic.

A major problem that occurs when working with constrained optimization is that the problem may be infeasible (Maciejowski [2002]). Constraints on inputs and outputs may prevent the optimization algorithm of finding a valid solution. It is important to have a back-up method if infeasible problems occur, such that the process is guaranteed to get an input. Maciejowski [2002] lists some back-up approaches that may be carried out. Two of them are avoiding hard constraints on $\boldsymbol{Z}$ by introducing slack-variables, or actively manage the horizons at each time step. If the controller reacts by imposing a very large change of input if a constraint on a system output is barely broken, this indicates that there is a hard constraint on $\boldsymbol{Z}$. Violating hard constraints makes the controller to react in an aggressive manner, which seldom is optimal for any system. The introduced slack-variables are non-zero only if the constraints of current interest are violated, and these non-zero values are heavily penalized such that the optimization algorithm's intuition will be to keep them at zero if possible (Maciejowski [2002]). Slack variables will be presented in more detail in Section 4.7.1.

The author of this thesis handles infeasible problems by

1. Introducing time-varying output constraints,
2. and by manipulating the system input.

The fact that the indoor and ventilation temperatures have different desired values during night and day causes some difficulties when implementing the output constraints. When the system is switching from night to day mode, the desired temperatures changes, thus altering the output constraints. But since the new desired temperatures are not reached instantly, the new output constraints will be violated if they are not modified. The output constraints have to be changed since the optimization problem does not contain a reference trajectory[10]. It is actually the output constraints that forces the system

[9] 35 time steps equals 175 minutes.

[10] The optimizer minimizes the magnitude and variation of the system input (4.59), and

input to rise. This is done by using the estimated system output from the current time step ($\hat{\boldsymbol{y}}(k)$) as a constraint. This entails that the output constraints do not get violated in the transition from night mode to day mode, simultaneously as the system input increases. However, a back-up method concerning system-input manipulation should also be available in case of constraint violations.

The optimization algorithm's output is a change of system input ($\Delta u(k)$). If one of the output constraints are broken, the optimization algorithm will respond by imposing a large input change in order to fulfill the broken constraint. This may cause the previous input ($u(k-1)$) plus the change of input to exceed the input constraints (4.38). The problem then becomes infeasible and action has to be taken. One possibility is to use the input change that was calculated in the previous time step ($\Delta u(k-1)$), or one can simply set the input change to 0 and proceed with the input from the previous time step ($u(k-1)$). As the next section will show, the latter approach leads to satisfying responses and is therefore chosen.

4.6 Simulations

Now, when the MPC controller is fully implemented, it is interesting to examine whether the supply water temperature (θ) behaves different from the temperature of the approach presented in Chapter 3. If this is the case, how does the system outputs react to the different behavior of θ? Desired system characteristics are important to have in mind when tuning the controller. Whether the building owner wants a quickly-responding system, or a low energy consuming system, the controller parameters have to reflect these wishes.

In Figure 4.6, the conventional-based reference and the MPC-based reference are plotted together, and as implied earlier in this chapter, the two reference schemes are different in great extent. When θ^{conv} varies with respect to the outdoor temperature, it is seen that θ^{MPC} is time dependent. The desired indoor and ventilation temperatures changes every 12 hours, and θ_{ref}^{MPC} clearly adapts to these variations by dropping its reference temperature during the night. θ_{ref}^{MPC} varies between 50 $^{\circ}C$ and 61 $^{\circ}C$ during the day, except from peaks that occur once a day, while it is 35 $^{\circ}C$ - 36 $^{\circ}C$ during the night. As stressed before, the MPC's objective is to minimize θ_{ref}^{MPC} with respect to the

without variation in the constraints the optimizer will not be able to distinguish night and day.

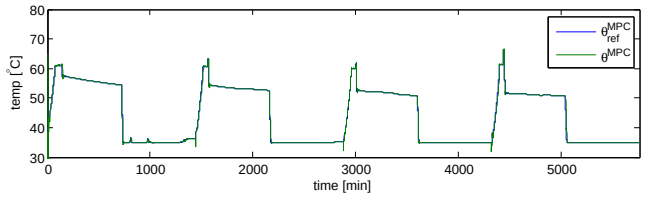

(a) MPC.

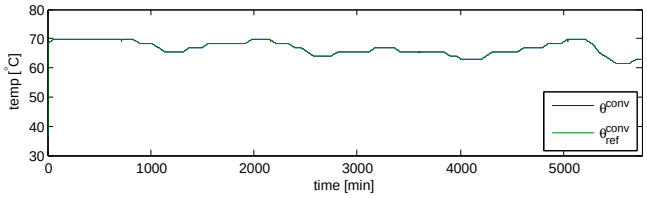

(b) Conventional.

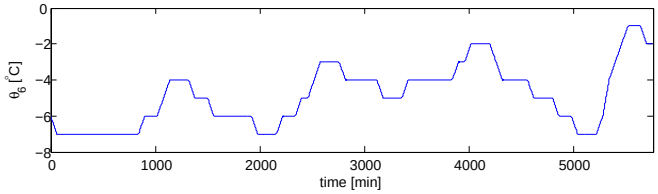

(c) Outdoor temperature.

Figure 4.6: MPC-generated reference (θ_{ref}^{MPC}), corresponding supply-water temperature (θ^{MPC}), conventional-based reference (θ_{ref}^{conv}), corresponding supply-water temperature (θ^{conv}), and outdoor temperature (θ_6) (during 4 days).

defined constraints (4.30). Even when θ_{ref}^{MPC} is minimized, these constraints make sure that it is large enough so that the indoor-climate demands will be fulfilled. The Figure 4.6 indicates that θ_{ref}^{MPC} is lower than θ_{ref}^{conv} during the entire simulation. The mentioned peaks that occur after every night-to-day switch[11] should be noticed. To keep the problem from becoming infeasible, an ad-hoc measure (which do not necessarily react in the same manner every time it is used) is implemented to soften the output constraints, and this measure is the probable cause of these peaks. The pros and cons of using this and the other ad-hoc solutions will be presented below. Also notice the inverted peaks that occur after every night-to-day switch. This may seem like a discontinuity, but the reason for the dip is that the ventilation system and the radiators increase their temperatures immediately after the mode switch. Therefore, the supply-water temperature (θ^{MPC}) decreases for a minute be-

[11]The system switches mode every 720 minutes (every 12 hours).

fore it starts its increase. These peaks will be present to a greater or lesser degree in all plots concerning the supply-water temperature. It is also seen that θ_{ref}^{MPC} varies in some degree during the first night (from 720 minutes to 1440 minutes). Since this behavior only occurs the first night, this seems like an initial issue that is eliminated when the system has simulated for a while. Actually, it is seen in Figure B.5a that this mentioned behavior only is present during the first night. These small variations are therefore ignored.

Table 4.1: MPC tuning parameters.

H_w	H_u	H_p	$\boldsymbol{R}$	$\boldsymbol{S}$	Extra
1	35	50	diag(1)	diag(100)	Feedforward

The indoor-temperature responses are quite different from the ones presented in Chapter 3. By studying Figure 4.7a, it is seen that θ_{2A} rises from 17 $^\circ C$ to 21 $^\circ C$ in about 62 minutes, which is significantly longer than the 26 minutes in the conventional case (Figure 3.3a). This was expected and can be explained by examination of θ^{MPC} and θ_{4A}. The constraints on the system outputs lead to a calm increase of the water temperature when switching from night to day mode. Naturally, θ_{4A} is increasing accordingly. θ_{ref}^{MPC} rises from 36 $^\circ C$ to 61 $^\circ C$ in 80 minutes, and during this time θ_{4A} increases with the same rate until θ_{2A} has settled on the desired 21 $^\circ C$. Using the conventional control strategy, θ_{ref}^{conv} is 67 $^\circ C$ (Figure 3.3) when the system switches mode. θ_{4A} can therefore increase at maximum rate which explains why the temperature response is faster using the conventional control scheme. As mentioned at the beginning in this section, it is up to the building owner to decide whether or not the system should be fast, economically beneficial, robust, or a combination of these. Pros and cons using a conventional strategy versus an MPC strategy will be discussed in Chapter 6. The same tendency appears when studying room B and C. θ_{2B} uses 88 minutes before it settles at 21 $^\circ C$ in the MPC case compared with 48 minutes in the conventional case. θ_{2C} uses 133 minutes using θ_{ref}^{MPC} as apposed to 88 minutes using θ_{ref}^{conv}.

The deviation in system behavior reveals itself most clearly when studying the ventilation temperature. Using the MPC-generated reference, θ_7 uses 43 minutes to reach the desired 22 $^\circ C$ compared with 1 minute in the conventional case! θ^{MPC}'s behavior is rather uneven when the system goes from night mode to day mode, and this because θ_{ref}^{MPC} increases in steps. This also explains the rough behavior of θ_7. However, the most interesting system feature occurs by examination of the valve openings in the ventilation system

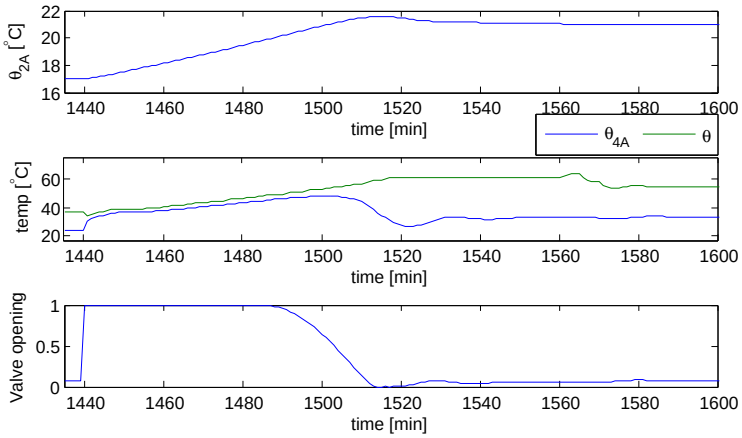

(a) Room A.

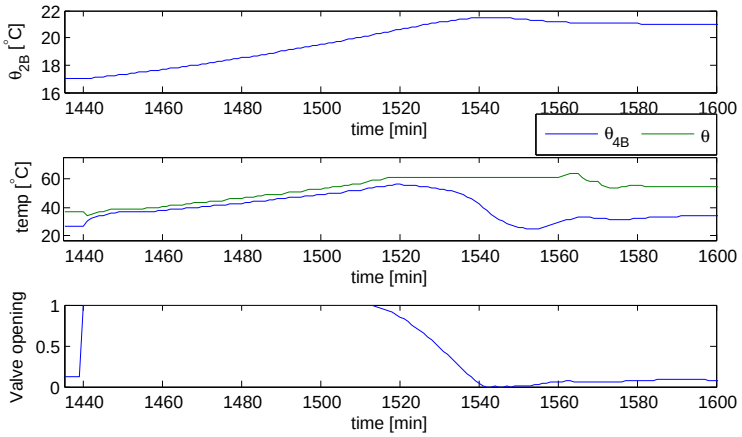

(b) Room B.

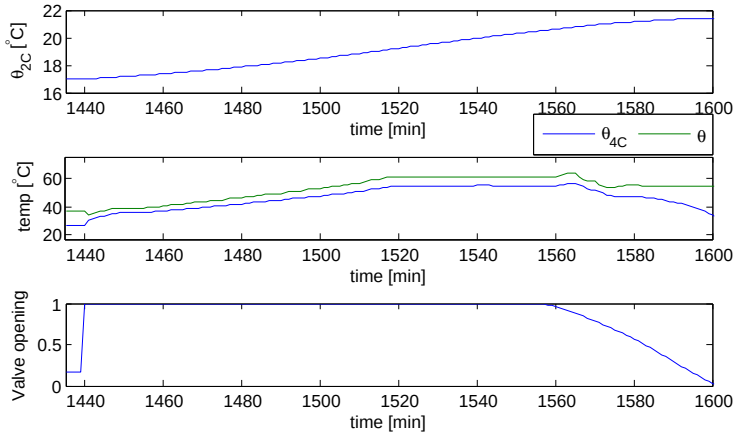

(c) Room C.

Figure 4.7: Indoor temperature (θ_2), radiator temperature (θ_4), supply-water temperature (θ), and control-valve opening of the radiator using the MPC scheme (from night to day).

(Figure 4.8) and in the radiators (Figure 4.7). The utilization of the available heat has improved compared with the conventional system. During the heating period, all the valves are completely open which means that they exploit the maximal amount of available energy. The valves are saturated for shorter periods during heating in the conventional case as well, but not in the same degree. The difference reveals itself clearly if the ventilation-temperature response is plotted over a longer interval.

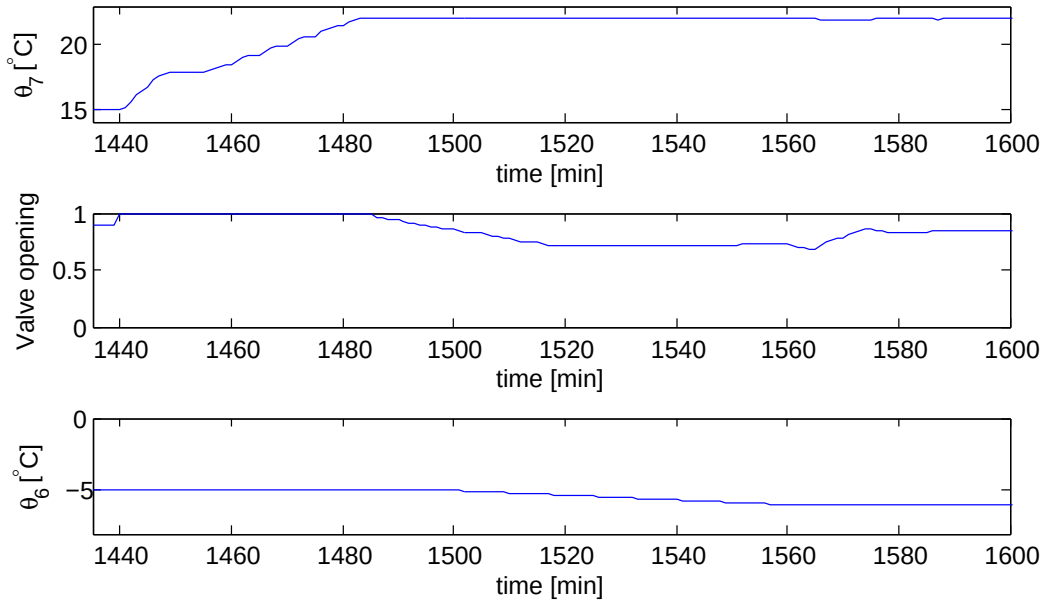

Figure 4.8: Ventilation-air temperature (θ_7), control-valve opening, and outdoor temperature (θ_6) using the MPC scheme (from night to day).

Figure 4.9a presents θ_7 during a period of 4 days. The valve opening varies between 0.7 and 1.0 (except from being 0.07 1 minute a day) over the entire period, and this suggests that θ^{MPC} almost is as low as it possibly can be while still fulfilling the desired indoor temperatures. In Figure 4.9b, it is seen that the valve opening in the conventional case is less open. However, during the day-to-night switch a weakness of the MPC scheme is revealed. Initially, θ_{ref}^{MPC} became too low such that θ_7 was unable to reach its desired night-time value. This is a violation of one of the output constraints and should theoretically not occur. This weakness is likely to descend from the Kalman-filter estimates. Recall that θ_7 is one of the four system outputs in the system and it consists of state 4 and 5 (see Figure 4.3). As mentioned in Section 4.3, these states are not estimated correctly, and it is therefore not surprising that the defined constraints on θ_7 are disregarded by the optimizer.

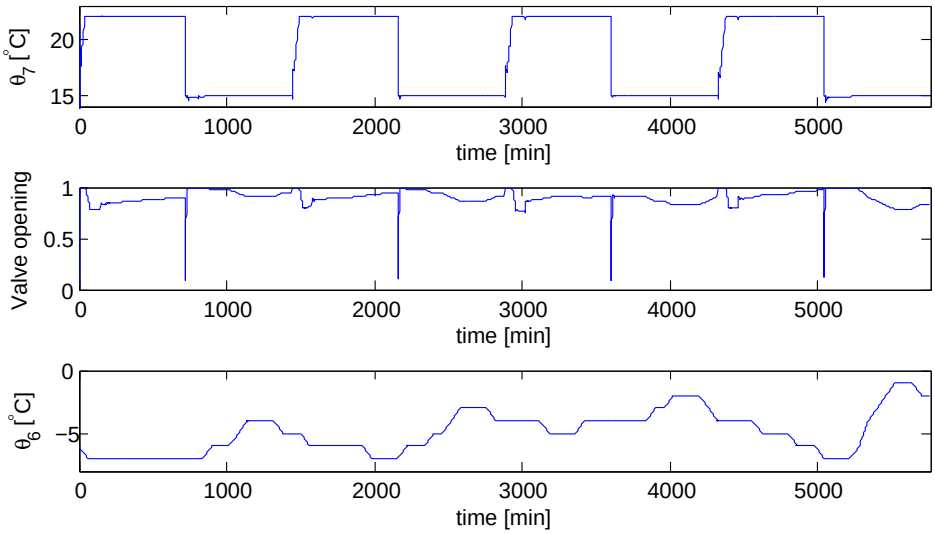

(a) MPC.

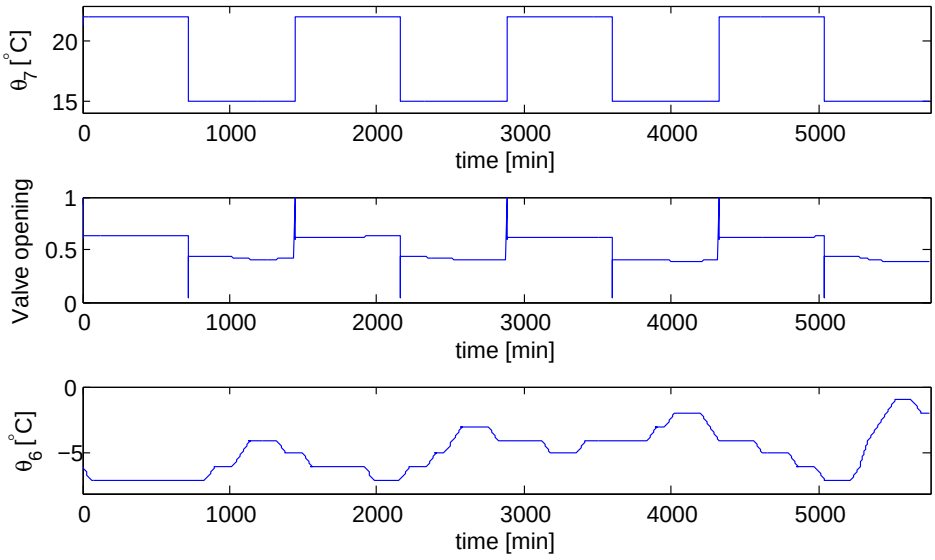

(b) Conventional.

Figure 4.9: Ventilation-air temperature (θ_7), control-valve opening, and outdoor temperature (θ_6) using the MPC scheme and the conventional scheme, respectively.

This problem was solved by setting the system-input's lower constraint to be 35 $^{\circ}C$, which made sure that θ_7 was able to fulfill its desired night-time values. This, together with the remaining ad hoc solutions will be presented below.

It should be mentioned that the temperature responses remain unchanged when the system is simulated with and without feedforward action. The outdoor temperature is slowly varying and its influence on the system outputs is hardly noticeable because of the effective behavior of the feedback action. Because of this, including future outdoor temperatures through feedforward action is unnecessary.

Day to night

Figure 4.11 indicates that the temperature responses from night to day are identical using the MPC control scheme versus the conventional. The matter of fact that θ^{MPC} drops to 35 $^{\circ}C$ during the night does not affect the radiators day-to-night response. The day-to-night responses are therefore still dependent on the radiator dynamics and the rooms inertia.

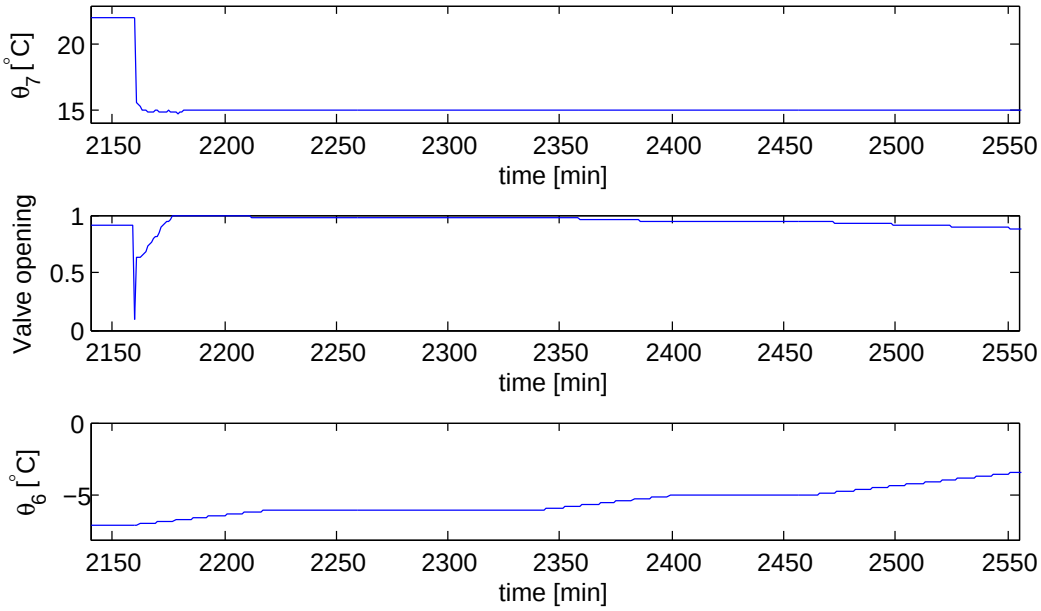

Figure 4.10: Ventilation-air temperature (θ_7), control-valve opening, and outdoor temperature (θ_6) using the MPC scheme (from day to night).

The ventilation-temperature response on the other hand, is slightly different than before. Figure 4.10 shows that θ_7 drops from 22 $^{\circ}C$ to about 15 $^{\circ}C$ in 4 minutes and settles after a small overshoot. As mentioned above, the system input's lower constraint (35 $^{\circ}C$) was introduced to ensure that θ_7 did not drop below its desired night-time temperature. This is still violated, but now only by under 0.3 $^{\circ}C$ and for a few minutes after the new input constraint was introduced. This makes it acceptable, even though it strictly speaking should have been taken care of by the output constraints. However, it is interesting to ascertain that the valve opening in the ventilation system still is almost wide open during the night time. This implies that the MPC does an approved job maximizing the utilization of the available energy in the supplied water.

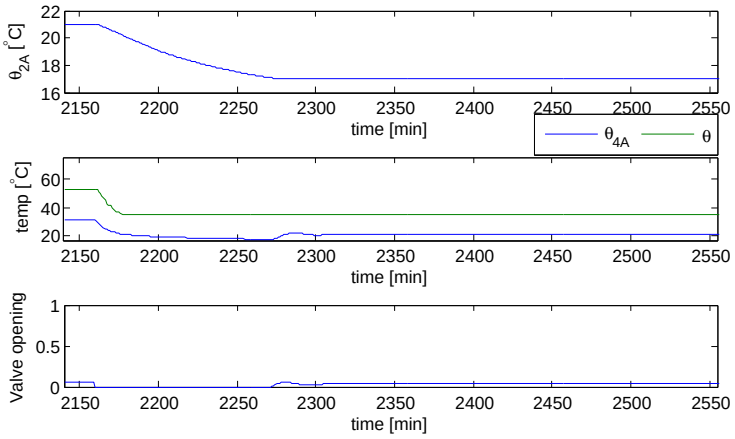

(a) Room A.

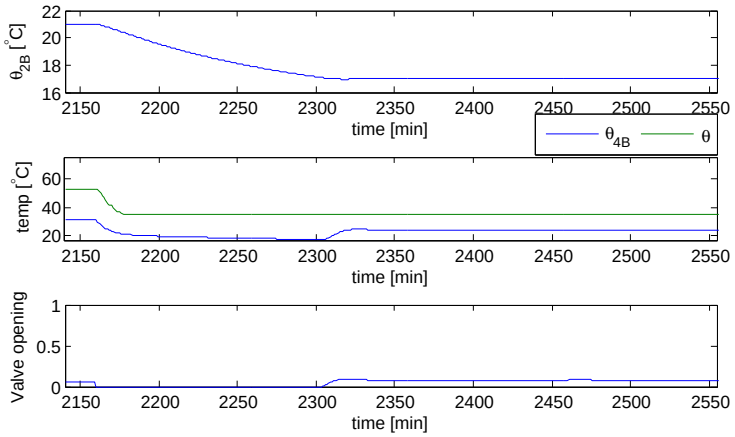

(b) Room B.

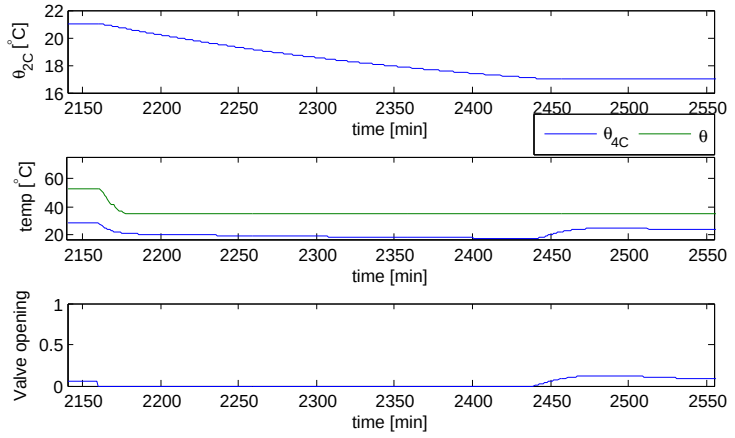

(c) Room C.

Figure 4.11: Indoor temperature (θ_2), radiator temperature (θ_4), supply-water temperature (θ), and control-valve opening of the radiator using the MPC scheme (from day to night).

Nevertheless, the MPC-control scheme does not function in an optimal manner. The introduced ad-hoc solutions are likely to cause this sub-optimal behavior.

Ad hoc

Theory and practice are two different things. The fact that the output constraints on θ_7 are not fulfilled, and that the system reacts in an nervous and aggressive manner close to constraints, enforces that measures have to be taken. In Example 4.3, the output constraints are defined to be equal to the desired day-time and night-time temperatures, and intuitively speaking, these values make sense. However, when the system was simulated, the reality proved to be different. Especially when the desired day-time temperatures was reached, θ_{ref}^{MPC} started to vary rapidly. A possible reason for this is that the temperature in one of the rooms may have dropped by 0.1 $^\circ C$ - 0.2 $^\circ C$ during the day. By defining the output constraints to be $[21, 21, 21, 22]^T$, θ_{ref}^{MPC} responds by increasing instantaneously if one of the room-air temperatures happens to be 20.95 $^\circ C$, for instance. The rapid variations occur because the optimization problem becomes infeasible when one of the constraints get violated (Maciejowski [2002]). The optimizer reacts intensely in order to reestablish the problem's feasibility. This behavior is resolved by redefining the day-time-output constraints to $[20.8, 20.8, 20.8, 21.8]^T$ and the night-time constraints to $[16.8, 16.8, 16.8, 14.8]^T$. It is common to operate with a margin of error when it comes to desired indoor temperatures, which make these new output constraints acceptable. Besides, the actual temperature control takes place inside each room and inside the ventilation system. The output constraints are defined to ensure that θ_{ref}^{MPC} is high enough such that the internal controllers are able to reach the desired temperatures. The 0.2 $^\circ C$ relaxation of the constraints does not harm this objective.

When the output constraints changes due to the switch from night mode to day mode, the problem's feasibility is yet again challenged. Immediately after the change of mode, the system outputs are still equal to (or maybe 0.1 $^\circ C$- 0.2 $^\circ C$ larger) their night-time values. If the day-time-output constraints are activated instantaneously after this mode change, they will most certainly be violated. This is taken care of by making the output constraints time dependent during the period the system outputs need before they have adapted to their new desired values. Instead of setting the output constraints to constant values, they are given a different value at each time step during the transition period, namely $\hat{\boldsymbol{y}}(k)$. By setting the output constraints equal

to $\hat{\boldsymbol{y}}(k)$, it is very likely that these will be fulfilled. In addition, the optimizer will keep increasing the system input such that the constraints continue to be satisfied with a certain margin (Figure 4.12). When the system outputs have reached their desired day-time values, the day-time constraints are activated and they remain constant until the next mode change. This measure can also be called a relaxation of the day-time-output constraints. Since the output constraints depend on the estimated outputs of an uncertain model, one is not guaranteed to get equal controller responses from day to day, which reveals a drawback using this ad-hoc measure. This is the probable reason why the peaks in 4.6a have different amplitudes. Introducing slack variables is a measure that could have eliminated the ad-hoc solutions mentioned above. This is the topic for Section 4.7.1.

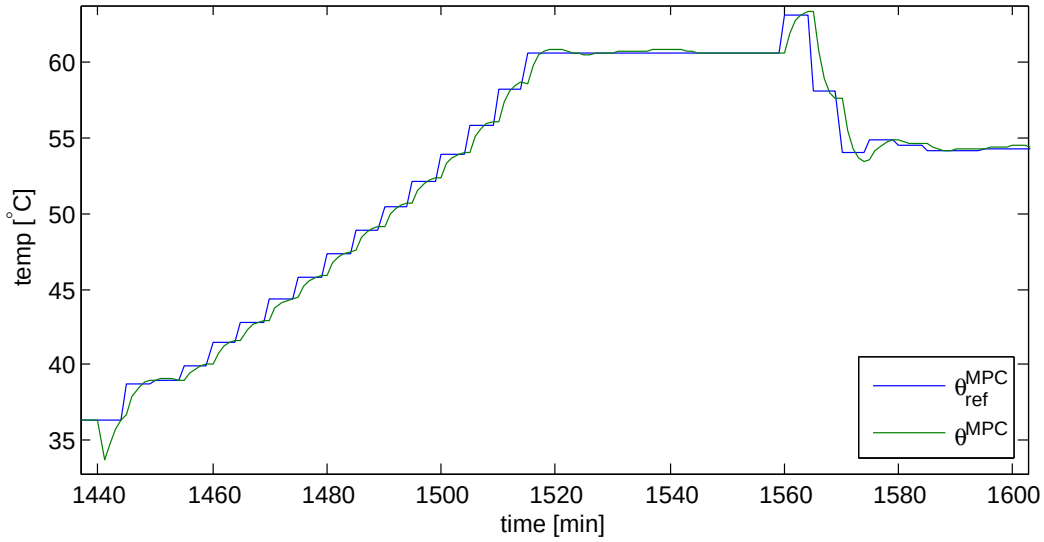

Figure 4.12: The MPC-generated reference (θ_{ref}^{MPC}) increases in steps during the period after the night-to-day switch.

The final special measure is that the lower input constraint is increased from 20 $°C$ to 35 $°C$. As mentioned above, this is done because the constraints on θ_7 are disregarded. θ^{MPC} has to maintain a certain temperature to be able to keep θ_7 near 15 $°C$ during night time, and the value 35 $°C$ was found by trail and error.

4.7 Making the MPC strategy robust

The definition of robust control is control of unknown plants with unknown dynamics subject to unknown disturbances, which primarily concern uncertainty and how the control system is able to deal with it (Rollins [1999]). When exploring a controller's robustness, two main items are how it responds to large variations in the disturbances and how it responds to model errors (Imsland [2011]). In this thesis, the disturbances are either slowly varying (outdoor temperature) or relatively small in amplitude (noise from people and equipment). However, since most of the Kalman-estimates in Figure 4.3 and Figure 4.4 deviates more or less from their real values, model uncertainty is the main concern. This uncertainty motivates implementation of a more robust control system.

The most common and often the first action that is taken to increase the robustness of a controller, is to restrict the change of system input ($\Delta u(k)$) (Imsland [2011]). This was already included in Section 4.1, so that the controller used in the simulations presented above was to some extent robust. However, some of the ad-hoc solutions listed above contribute to make the control scheme less robust, and should be removed. Especially the relaxation of the system-output constraints. As mentioned above, the output constraints are set to $\hat{\boldsymbol{y}}(k)$ when relaxed, which actually make them dependent of the uncertain model. It can be seen in Figure 4.6a that θ_{ref}^{MPC} behaves differently during the night-to-day switches. Shortly after these switches, small peaks can be spotted in the figure. By setting the constraints equal to $\hat{\boldsymbol{y}}(k)$, the optimization problem will constantly be on the feasibility limit, which makes the probability of violation considerable. This may be the reason why the peaks exist but also why the maximum value varies from day to day.

The softening of the output constraints should be solved in manner that removes the chance of constraint violations. This can be done straightforward by defining a constant set-point value that is valid only during the transition (Figure 4.13). This will remove the uncertainty about $\hat{\boldsymbol{y}}(k)$ at every time step, since θ_{ref}^{MPC} will increase at maximum allowed rate in order to reach the defined set point. If this is carried through, the cost function (4.56) has to be expanded to include $\boldsymbol{Z}(k)$ since $\boldsymbol{Q}$ no longer is equal to $diag(0, \cdots, 0)$. $\boldsymbol{Q}$ should not be equal to $diag(0, \cdots, 0)$ during the transition after the night-to-day switch, and it should be equal to $diag(0, \cdots, 0)$ otherwise.

A more theoretical approach is to introduce slack variables

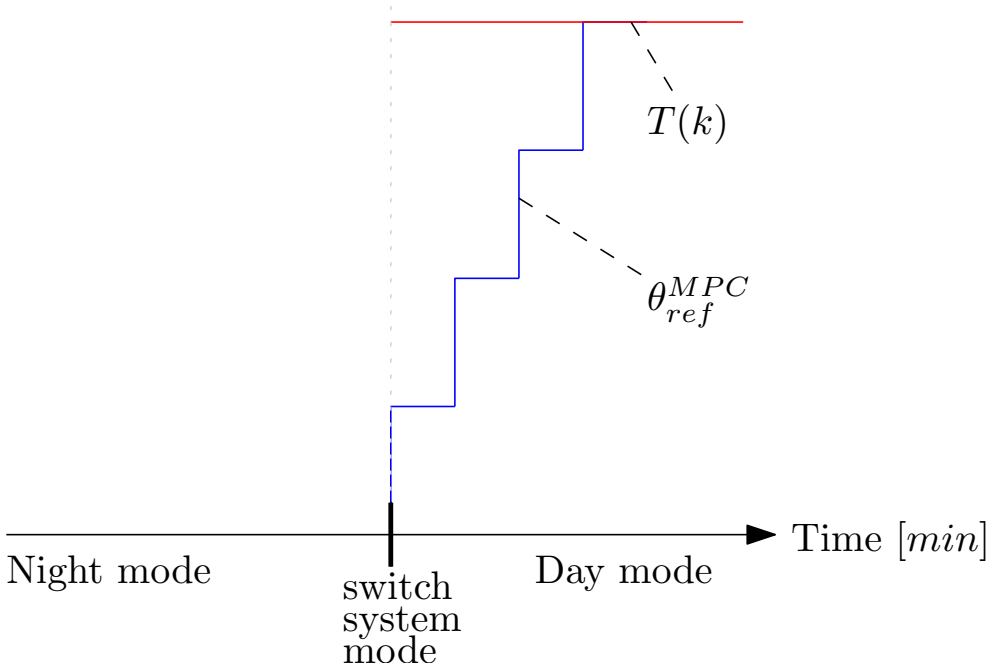

Figure 4.13: The output constraints may be softened by defining a desired trajectory that is valid only during the transition from night to day.

4.7.1 Slack variables

This section will be based on Maciejowski [2002]. Slack variables are included to soften the output constraints[12] and are defined in such a way that they are non-zero only if the constraints are violated. If a non-zero value occurs, it is heavily penalized in the cost function such that the optimizer's intuition will be to keep them at zero if possible. The slack variables are added into the cost function and the constraints as follows:

$$\min \frac{1}{2}\boldsymbol{\Delta U}(k)^T \boldsymbol{H} \boldsymbol{\Delta U}(k) + \boldsymbol{\Delta U}(k)^T \boldsymbol{G} + \boldsymbol{\rho} \|\boldsymbol{s}|^2 \tag{4.102}$$

subject to

$$\boldsymbol{\Omega \Delta U}(k) \leq \boldsymbol{\omega} + \boldsymbol{s} \tag{4.103}$$

$$\boldsymbol{s} \geq 0 \tag{4.104}$$

[12]Input constraints are often hard constraints (e.g. a valve opening) and are rarely softened (Maciejowski [2002]).

where $\boldsymbol{\rho}$ penalizes non-zero values of the slack variables. $\boldsymbol{\rho} = 0$) leads to an unconstrained problem, while $\boldsymbol{\rho} \to \infty$ denotes a hard-constrained problem. A problem by having a quadratic penalization of constraint violations is that activated constraints will, in some extent, be violated if $\boldsymbol{\rho}$ has a finite value, even though this is unnecessary. A solution to this problem is to penalize 1-norm[13] or 2-norm of the constraint violations. If the 1-norm is used to penalize the violations, every constraint is required to have their own slack variable. As mentioned above, it is not desirable to soften the input constraints, which means that the penalization values corresponding to the system inputs are set to ∞. It can be shown that if $\boldsymbol{\rho}$ is chosen to be large enough, the 1-norm-violation penalty leads to an exact penalty method, which means that the constraints will not be violated unless the problem becomes infeasible. In other words, as long as the optimizer is able to find a feasible solution, the solution will be equal to the solution of the original hard-constrained problem.

The implementation can be done by augmenting the state vector such that the slack variables are included. And as implied by (4.102) and (4.104), the objective function and the constraints must be expanded to include the slack variables as well. Eric C. Kerrigan, one of Jan Marian Maciejowski's former PhD students, has written a `MATLAB` function that includes the slack variables into the QP problem such that it can be solved using `quadprog()`. This function is found in Kerrigan [1999]. Before using the function, the system designer has to decide which norm to use for penalization of constraint violations, and choose the value(s) in the penalization vector. A 1-norm is used in this thesis because of the ability to provide exact penalty. The penalization values corresponding to system input and system-input change are set to ∞ since it is desirable to keep these as hard constraints. Strictly speaking, the constraints corresponding to system input do not need to be augmented by slack variables. However, if Kerrigan's function is to be used, it is convenient to use exact penalization and set the system-input penalization values to ∞. The penalization values corresponding to the system outputs are set to 10^5. These are set to be high for the reason mentioned above, namely that high enough values in $\boldsymbol{\rho}$ lead to exact penalization of constraint violations.

Figure 4.14 presents how θ_{ref}^{MPC} behaves using the introduced slack variables. The ad-hoc solution that made the output constraints time dependent are now removed. It is seen that θ_{ref}^{MPC} is able to increase after the mode switches, and this is done without feasibility issues. This is solely the work of the slack

[13]The 1-norm is defined by Khalil [2002]: $\|v\|_1 = [\sum_i \sigma_i]$.

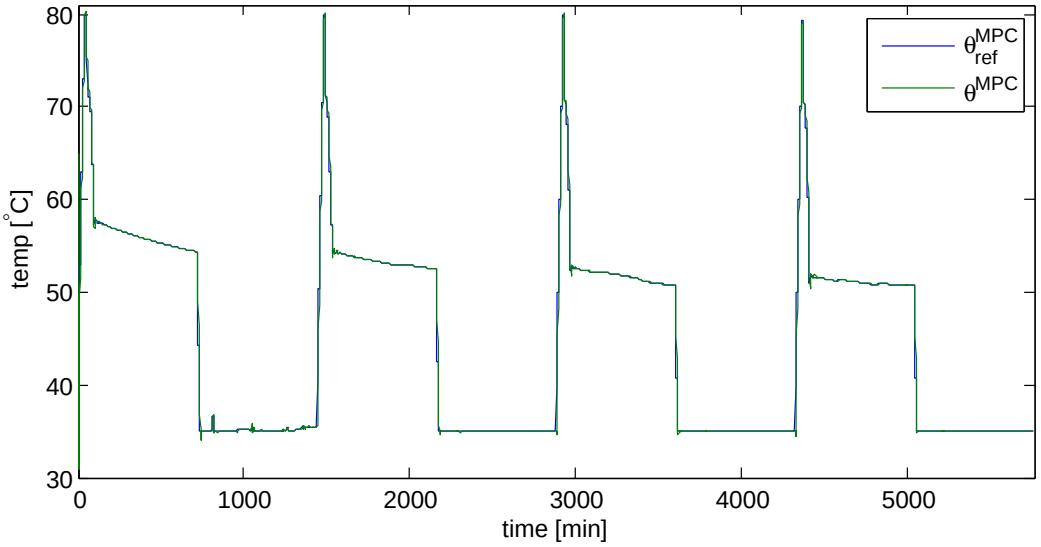

Figure 4.14: Behavior of the MPC-generated reference (θ_{ref}^{MPC}) and the corresponding supply-water temperature θ^{MPC} using the robust MPC scheme.

variables. Immediately after the mode switch, the system-output constraints are changed, and this leads to violation. However, the slack variables allow them to be violated, but the violation get heavily penalized. Further, this causes θ_{ref}^{MPC} to rise since the optimizer tend to retain a hard-constrained solution of the problem. θ_{ref}^{MPC} varies between 80 $°C$ and 51 $°C$ during day time. The reason why it becomes as high as 80 $°C$ is that the optimizer tend to get the slack variables equal to zero and thereby fulfill the day-time constraints, as fast as possible. When this is obtained θ_{ref}^{MPC} settles on a lower and more appropriate value, which varies from day to day because of a varying outdoor temperature. Because of the lower input constraint, θ_{ref}^{MPC} is 35 $°C$ during the night as before, except from the first 1440 minutes (the first day). During the night time, θ_{ref}^{MPC} behaves unevenly like it did the first night in Figure 4.6a. The reason is the same as before, namely that it is an initial issue that is eliminated after the first night. Figure B.5b shows that this behavior is only present the first night when the system is simulated for 8 days.

θ_{ref}^{MPC}'s rapid increase draws notice to itself when the indoor temperatures are examined in Figure 4.15. The tuning parameters are set to be the same as in Table 4.1, such that the responses using the old scheme and new scheme can be compared.

The indoor temperature in room A (θ_{2A}) rises from 17 $°C$ to 21 $°C$ in only

26 minutes, which is 36 minutes faster than the previous case and actually as fast as in the conventional case. The reason for this is that θ_{ref}^{MPC} rises faster and higher than in the previous case, thus the radiator (θ_{4A}) increases its temperature faster. The same tendency is seen in the other rooms. θ_{2B} uses 53 minutes to reach 21 $^{\circ}C$, which is 35 minutes faster than before and only 5 minutes slower than in the conventional case, while θ_{2C} uses 97 minutes, 36 minutes less than in the previous case and 9 minutes slower than in the conventional case. Due to the larger available heat amount during heating, the radiators remain saturated for a shorter period than they did in Figure 4.7. The ventilation temperature in Figure 4.16 now uses 11 minutes to reach the desired 22 $^{\circ}C$ as apposed to 43 minutes before. The indoor-temperature responses and the ventilation-temperature response during a 4 day period are found in Appendix B. The day-to-night responses are still similar as they have been all along since the room inertia and radiator dynamics have not changed.

There are several reasons why the controller has become more robust after having introduced slack variables. First and most important, the ad-hoc solution on the output constraints has been eliminated by the slack variables. By using the estimated system output ($\hat{\boldsymbol{y}}(k)$) as output constraints during the night-to-day transitions contributes with extra uncertainty, given that the Kalman filter does not estimate the states perfectly. This measure has now been removed since the slack variables allow the output constraints to be violated when it is needed. Another reason why the robustness of the controller has increased is that the system is able to respond faster than before. Figure 4.17 presents the behavior of θ_{ref}^{MPC} after the system has switched from night mode to day mode. θ_{ref}^{MPC} now increases at maximum rate, 5 $^{\circ}C$ per time step, so that the radiators are able affect the room temperatures faster. The control system is therefore more suitable to take care eventual unforeseen events. If a room temperature for some reason do not increase from one time step to the next (if a window is opened), the optimizer may stop to increase θ_{ref}^{MPC} if $\hat{\boldsymbol{y}}(k)$ is used as output constraints. Such incidents are very unlikely to occur using slack variables.

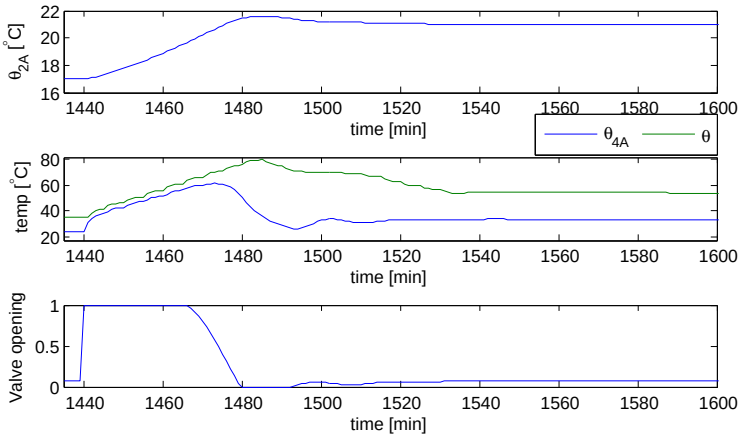

(a) Room A.

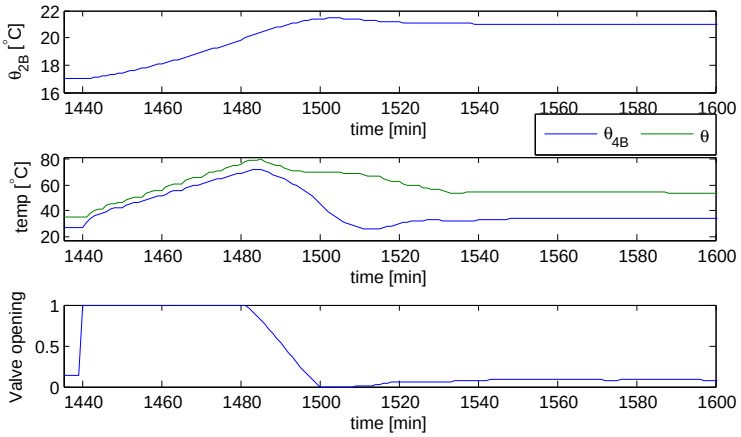

(b) Room B.

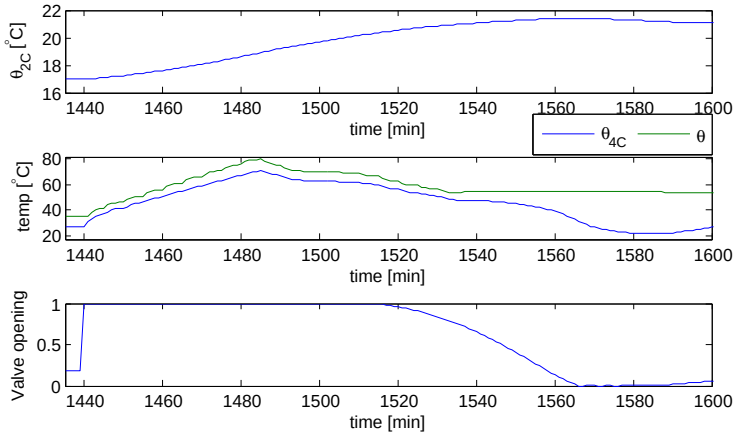

(c) Room C.

Figure 4.15: Indoor temperature (θ_2), radiator temperature (θ_4), supply-water temperature (θ), and control-valve opening of the radiator using the robust MPC scheme (from night to day).

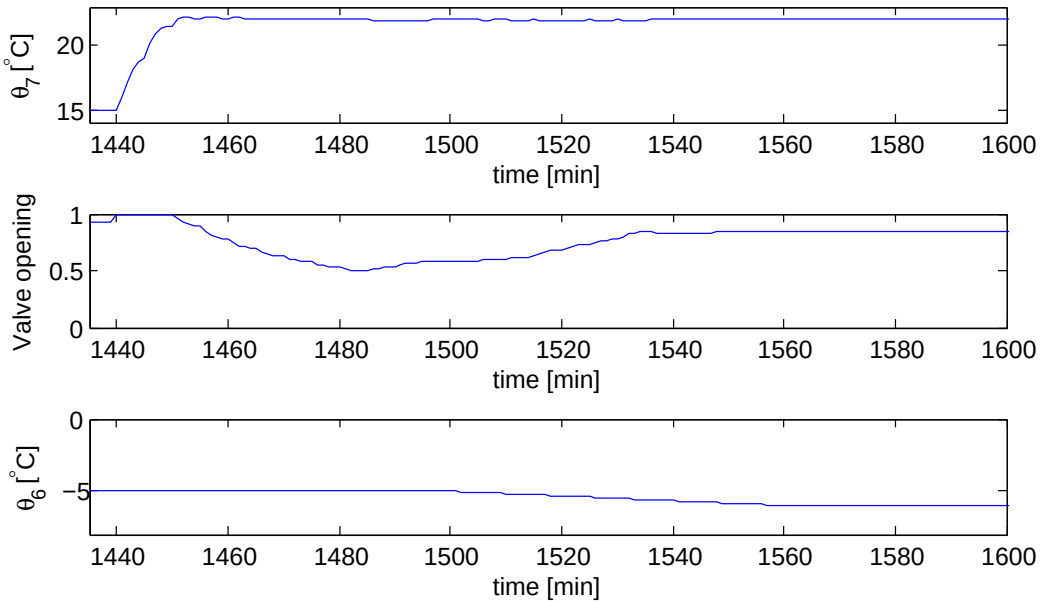

Figure 4.16: Ventilation-air temperature (θ_7), control-valve opening, and outdoor temperature (θ_6) using the robust MPC scheme (from night to day).

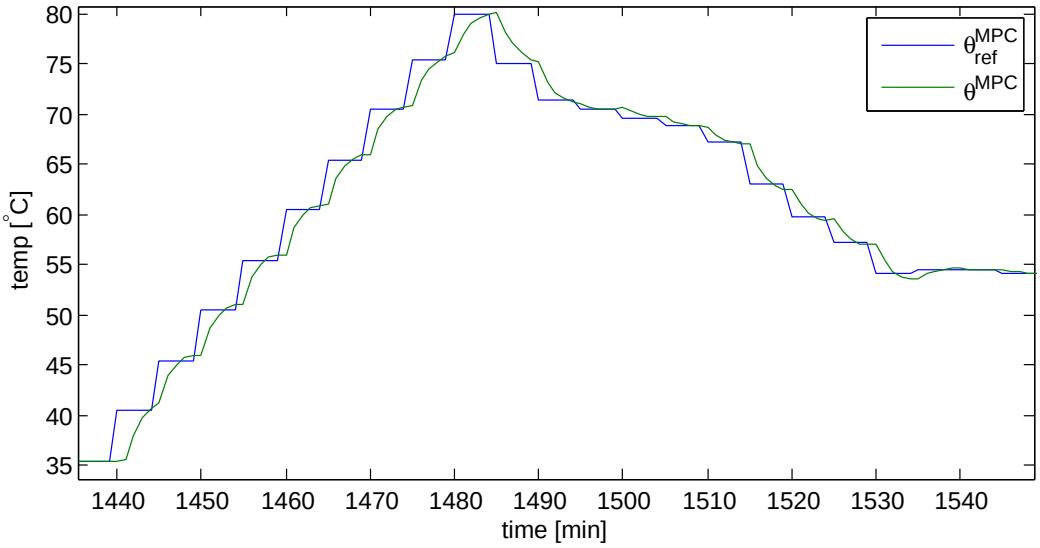

Figure 4.17: The MPC-generated reference (θ_{ref}^{MPC}) increases in steps at maximum allowed rate after the night-to-day switch in the robust MPC scheme.

Chapter 5

Energy Consumption

As mentioned in Chapter 1, energy usage in buildings represent 40 % of the total energy consmumption in industrialized countries. However, it should be said that in European countries, the total heating demand to the building stock has decreased despite that the number of buildings is constantly increasing, and this is because of energy-saving measures and new building technology (Abel and Elmroth [2007]).

When studying the energy consumption in this thesis, there are two matters that have to be addressed, namely

- the used amount of energy in the system, but also
- the amount of energy that is available in the system.

Intuitively, the most interesting matter is to examine the amount of used energy. However, since the purpose of the MPC scheme is to minimize the amount of available energy in the system, it is important to study the extent of the variation between the control schemes. Nevertheless, even though heat loss to the surroundings has been neglected in this thesis, this will always be a concern when a hot fluid is transported through pipes. The amount of energy that is used by the different control schemes is also subject for examination. Although minimizing the amount of used energy was not the purpose of the MPC, it is of interest to explore if removal of redundant heat in the system actually affects the energy that is consumed.

5.1 Calculating energy consumption

It is desirable to study the energy consumption on an hourly basis, to see how the consumption varies during and after working hours, for example. The energy is described as

$$E = \eta^{dh} w^{dh} c_w \rho_w \Delta\theta^{dh}. \tag{5.1}$$

where η^{dh} [-] is the efficiency factor in the district-heating heat exchanger, w^{dh} $[m^3/h]$ is the water flow through the heat exchanger, and $\Delta\theta^{dh}$ $[^\circ C]$ is the temperature difference between the supplied water and the water that is returned from the building. The efficiency factor is given by the relationship between the effect given into the system, and the effect supplied to the system, $\eta^{dh} = \frac{P_{in}}{P_{supplied}}$. It is assumed that no effect is lost, $\eta^{dh} = 1$. The amount of water flowing through the heat exchanger is taken from a heat-exchanger example in Novakovic [1995]. The reason why not the actual water amount from Bassengbakken 1's system is used will be discussed in Chaper 6.

This model is very simplified since it does not include any energy consuming components, nor heat loss to the surroundings. However, it can detect energy variations within hours, even seconds. This will be important when investigating the energy levels using the various control schemes.

5.2 Case 1 - Conventional control strategy

Figure 5.1 presents how the amount of available and used energy in the system varies during the day. As implied before, the available energy amount is not time dependent by not behaving a certain way during night time and day time, but by varying according to the outdoor temperature. When studying Figure 5.1, it is seen that the energy consumption is larger during day time compared to night time. Since the desired temperature values are higher during the day, this result makes sense. An important reason why an MPC scheme was introduced in the first place appears if the available energy is compared with the used energy. The large difference indicates that the amount of available energy in the system is unnecessary high as apposed to the used energy, which in real life is likely to cause a sustainable heat loss to the surroundings. When using the conventional control scheme, 13.45 % of the available energy is used.

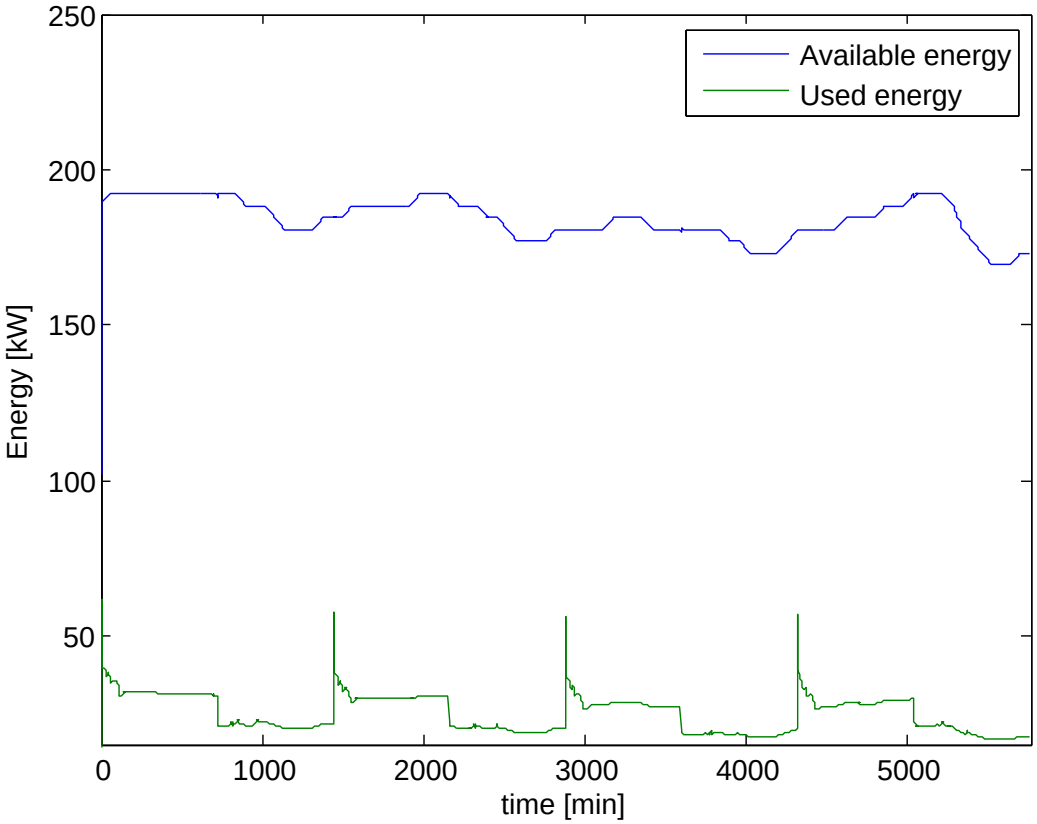

Figure 5.1: Used amount of energy and available amount of energy in the system using the conventional control scheme (during 4 days).

5.3 Case 2 - The MPC scheme

Figure 5.2 shows the available amount of energy and the used amount of energy using the MPC scheme. As mentioned in Chapter 4, the available energy is lower during the entire simulation when using the MPC scheme instead of the conventional scheme. As apposed to the conventional case, the available energy in the MPC case varies in a similar manner as the used energy. This is simply because the available energy amount is time dependent, and therefore decreases during night time when the demanded energy level is lower than during day time. The used energy amount is almost identical as in the conventional case. This is not surprising since minimization of the actual energy consumption was not the MPC's objective. However, a small decrease in used energy can be spotted, and this is an effect of the low energy amount that is available during the heating of the rooms. Using the MPC scheme, 20.29 % of the available energy is used. The reason why this

amount is not not bigger will be discussed in Chapter 6. After Case 3 has been presented, both the used energy and the available energy in the three cases will be compared.

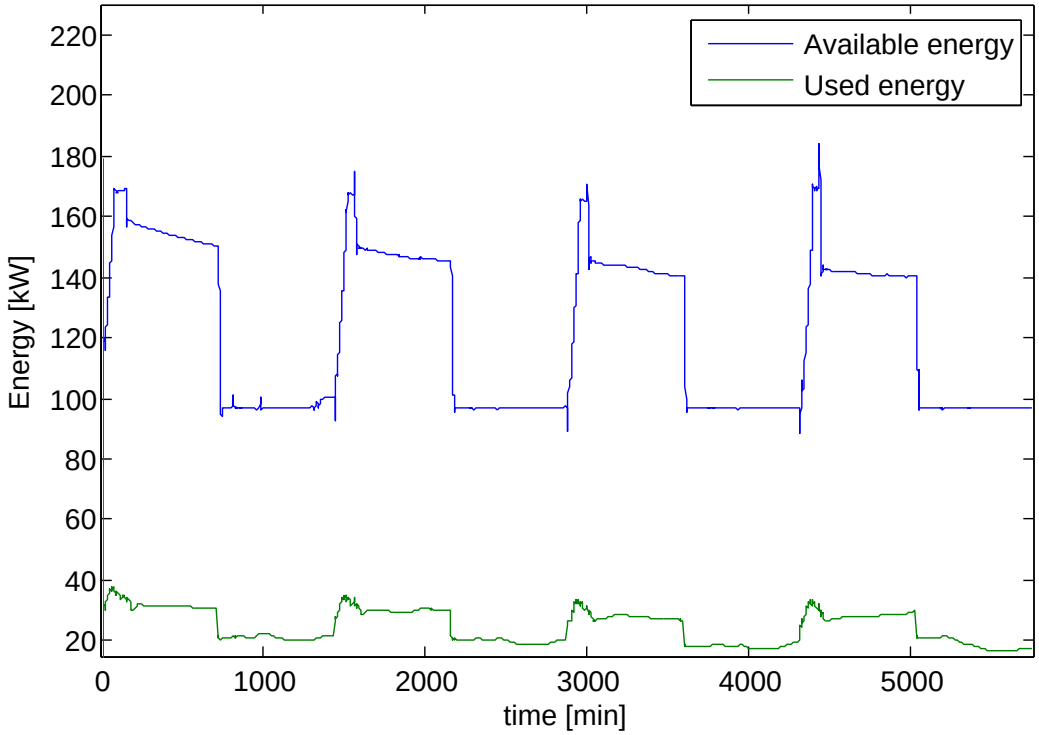

Figure 5.2: Used amount of energy and available amount of energy in the system using the MPC scheme (during 4 days).

5.4 Case 3 - The robust MPC scheme

By studying Figure 5.3, it is seen that both the available amount of energy and the used amount of energy are pretty similar as in Case 2. The increase of θ_{ref}^{MPC} in the robust case constitutes the difference, by increasing faster and further after the night-to-day switches. When the robust MPC scheme is used, 20.03 % of the available energy is used. This amount is a bit smaller than in Case 2, but on the other hand, the system responds quicker now than when using the ordinary MPC scheme. System response versus energy efficiency and other pros and cons using the three suggested schemes, will be discussed in Chapter 6.

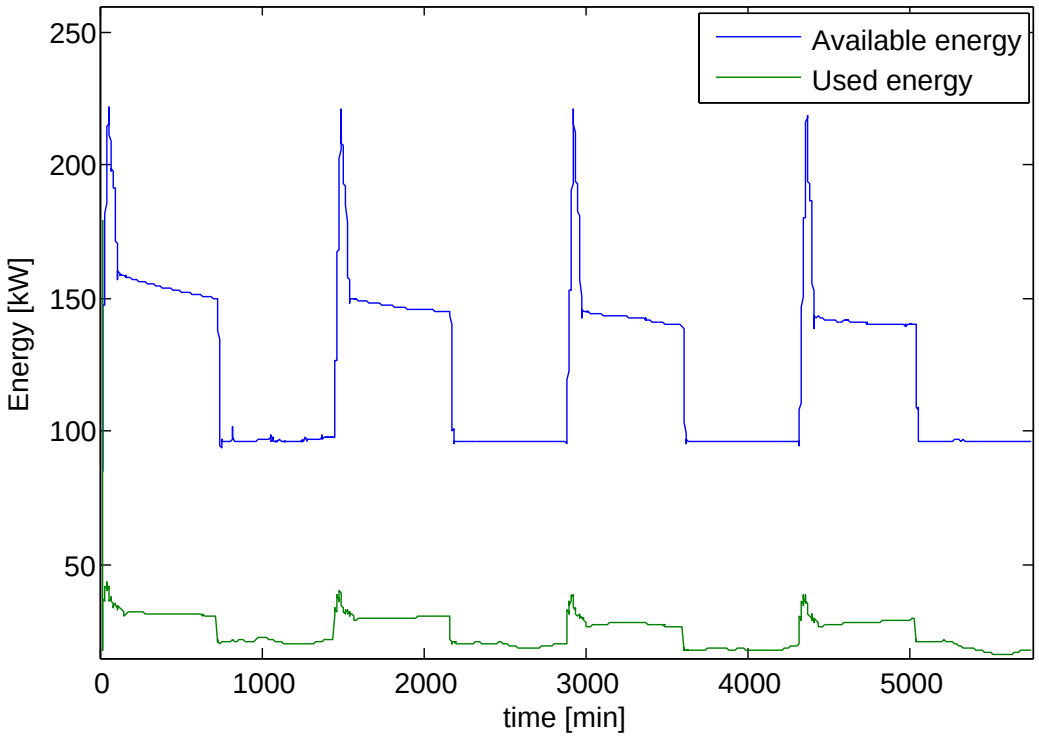

Figure 5.3: Used amount of energy and available amount of energy in the system using the robust MPC scheme (during 4 days).

5.5 Comparison

It is clear that both the ordinary MPC case and the robust MPC case have considerably less available energy during the simulation than the conventional case, while the actual consumption is almost identical in the three cases. The improvement from Case 1 to Case 2 is 0.43 %, and 0.083 % from Case 1 to Case 3. However, be aware that the calculations of energy consumption are inaccurate, since important factors like heat losses have been neglected. As stressed before, heat losses to the surroundings and energy consumption in general will increase the larger the amount of available energy becomes. Thus, a reduction in available heat in the system can be seen as an energy reduction potential. And this energy reduction potential is substantial when an MPC scheme is used. If Case 2 is used instead of Case 1, the energy reduction potential is 34 %. If this scheme is chosen, the building owner gets a system with some uncertain ad-hoc solutions that does not respond as fast as in Case 1, but that has a great energy reduction potential.

If Case 3 is chosen in stead of Case 1, the energy reduction potential is 32.92 %. As apposed to Case 2, Case 3 provides the building owner with a robust control system that responds faster than Case 2 with nearly equal energy reduction potential. Given Case 3's robustness and quick-responding abilities, this is recommended rather than Case 2 exclusively, despite the fact that the energy reduction potential is even larger in Case 2 than in Case 3. The choice between Case 1 and Case 3 on the other hand, depends on the building owner's demands and wishes. If a well known, conventional and quickly responding control system is desirable, Case 1 should be chosen. However, if the building owner is willing to compromise in terms of a well known and quickly responding system, Case 3 provides a robust control scheme with a considerable energy reduction potential.

Chapter 6

Discussion

Throughout this thesis, a model of a building has been derived by studying the most fundamental thermodynamical relations and by using an electrical analogy. Specific building information like wall thickness, insulation amount, and window area are taken from Bassengbakken 1 in Trondheim. A ventilation system and a district heating system are also included. In order for the system to be able to reach desired room temperatures and ventilation temperatures, internal controllers are added to the system. The supply temperature in the district heating system is decided either by

- a conventional control scheme that decides the supply temperature with regard to the outdoor temperature, or
- by an MPC scheme that minimizes the supply-water temperature with respect to a set of constraints.

In this chapter, simplifications done in the modeling, like neglecting floor and ceiling, disregarding the influence from the sun, and arbitrarily choosing certain values, will be justified. Problems during implementation and the working procedure in general will be discussed. The control strategies, including the preparations and simplifications that had to be done in order for the MPC scheme to function properly, will be subject for deliberation. Finally, the results will be evaluated. Are they realistic? What could have been done to improve the control scheme?

Although the results imply that the proposed scheme will increase the energy efficiency, it is far from theory to reality. Is the proposed idea actually achievable? Will the conservative construction industry approve? And most importantly, will building owners be willing to invest the time and the money

that is needed in order to make implementation of such a solution in existing and new buildings even possible?

6.1 Model review

The model that was derived in Chapter 2 was on a L3 level according to Table 2.1. The fundamental thermal relationships in a building were described using first-principle modeling. A simplification was to treat a segment of a building, three rooms to be precise, as a total building. However, since the fundamental thermal relations in a building are comprehended to a considerable extent by studying three rooms next to each other (see Figure 2.1), this simplification was acceptable. A more harsh simplification on the other hand, was to neglect the floor and the ceiling when deriving the model. Heat transmissions from rooms on the floor over or below are therefore not included in the model. Regardless of the number of rooms, and the absence or presence of a floor and a ceiling, the temperature responses in the system would have remained similar, since the most fundamental thermal properties were described. Besides, considering that the model acted as a tool for comparison of different control schemes, it was sufficiently accurate.

Specific building information like wall thickness, insulation material, U-values, and type of heating system, were given by Grini et al. [2009]. However, pipe dimensions and water amount in the heating and ventilation system were not taken from Bassengbakken 1. Since only a segment of the building was subject for examination in this thesis, the author did not want to include pipe dimensions and water amounts that were dimensioned for a large building. The radiator-pipe dimensions were chosen by studying the actual system dimensions in an office of the same size as one of the rooms in the segment. The dimensions in the ventilation system were chosen to be the same as an example in Novakovic [1995]. In terms of the amount of water that is sent to the radiators and the ventilation system, this was determined by intuition. First, the water amount should increase for larger rooms. Second, the ventilation system should get the largest amount of water because it probably is more demanding to heat up air from $-6\ ^{\circ}C$ to $22\ ^{\circ}C$ than it is to provide heat to a well insulated room containing disturbance elements that emit heat. However, to hedge one's bets, the amount sent to the different consumers was chosen to be fairly equal. The different water amounts added together then made up the total water amount in the system. This simplification was rather gross, and in the hindsight's spirit, this should have been

carried out differently. By doing some research, it would have been possible to figure out used typical water amounts for the different types of equipment.

The heat exchangers in the ventilation system and in the district-heating system were derived using first order differential equations. Their thermal abilities, like heat-transmission time constants, were given when initializing the heat-exchanger transfer functions, which was done according to an example in Novakovic [1995]. This made sure that heat-exchanger characteristics became realistic. However, the values should have been evaluated in terms of which application they were applied to. The heat transmissions might have been too quick and therefore unrealistic. This could have been done differently by obtaining the characteristics of similar systems, and apply these in the model. However, even though the heat-transmission time constants had been more realistic, this would not have affected the comparison of the control schemes. When it comes to the radiators in the model, these were modeled using a heat balance, and it was assumed that the valves in the radiators were perfect[1](see Figure 2.8), which is not realistic. However, exact radiator dynamics was not a particular goal during the modeling. Initially, they were modeled simply by using a time delay, but because this created problems during the linearization of the model, the heat-balance model had to be used.

Despite the simplifications (some of them harsh) that were carried out when deriving the model, it should be emphasized that the model is suited for its purpose. The goal was to derive a model such that one could examine how the system responded when different control schemes were tested. As stressed above, it was not a defined goal to derive a model as realistic as possible. It was important that the model captured the most fundamental thermal relations in a building, and last but not least, that the model was fitted for optimization. Simulating completely realistic models often tend to be time consuming, which makes simplification of the model necessary in order for the MPC to be able to run in real time. The mentioned simplifications were carried through to keep the model complexity and thus the number of states at a moderate level.

[1]No dynamics, no slack. The valves opening were determined by a number between 0 and 1.

6.2 Implementation and working procedure

One of the items in the feature-work section in Magnussen [2010] was to become independent of `Simscape`, because `MATLAB` functions like `linmod(system)` could not be used in `Simscape`. The reason why `Simscape` was used in the first place, was because the electrical analogy used in the model could be implemented by using electrical components instead of transfer functions, which made the implementation less complex. Becoming independent of `Simscape` was cumbersome, especially since the model had been augmented with two additional rooms, a ventilation system, and a more complex heating system than in Magnussen [2010].

A matter that should seem obvious when deriving and implementing large models, is to test the model thorough in between the augmentations. In particular if the model is going to be used in further analysis. However, this was not done thorough enough, and this caused problems when the model was to be linearized. Different approaches were tested in the pursuit of a correct linearized model. When the linearization of the entire system did not behave as is should, the model was dismantled and re-linearized until it turned out that the radiators were implemented in a way that kept the linearization from becoming correct. The problem was that the radiators' internal controllers contained saturation and anti wind-up abilities, and this made the behavior from the defined system input to the system outputs not obtainable. Saturation is highly nonlinear and the `MATLAB` function that included anti wind-up was discontinuous, which make linearization very difficult(Imsland [2011]). However, when the radiators were modeled using a heat balance, the linearized model became correct. Testing the model underway will delay the implementation in some extent, but in the long run it is actually likely to be time saving.

6.3 Control schemes

6.3.1 Conventional scheme

In order to be able to evaluate the proposed MPC scheme, a conventional control scheme was introduced in Chapter 3 as a foundation of comparison. In this scheme, the supply-water temperature varies in an approximately linear manner with respect to the outdoor temperature. The amount of available energy using this scheme never becomes low enough to slow down

the temperature responses in the system. Thus, the temperature responses are dependent on the dynamics of the radiators and heat exchangers. This results in a quickly-responding system that is robust considering that it will be able to handle large variations in disturbances. On the other hand, such control schemes do not seem to be very energy efficient with regard to available amount of energy versus used amount of energy. Nevertheless, as implied in both Djuric et al. [2007] and in Nilsson et al. [2003], this is the most common way to control the supply-water temperature. A robust control scheme is naturally important, and this scheme is undoubtedly robust, but it seems unnecessary that the supply-water temperature should be that high (see Figure 3.1). As implied in Chapter 1, it seems like a majority of the research within energy efficiency in buildings concern improvement of low-level control schemes. However, the author of this thesis believes that minimization of the supply-water temperature will lead to increased energy efficiency.

6.3.2 MPC scheme

This was the main purpose of the thesis, and the reason why an MPC scheme was introduced. A model forms the basis of an MPC scheme, so it was important that the derived model was both accurate, but also that its complexity level was limited. This was ensured by, among others, leaving out the district-heating dynamics and the thermal disturbances. As mentioned before, the matrices that are obtained when linearizing the system can be badly scaled, which again may affect the optimization problem negatively. However, it turned out that the scaling did not improve the MPC scheme's behavior, such that the proposed scaling introduced in Section 4.2.2 was left out.

Since only 4 of the 17 states in the model were measured, a state estimator had to be included such that the MPC could be provided with an estimate of the total state vector. A Kalman filter was used because it is fairly easy to implement and not complex to tune. The estimates obtained by the Kalman filter deviated more or less from their real values, but the responses were similar. However, deviations in some of the estimates led to problems during the optimization. The linearized model turned out to be unobservable, which caused problems in the estimation. Errors in the estimates of state 4 and 5 in particular caused one of the output constraints in the optimization problem to be repeatedly violated. Recall that this problem was resolved by increasing the system input's lower constraint. The controller would have become more robust if the estimates had been fixed instead of including this

ad-hoc solution, and this reveals another shortcoming in the control scheme. Adding an additional measurement at state 4 or 5 could have made the model observable, which again could have improved the estimates. Changing the model or improving the initial conditions in the Kalman filter may also have improved the estimates (Imsland [2011]). On the other hand, increasing the system input's lower constraint to 35 $^{\circ}C$ was a decent solution in this thesis, because when the supply-water temperature is 35 $^{\circ}C$, the control valve in the ventilation system is almost entirely open. However, if the system had been dimensioned differently, the system input could have been decreased further. According to Nilsson et al. [2003], the supply-water temperature should not be lower than 65 $^{\circ}C$ because hot tapping water has to be ensured. However, by studying Figure 15 in Djuric et al. [2007], it is seen that hot tapping water constitutes a negligible part of the energy consumption. This demand is therefore ignored in this thesis. Hot water can be provided by a separate supply line, for example. It seems unnecessary that the temperature of the main water supply to the building have to be kept as high as 65 $^{\circ}C$ to satisfy the least prominent consumer.

Tuning and results

Choosing the correct tuning parameters is important in order for the MPC to function in an optimal manner. All the tuning parameters were kept constant when simulating the system with the two MPC schemes, such that comparison of the results should make sense. The initial tuning parameters suggested in Section 4.5 turned out to function well. Recall that the control horizon should be chosen to be large enough such that no additional inputs to the system are necessary. θ_{ref}^{MPC} in both Figure 4.12 and Figure 4.17 settles to constant values after 140 and 90 minutes, respectively, which imply that no additional inputs are needed after this. $H_u = 35$ (175 minutes) covers this with a safe margin. The prediction horizon was kept equal to 50. This may seem odd since according to the mentioned rule of thumb, the prediction horizon should be chosen to be equal to, or larger than, the largest time constant in the system. However, this turned out to be unnecessary. When the system was simulated with $H_p = 450$ and $H_u = 80$, the results remained almost identical (compare Figure 6.1 and Figure 4.6a). The corresponding indoor temperature responses using these horizons are found in Appendix B. Besides, long prediction horizons can lead to numerical problems when calculating $\mathbf{\Psi}$ (4.12), especially in unstable plants (Maciejowski [2002]). As de Jager [2004] implies, the prediction horizon should be limited if it does not affect the system response negatively.

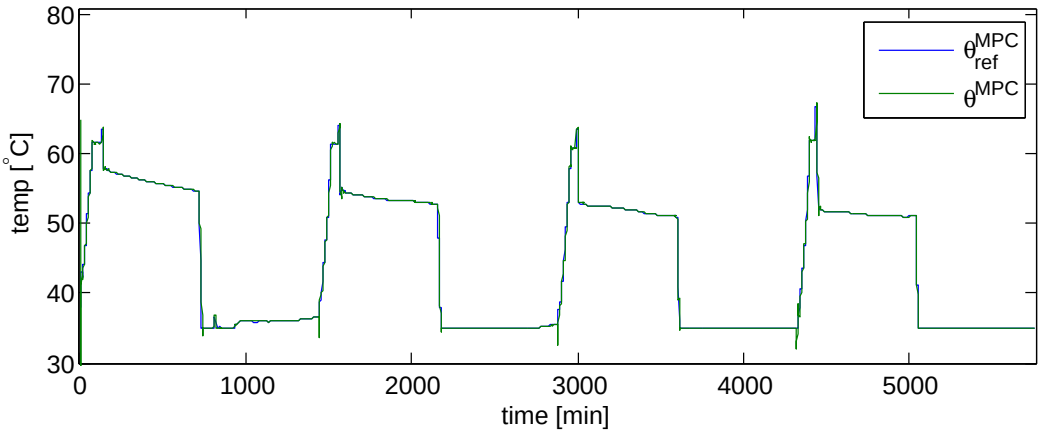

Figure 6.1: The behavior of the MPC-generated reference (θ_{ref}^{MPC}) does not get affected by longer control or prediction horizons.

As mentioned before, infeasible problems were handled by setting $\Delta u(k) = 0$, thus use the same input as in the previous time step. This approach was not very sophisticated, and this combined with the ad-hoc solution where $\hat{\boldsymbol{y}}(k)$ periodically acted as output constraints, are likely to be the main reason for the peaks and out-of-level behavior of θ_{ref}^{MPC} after every night-to-day switch. Both the these ad-hoc solutions and the unequal behavior of θ_{ref}^{MPC} were eliminated after the slack variables were introduced.

Recall that the constraints on the change of system input (Δu) were chosen to be $-5 \leq \Delta u \leq 5$. These values were arbitrarily chosen. If these constraints had been chosen to be less strict, $-10 \leq \Delta u \leq 10$, for example, θ_{ref}^{MPC} could have avoided the overshoot and to reach high temperatures like 80 $^{\circ}C$. This is because the radiators would have increased their temperatures faster if θ_{ref}^{MPC} could increase by 10 $^{\circ}C$ each time step, and thereby reached their desired values as quick as before. On the other hand, in terms of the different abilities of different heat exchangers, the chosen constraints on Δu seemed to be appropriate. Another measure that could have been taken to avoid such high values of θ_{ref}^{MPC}, is to penalize violations of the slack variables in a less strict manner. But, since θ_{ref}^{MPC} only is 80 $^{\circ}C$ for a few minutes before settling on a lower value, the tuning of the MPC seem to be satisfying. However, by applying an optimal set of tuning parameters, the overshooting response that reached 80 $^{\circ}C$ could have been avoided.

Now, when the control schemes have been presented and the system has been simulated with all of them, it seems obvious that either Case 1 or Case 3 should be chosen. The ordinary MPC formulation in Case 2 is really a

checkpoint towards the robust formulation in Case 3. Besides, since Case 3

Table 6.1: Comparison of results. The conventional Case 1 is basis for comparison.

	Night-to-day behavior				Energy reduction potential	Used amount of available energy
	θ_{2A}	θ_{2B}	θ_{2C}	θ_7		
Case 1	26 min	48 min	88 min	1 min	-	13.45 %
Case 2	62 min	88 min	133 min	43 min	34 %	20.29 %
Case 3	26 min	53 min	97 min	11 min	32.92 %	20.03 %

is almost as energy efficient as Case 2, in addition to its superior behavior, and the fact that it is more robust, the choice between these two is obvious. Deciding between Case 1 and Case 3 on the other hand, is a matter of traditional and well known versus ambitious but unknown, since the indoor temperature responses are pretty similar. The fact that it takes 9 extra minutes to heat up an office landscape (room C) is nothing to speak of.

Potential improvements

Getting the Kalman-filter to work properly such that some of the ad-hoc solutions could have been eliminated, should have been prioritized. A nimbly solution that probably would have improved the estimates, is to add additional measurements. However, this would increase the investment in terms of additional sensors, besides, in a real application not all states are measurable. Another measure is to add integral action in the estimator, and through knowledge about the system states, removed the stationary errors between estimate and state.

Computational complexity is another major concern when solving constrained optimization problems (Maciejowski [2002]), and no measures were taken to handle this. The computational complexity can be reduced using input blocking, by forcing the input to remain the same over a certain amount of samples (Cagienard et al. [2007]). It is shown that input blocking provides good results for stable systems.

If the optimization problem had been formulated differently, the ad-hoc solution on the output constraints and the introduced slack variables might have been unnecessary. Recall that the matrix that penalizes deviations from the

desired trajectory ($\boldsymbol{Q}$) was set to be $diag(0, \cdots, 0)$ since no desired trajectory was defined. If a desired trajectory had been created, the feasibility problems during the transition from night to day would not have been an issue. This could have been done by defining an additional optimization problem that calculates an optimal desired input trajectory that would have been inserted into the main optimization problem. This is also a matter of software and would not demand extraordinary components in the building's automation system. However, the computational complexity would have been increased because of the additional optimization problem.

It was mentioned above that the pipe dimensions and water amounts in the system were chosen unwisely. Both the energy reduction potential and the amount of used energy could have been improved if the system had been dimensioned in an optimal manner. The indoor temperature responses in both the MPC schemes (Figure B.1 and Figure 4.15) indicate that the valve position in the radiators were more closed than open. As apposed to this, the valve position in the ventilation system was accordingly more open than closed (Figure 4.9a and Figure B.3). If more water had been sent to the ventilation system, this would have increased the percentage of used amount of available energy. However, this must be carried out with caution such that the indoor temperature responses do not get too slow.

6.4 Credibility

The life span of buildings can be 10, 20 or 50 years. Such long lasting systems impose substantial demands when it comes to reliable control systems. Thorough testing and further development is an absolute requirement if an MPC scheme is going to be considered implemented in a building. In many ways, it is the building owners that set the pace for development of smart solutions in the construction industry. If the owner is renting out the building, running costs are probably not a high priority, which makes development of new technology, like the proposed MPC scheme, uninteresting. However, on a long-term basis, a well-developed MPC scheme is likely to be economically beneficial, which is interesting if the building owner is going to use the building. It should be repeated that the imposed high-level control scheme in principle only need to be developed one time. The intention is that it should be applicable in every existing building containing a waterborne heating system. Nevertheless, testing have to be carried out before the control scheme is put into use, but this cost represents a drop in the ocean considering the

long-term energy-saving potential.

It should be mentioned that according to Nilsson et al. [2003], the largest potential for increasing the energy efficiency in commercial buildings is to decrease the internal heat generation, thus make the cooling systems more efficient. Nevertheless, this may not be true in countries with cold winters, like Norway. Actually, in Grini et al. [2009], it is seen that 46.7 % of the delivered energy to Bassengbakken 1 is used to heat up ventilation and room temperatures. As apposed to this, cooling of ventilation and room temperatures represent 9 % of the delivered energy. This imply that there is a lot of energy to be saved if the heating process of an office building is carried out in an optimal manner.

Chapter 7

Conclusion and Further Work

7.1 Conclusion

Throughout this thesis, a mathematical model of a building, including its ventilation system and a heating system has been used to simulate indoor temperature responses when different control schemes has been applied. A conventional control scheme and two MPC schemes that generated supply-water-temperature references in different manners were compared. The simulations implied that a considerable amount of energy can be saved when using the MPC schemes. Given that a substantial amount of the supplied energy to Bassengbakken 1 is used for heating purposes, the 33 % - 34 % energy reduction potential imply that energy can be saved by introducing an MPC control scheme. The MPC's ability to minimize an objective function and maintaining defined system demands at the same time, makes it highly suitable for increasing the energy efficiency in buildings.

Case 2 had a greater energy reduction potential than Case 3, however, the controller in Case 3 was more robust and the system responses were superior when this was applied. If an MPC scheme is to be implemented, Case 3 is recommended. It was also interesting to ascertain that the generated system inputs remained unchanged when using a finite and relatively small prediction horizon, as well as a long prediction horizon. If the water amounts in the system had been chosen differently, the used amount of the available energy would have been improved. Regardless of this, this thesis implies that the energy efficiency in buildings can be increased if an MPC scheme is implemented.

7.2 Further work

Modeling

If heat losses to the surroundings from the ventilation system, and especially from the district heating system, are included in the model, this may highlight the importance of keeping the supply-water temperature as low as possible in a more distinct degree.

Optimization

It should be a top priority to ensure that the state estimator is able to obtain accurate estimates. This will make the control system more robust, and it will make some of the ac-hod solutions superfluous. Another measure that may increase the robustness of the system, is to add an additional optimization problem that calculates optimal set-points for the MPC controller. By doing this, the optimizer do not have to depend on the slack variables when increasing the supply-water temperature from night to day.

Low-level control

It should be considered to optimize the low-level controllers in the system. Even though this will make the control scheme tailor made, and therefore building specific, this may decrease the actual energy consumption.

Include energy prices

In order to increase the energy efficiency further, electricity prices may be included as a variable in the optimization problem. If hourly electricity prices are available, the optimizer can predict how they vary and thus initiate high energy-demanding tasks when the prices are low, and vice versa. These mentioned items may help leading the proposed MPC scheme forward towards a future realization.

Nomenclature

Building

θ_6 $[°C]$ Outdoor air temperature

θ_{16C} $[°C]$ Wall temperature (mass center), towards outdoor air, Room C

θ_{1AC} $[°C]$ Wall temperature (mass center), towards room A, Room C

θ_{1BC} $[°C]$ Wall temperature (mass center) between room B and C

θ_{2C} $[°C]$ Room air temperature, room C

θ_{36C} $[°C]$ Wall surface temperature, towards outdoor air, Room C

θ_{3AC} $[°C]$ Wall surface temperature, towards room A, Room C

θ_{3BC} $[°C]$ Wall surface temperature, towards room A, Room C

θ_{3BC} $[°C]$ Wall surface temperature, towards room A, room C

θ_{3CA} $[°C]$ Wall surface temperature, towards room C, Room A

θ_{3CB} $[°C]$ Wall surface temperature, towards room C, Room B

θ_{3CB} $[°C]$ Wall surface temperature, towards room C, room B

θ_{4C} $[°C]$ Radiation temperature, room C

θ_{5C} $[°C]$ Window surface temperature, room C

θ_{7C} $[°C]$ Ventilation air temperature, room C

A_{ob} $[m^2]$ Area of an object

C_{2C} $[W/K]$ Capacity of room air, room C

C_{6C} $[W/K]$ Outer wall capacity, Room C

C_{AC} $[W/K]$ Capacity of wall between room A and C

C_{BC} $[W/K]$ Capacity of wall between room B and C

H $[m]$ Room height

h_{mat} $[W/m^2K]$ Convective heat-transmission coefficient of a material

k_{eC} $[W]$ Heat ratio due to electrical equipment, room C

k_{eC} $[W]$ Heat ratio due to lighting, room C

k_{eC} $[W]$ Heat ratio due to people, room C

R_{10C} $[K/W]$ Convective heat transport from radiator to room air, room C

R_{16C} $[K/W]$ Convective thermal resistance of wall (mass center) towards outdoor air, Room C

R_{1tC} $[K/W]$ Resultant thermal resistance of wall (mass center) towards outdoor air, Room C

R_{26C} $[K/W]$ Convective thermal resistance of wall (mass center) towards outdoor air, Room C

R_{2AC} $[K/W]$ Convective thermal resistance of wall (mass center) between room A and C

R_{2BC} $[K/W]$ Convective thermal resistance of wall (mass center) between room B and C

R_{2tBC} $[K/W]$ Resultant thermal resistance of room air, room C

R_{36C} $[K/W]$ Convective thermal resistance of wall surface towards outdoor air, room C

R_{3AC} $[K/W]$ Convective thermal resistance of wall surface towards room A, room C

R_{3BC} $[K/W]$ Convective thermal resistance of wall surface towards room B, room C

R_{3tAC} $[K/W]$ Resultant thermal resistance of wall (mass center) between room A and C

R_{3tBC} $[K/W]$ Resultant thermal resistance of wall (mass center) between room A and C

R_{4tC} $[K/W]$ Resultant thermal resistance of wall surface towards outdoor air, Room C

R_{5C} $[K/W]$ Convective thermal resistance of window surface, room C

R_{5tC} $[K/W]$ Resultant thermal resistance of wall surface towards room A, Room C

R_{6tC} $[K/W]$ Resultant thermal resistance of window surface, Room C

R_{7C} $[K/W]$ Convective heat transport with ventilation air, room C

R_{8C} $[K/W]$ Convective heat transport with infiltration air, room C

R_{9C} $[K/W]$ Thermal radiation from radiator, room C

T_{1C} $[s]$ Time constant of wall (mass center) towards outdoor air, Room C

T_{2C} $[s]$ Time constant room air, room C

T_{3C} $[s]$ Time constant of wall (mass center) between room A and C

T_{4C} $[s]$ Time constant of wall (mass center) between room B and C

U_{mat} $[W/m^2K]$ U-value of a material

W_{eC} $[W]$ Heat emitted from electrical equipment, room C

W_{lC} $[W]$ Heat emitted from lighting, room C

W_{pC} $[W]$ Heat emitted from people, room C

Heating system

α [-] Valve opening in the radiator, room C

ρ_{mat} $[kg/m^3]$ Density of a material

θ $[^\circ C]$ Temperature of supply water that is sent into the building

θ^{conv} $[^\circ C]$ Temperature of supply water that is sent into the building using a conventional scheme

θ^{MPC} $[^\circ C]$ Temperature of supply water that is sent into the building using an MPC scheme

θ_4^{out} $[^\circ C]$ Temperature of water flowing out of a radiator

θ_{fb} $[^\circ C]$ Temperature of water flowing out of the building into the heat exchanger

θ_{hi}^{dh} $[^\circ C]$ Temperature of water flowing into the heat exchanger

θ_{ho}^{dh} $[^\circ C]$ Temperature of water flowing out of the heat exchanger

θ_i^{dh} $[^\circ C]$ Temperature of water flowing from a district heating distribution line into the heat exchanger

θ_{mi}^{dh} $[^{\circ}C]$ Temperature of water flowing out of the district heating main supply

θ_{mo}^{dh} $[^{\circ}C]$ Temperature of water flowing back to the district heating main supply

θ_{o}^{dh} $[^{\circ}C]$ Temperature of water flowing out of the heat exchanger, back to the district heating distribution

θ_{ref} $[^{\circ}C]$ Reference temperature of supply water that is sent into the building

θ_{ref}^{conv} $[^{\circ}C]$ Reference temperature of supply water that is sent into the building using a conventional set-point scheme

θ_{ref}^{MPC} $[^{\circ}C]$ Reference temperature of supply water that is sent into the building using an MPC set-point scheme

θ_{tb} $[^{\circ}C]$ Temperature of water flowing out of the heat exchanger into the building

C_{4C} $[W/K]$ Capacity of the radiator, room C

c_{mat} $[J/kgK]$ Specific heat capacity of a material

$f_{CP}^{dh}(z)$ [-] Control port valve characteristic in shunt connection towards district heating

$f_{SP}^{dh}(z)$ [-] Shunt port valve characteristic in shunt connection towards district heating

Q_{4C} $[W]$ Heat dissipation from the radiator to the surroundings, room C

R_{CP}^{dh} [-] Water-flow relationship between water flow through entirely open and closed control valve

R_{SP}^{dh} [-] Water-flow relationship between water flow through entirely open and closed shunt valve

T^{dh} $[s]$ Time constant of heat exchanger in the district-heating system

T_{5C} $[W]$ Time constant of the radiator, room C

z^{dh} [-] Valve opening of shunt connection

Ventilation

$(UA)_h$ $[W/K]$ Heat exchanger's heat-transmission number

Δp_{CPz} $[Pa]$ Pressure drop over an open control port

Δp_{IIIz} $[Pa]$ Pressure drop over the shunt pipe by an open shunt valve

Δp_{IIz} $[Pa]$ Pressure drop over the pipe lines A and B

Δp_{SPz} $[Pa]$ Pressure drop over an open shunt port

$\dot{m}_7$ $[kg/s]$ The ventilation air amount

$\dot{m}_8$ $[kg/s]$ The infiltration air amount

$\dot{m}_a$ $[kg/s]$ Air flow through heat exchanger

$\dot{m}_w$ $[kg/s]$ Water flow through heat exchanger

$\dot{Q}_{CP}$ $[m^3/s]$ Water amount through the control valve

$\dot{Q}_{max}$ $[m^3/s]$ Maximum flow through a valve (z = 1)

ϵ_a [-] Relative air heating

ϵ_w [-] Relative water cooling

θ_h $[^\circ C]$ Metal temperature in heat exchanger

θ_{ai} $[^\circ C]$ Air temperature flowing into the heat exchanger

θ_{ao} $[^\circ C]$ Temperature of the air flowing out of the heat exchanger

θ_{hi} $[^\circ C]$ Temperature of water flowing into the heat exchanger

θ_{ho} $[^\circ C]$ Temperature of water flowing out of the heat exchanger

θ_{mi} $[^\circ C]$ Temperature of water flowing out of the building's main supply

θ_{mo} $[^\circ C]$ Temperature of water flowing back to the building's main supply

θ_{wi} $[^\circ C]$ Water temperature flowing into the heat exchanger

θ_{wo} $[^\circ C]$ Water temperature flowing out of the heat exchanger

$f_{CP}(z)$ [-] Valve characteristic control valve

$f_{SP}(z)$ [-] Valve characteristic shunt valve

K_h $[s]$ Transfer function gain

k_{vs} [-] Capacity number

m_{ob} $[kg]$ Mass of an object

q [-] Relative water flow through the control valve

q_s [-] Relative water flow through the shunt valve

$R_{CP}(z)$ [-] Water-flow relationship between water flow through entirely open and closed control valve

$R_{SP}(z)$ [-] Water-flow relationship between water flow through entirely open and closed shunt valve

T_h [s] Heat exchanger time constant

z [-] Valve opening of the shunt connection

Bibliography

Enno Abel and Arne Elmroth. *Buildings and Energy - a systematic approach.* Formas, 1st edition, 2007.

Robert Grover Brown and Patrick Y.C. Hwang. *Introduction to Random Signals and Applied Kalman Filtering.* John Wiley and Sons, Ltd, 3rd edition, 1997.

Byggforsk. Byggforskserien: Varmeisolasjonsmaterialer - Typer og egenskaper, 2004.

R. Cagienard, P. Grieder, E.C. Kerrigan, and M. Morari. Move Blocking Strategies in Receding Horizon Control. *Journal of Process Control*, 17(6): 563–570, 2007.

Chi-Tsong Chen. *Linear System Theory and Design.* Oxford University Press, Inc, 3rd edition, 1999.

Bram de Jager. The horizon in predictive energy storage control. In *American Control Conference*, Boston, Massachusetts, 2004.

Natasa Djuric, Vojislav Novakovic, and Frode Frydenlund. Heating system performance estimation using optimization tool and BEMS data. *Energy and Buildings*, 40:1367–1376, 2007.

Olav Egeland and Jan Tommy Gravdahl. *Modeling and Simulation for Automatic Control.* Tapir akademisk forlag, 1st edition, 2002.

Anne Mai Ersdal. Methods for Ice Model Updating Using a Mobile Sensor Network. Master's thesis, Norwegian University of Science and Technology, 2011.

Cathrine Grini, Hans-Martin Mathisen, Igor Sartori, Matthias Haase, Helle Wølhk Jæger Sørensen, Arnkell Petersen, Ida Bryn, and Tore Wigenstad. LECO – Energibruk i fem kontorbygg i Norge. Technical report, SINTEF, 2009.

Dimitrios Gyalistras and Markus Gwerder. Use of Weather and Occupancy Forecasts For Optimal Building Climate Control (OptiControl): Two Years Process Report. Technical report, Terrestrial Systems Ecology ETH Zurich, Building Technologies Division, Siemens Switzerland Ltd., 2009.

Eivind Hiis Hauge and Jon Andreas Støvneng. *Grunnleggende fysikk - klassisk mekanikk og varmelære*. Tapir akademisk forlag, 1st edition, 2009.

Lars Imsland. Introduction to Model Predictive Control. Note on MPC - Norwegian University of Science and Technology, 2007.

Lars Imsland. Personal conversation with supervisor, 2011.

Eric C. Kerrigan. Webpage: http://www.control.eng.cam.ac.uk/jmm/mpcbook/software/software.html. Page read 01.06.2011, 1999.

Hassan K. Khalil. *Nonlinear Systems*. Prentice-Hall, Inc, 3rd edition, 2002.

Jan F. Kreider, Peter S. Curtiss, and Ari Rabl. *Heating and Cooling of Buildings - Design for Efficiency*. McGraw-Hill Higher Education, 2nd edition, 2002.

Jan Marian Maciejowski. *Predictive Control with Constraints*. Pearson Education Limited, 1st edition, 2002.

Jonas Magnussen. Increased Energy Efficiency in Buildings using Model Predictive Control. Technical report, Norwegian University of Science and Technology, 2010.

MathWorks. Webpage: http://www.mathworks.com/help/toolbox/control/ref/obsv.html. Page read 20.05.2011, 2011.

Petru-Daniel Morosan, Romain Bourdais, Didier Dumur, and Jean Buisson. Building temperature regulation using a distributed model predictive control. *Energy and Buildings*, 42:1445–1452, 2010.

Per Erik Nilsson, Enno Abel, Roger Clark, Lars E. Ekberg, Per Fahlèn, P. Ole Fanger, Klaus Fitzner, Lars Gunnarsen, Lennart Jagemar, Peter V. Nielsen, John L. Stoops, Anders Trüschel, and Pawel Wargocki. *Achieving the desired indoor climate - energy effiency aspects of system design*. Studentlitteratur, Lund, 1st edition, 2003.

Jorge Nocedal and Stephen J. Wrigth. *Numerical Optimization*. Springer, 2nd edition, 2006.

Vojislav Novakovic. Curriculum compendium in TEP15, NTH - The Norwegian Institute of Technology, 1995.

Frauke Oldewurtel, Alessandra Parisio, Colin N. Jones, Manfred Morari, Dimitrios Gyalistras, Markus Gwerder, Vanessa Stauch, Beat Lehmann, and Katharina Wirth. Energy Efficient Building Climate Control using Stochastic Model Predictive Control and Weather Predictions. *In Gyalistras and Gwerder [2009]*, 2009a.

Frauke Oldewurtel, Andreas Ulbig, Alessandra Parisio, and Manfred Morari Gran Andersson. Reducing Peak Electricity Demand in Building Climate Control using Real-Time Pricing and Model Predictive Control. *In Gyalistras and Gwerder [2009]*, 2009b.

Samuel Privara, Jan Siroky, Lukas Ferkl, and Jiri Cigler. Model predictive control of a building heating system: The first experience. *Energy and Buildings*, 43:564–572, 2010.

S. Joe Qin and Thomas A. Badgwell. An Overview Of Industrial Model Predictive Control Technology. *Control Engineering Practice*, 11:733–764, 2003.

Rockwool. Webpage: http://guiden.rockwool.no/media/61326/8-25.pdf. Page read 10.12.2010, 2010.

Leo Rollins. Robust Control Theory. Technical report, Carnegie Mellon University, 1999.

Gaurang Shah and Sebastian Engell. Tuning MPC for Desired Closed-Loop Performance for SISO Systems. In *18th Mediterranean Conference on Control and Automation*, Marrakech, Morocco, 2010.

Dan J. Simon. *Optimal State Estimation.* John Wiley and Sons, Ltd, 1st edition, 2006.

Jan Siroky, Frauke Oldewurtel, Jiri Cigler, and Samuel Privara. Experimental analysis of model predictive control for an energy efficient building heating system. *Applied energy*, 88:3079–3087, 2011.

Sigurd Skogestad and Ian Postlethwaite. *Multivariable Feedback Control.* John Wiley and Sons, Ltd, 2nd edition, 2008.

Appendix A

Calculation of Thermal Values

A.1 Building

The electrical elements in Figure 2.2 and Figure 2.3 in Section 2.2 have to be determined in order to get the model to behave realistically. There are a set of determination rules in Novakovic [1995], and these will be the base of the following calculations. Specific thermal values are taken from Grini et al. [2009]. The model contains convective thermal resistors, in addition to thermal resistors due to radiation. Convection is heat transfered from a fluid in motion to a solid object, and radiation is the heat that is absorbed, reflected (or passed through) an object exposed of radiation (Hauge and Støvneng [2009]).

R_{16C} is the convective thermal resistance from the outside air through the outer part of the wall, and this can be calculated approximately as

$$R_{16C} \approx \frac{1}{U_{16C} A_{6C}}, \tag{A.1}$$

and has the denomination $[K/W]$ (all the thermal resistors have this denomination). U_{16C} represents the U-value [1] of the outer part of the wall. U-values are denominated $[W/m^2K]$. Typical U-values for outer walls are 0.2 W/m^2 - 0.4 W/m^2K. U_{16C} is set to be 0.25 W/m^2K. A_{6C} is the area of the outer

[1] Abel and Elmroth [2007] defines the U-value as the quantity of heat per unit time passing through a unit area of the structure when the difference in the temperature between each side of the structure is 1 $°C$.

walls in room C. From Figure 2.1 it can be seen that room C has two outer walls, $A_{6C} = (4.5 + 6) \cdot H = (4.5 + 6) \cdot 3\ m^2$.

R_{2AC} is the convective resistance from the thermal mass in the wall between room A and C to the inner surface of the wall, and is calculated in the same way as R_{16C}.

$$R_{2AC} \approx \frac{1}{U_{2AC} A_{AC}}, \tag{A.2}$$

where $U_{2AC} = 0.5\ W/m^2K$ and $A_{AC} = 4.5 \cdot 3\ m^2$.

$$R_{2BC} \approx \frac{1}{U_{2BC} A_{BC}}, \tag{A.3}$$

where $U_{2BC} = 0.5\ W/m^2K$ and $A_{BC} = 6 \cdot 3\ m^2$.

R_{36C} is a convective resistance from the inner surface of the outer wall, to the room air, and it is defined as

$$R_{36C} = \frac{1}{h_{36C} A_{6C}}, \tag{A.4}$$

where h_{36C} is the convective heat-transmission coefficient by the inner surface of the wall. It is set to $3\ W/m^2K$.

R_{3AC} is a convective resistance from the inner surface of the wall towards room A, to the room air, and is calculated as above

$$R_{3AC} = \frac{1}{h_{3AC} A_{AC}}, \tag{A.5}$$

where $h_{3AC} = h_{36C}$.

$$R_{3BC} = \frac{1}{h_{3BC} A_{BC}}, \tag{A.6}$$

$h_{3BC} = h_{36C}$.

R_{4C} is the radiation between from the window to the inner part of the wall.

$$R_{4C} = \frac{1}{h_{4C} A_{wC}} \tag{A.7}$$

h_{4C} is the radiation coefficient by the inner surface of the window, and is set to $5\ W/m^2K$. The window area (A_{wC}) is 25.8 % of A_C, which is the total room area.

Convective resistance between the window's inner surface and the room air, R_{5C}, is

$$R_{5C} = \frac{1}{h_{wC} A_{wC}}, \tag{A.8}$$

h_{wC} is set to 3 W/m^2K.

R_6 is the convective thermal resistance between the window and the outside air.

$$R_{6C} = \frac{1}{U_{wC} A_{wC}} - \frac{1}{\frac{1}{R_{4C}} + \frac{1}{R_{5C}}}, \tag{A.9}$$

$U_{wC} = 1.2$ W/m^2K.

R_{7C} is the convective heat transport from ventilation air to room air

$$R_{7C} = \frac{1}{\dot{m}_7 c_a}, \tag{A.10}$$

where $\dot{m}_7$ $[kg/s]$ is the ventilation-air amount, and $c_a = 1005$ J/kgK is the specific heat capacity of air. The ventilation provides an air exchange of 8.9 m^3/hm^2. In order to get the correct denomination, this air amount is multiplied by the air density and the area of the room, and divided by 3600 s.

R_{8C} is convective heat transport from the infiltration air[2] to the room air. This variable is often described as units of air changes per hour (Kreider et al. [2002]).

$$R_{8C} = \frac{1}{\dot{m}_8 c_a}, \tag{A.11}$$

where $\dot{m}_8$ $[kg/s]$ is the infiltration air amount in. Typical values for the infiltration air amount is 0.1 - 0.3 h^{-1}. However, in Bassengbakken 1, the air exchange per hour is 1.5 h^{-1}. This is multiplied by the air density and the volume of the room, and divided by 3600 s to get the correct denomination.

R_{9C} is the radiation between from the radiator to the wall surface

$$R_{9C} = \frac{1}{h_{rad} A_4 C}. \tag{A.12}$$

The area of the radiator (A_4C) is set to $0.75 \cdot 2$ m^2, while a typical value for h_{rad} is 7 W/m^2K.

R_{10C} is the convective thermal resistance between radiator and room air

[2]Kreider et al. [2002] defines infiltration air as uncontrolled airflow through all the little cracks and openings in a real building.

$$R_{10C} \approx |R_C^{PROD} - R_{9C}|, \tag{A.13}$$

where

$$R_C^{PROD} = \frac{\Delta\theta_{4C}}{P_C^{RAD}}. \tag{A.14}$$

$\Delta\theta_{4C}$ $[^\circ C]$ is the temperature difference between the radiator surface and the air temperature, while P_C^{RAD} $[W]$ is the radiators effect. These values were not defined in Grini et al. [2009] , and are therefore set arbitrarily to 30 $^\circ C$ and 3200 W, respectively.

Since there are only two types of walls, no ceiling and no floor, 3 heat capacities have to be calculated for the walls (outer walls, walls towards room A and B).

$$C_{6C}^{tot} = \delta_w A_{6C} \rho_{6C} c_{6C} \tag{A.15}$$

The outer walls consist of bricks (30.56 %), gypsum (6.11 %), insulation (55 %) (rock wool), and air gaps (8.33 %). $\delta_w = 0.36\ m$ is the total thickness of the wall.

$$\rho_{6C} = 0.3056\rho_{bricks} + 0.0611\rho_{gypsum} + 0.55\rho_{insulation} + 0.0833\rho_{air}, \tag{A.16}$$

where $\rho_{bricks} = 830\ kg/m^3$, $\rho_{gypsum} = 800\ kg/m^3$, $\rho_{insulation} = 1030\ kg/m^3$ and $\rho_{air} = 1005\ kg/m^3$.

c_{6C} is calculated in the same manner, where $c_{bricks} = 1800\ J/kgK$, $c_{gypsum} = 900\ J/kgK$ and $c_{insulation} = 31\ J/kgK$. The insulation values are taken from Rockwool [2010] and Byggforsk [2004].

The walls towards room A and B consist of gypsum (18, 03 %), air gaps (40, 98 %), and insulation (40, 98 %). Except from this different composition, C_{AC}^{tot} and C_{BC}^{tot} are calculated in the same manner as C_{6C}^{tot}.

The heat capacity of the air is dependent on the inventory in the room and the room air itself. $C_{inventory}$ is set to 50 times the C_{2C}, which is

$$C_{2C} = HA_C\rho_a c_a. \tag{A.17}$$

$C_{inventory}$ is contributions to the heat capacity from office furniture, books, computers and other equipment.

A.2 Ventilation

The introduced variables relative heating and relative cooling in Section 2.3.1 are calculated by using the heat exchanger's nominal (or design) temperatures. This means that these variables are valid in a neighborhood of the nominal values. The design temperatures are $\theta_{wi} = 70\ ^\circ C$, $\theta_{ai} = 18\ ^\circ C$, $\theta_{ao} = 45\ ^\circ C$. The nominal value of the outgoing water temperature is dependent of the remaining temperatures and is calculated by

$$\theta_{wo} = \theta_{wi} - \frac{\dot{m}_a \rho_a c_a}{\dot{m}_w \rho_w c_w}(\theta_{ao} - \theta_{ai}), \tag{A.18}$$

where $\rho_w = 1000\ kg/m^3$ and $c_w = 4200\ J/kgK$. $\dot{m}_a = 0.857\ m^3/s$ and $\dot{m}_w = 2.05 \cdot 10^{-4}\ m^3/s$ are the air flow and water flow through the heat exchanger, respectively. The heat exchanger consists of 67 % aluminum ($\rho_{alu} = 2700\ kg/m^3$, $c_{alu} = 900\ J/kgK$) and 33 % copper ($\rho_{cop} = 8900\ kg/m^3$, $c_{cop} = 390\ J/kgK$).

The pressure drops in Figure 2.6 are taken from an example in Novakovic [1995]. $\Delta p_{CP} = \Delta p_{SP} = 1736\ bar$ and $\Delta p_A = \Delta p_B = 150\ bar$. The relationships between the volume flows through an open valve and a closed valve are taken from the same example, $R_{SP} = R_{CP} = 50$.

A.3 Heating

The heat capacity of the radiator depends on its material and size.

$$C_{4C} = \delta_{4C} A_C^{rad} \rho_{steel} c_{steel}, \tag{A.19}$$

where $\delta_{4C} = 0.01\ m$, $\rho_{steel} = 7750\ kg/m^3$ and $c_{steel} = 460\ J/kgK$.

The heat exchanger's relative heating and cooling coefficients are calculated in the same manner as in the ventilation system, but the nominal values are slightly different. They are $\theta_{tb} = 78\ ^\circ C$, $\theta_{fb} = 48\ ^\circ C$ and $\theta_i^{dh} = 95\ ^\circ C$. θ_o^{dh} is calculated as (A.18).

$$\theta_o^{dh} = \theta_i^{dh} - \frac{\dot{m}_w^b \rho_w c_w}{\dot{m}_w^{dh} \rho_w c_w}(\theta_{tb} - \theta_{fb}), \tag{A.20}$$

$\dot{m}_w^b = 6.57 \cdot 10^{-4}\ m^3/s$ and $\dot{m}_w^{dh} = 6.57 \cdot 10^{-4}\ m^3/s$ are the water flows on the building side and district-heating side, respectively.

Appendix B

Additional plots

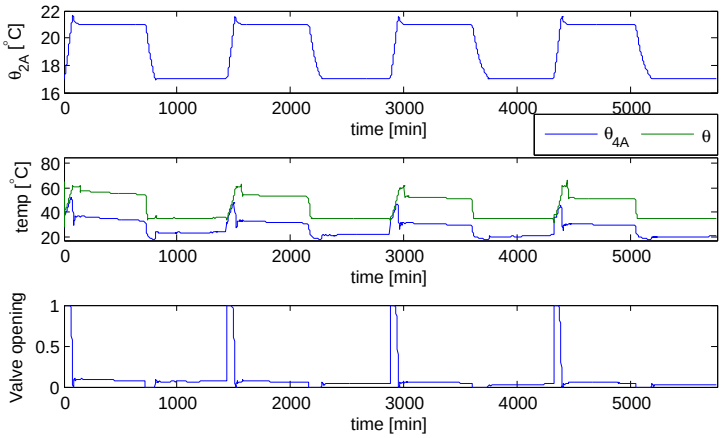

(a) Room A.

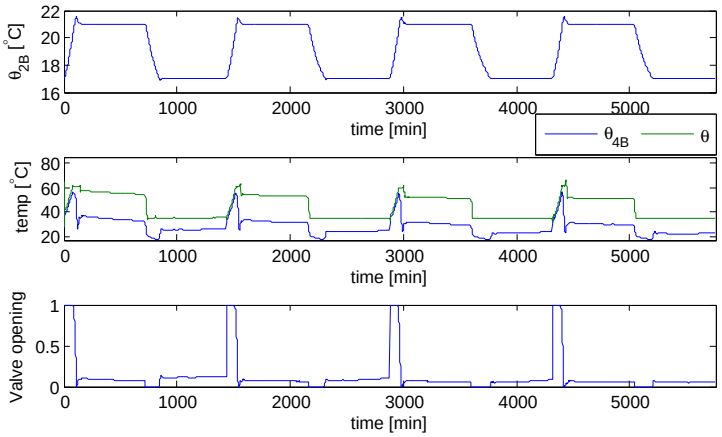

(b) Room B.

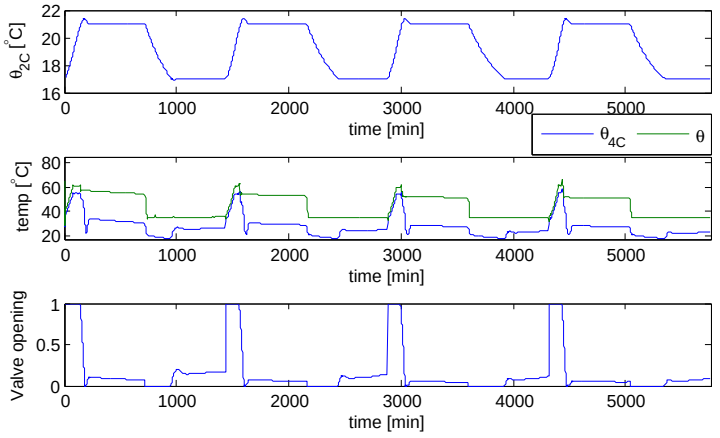

(c) Room C.

Figure B.1: Indoor temperature (θ_2), radiator temperature (θ_4), supply-water temperature (θ), and control-valve opening of the radiator using the MPC scheme (during 4 days).

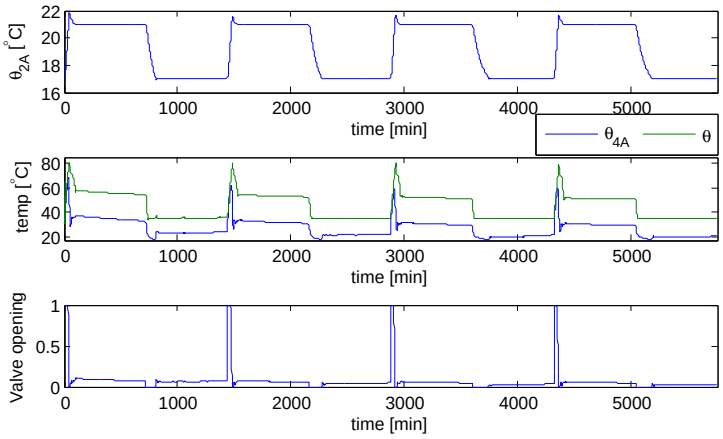

(a) Room A.

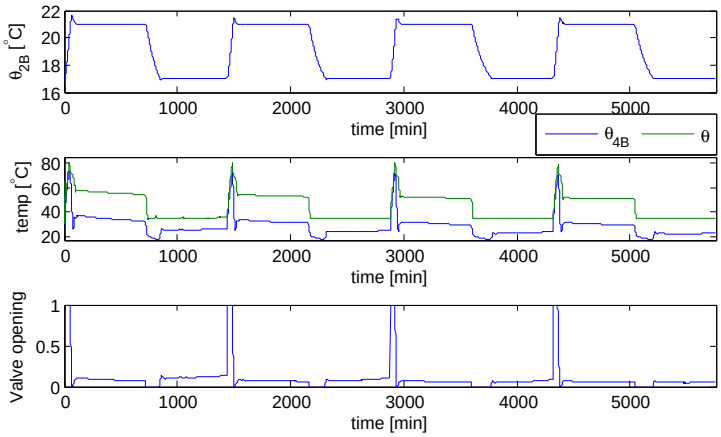

(b) Room B.

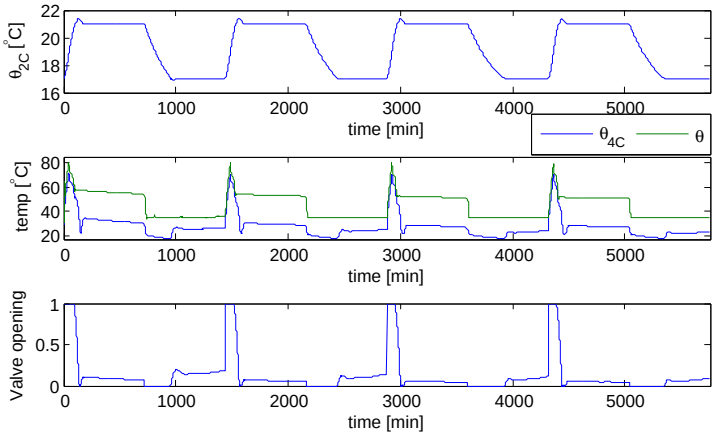

(c) Room C.

Figure B.2: Indoor temperature (θ_2), radiator temperature (θ_4), supply-water temperature (θ), and control-valve opening of the radiator using the robust MPC scheme (during 4 days).

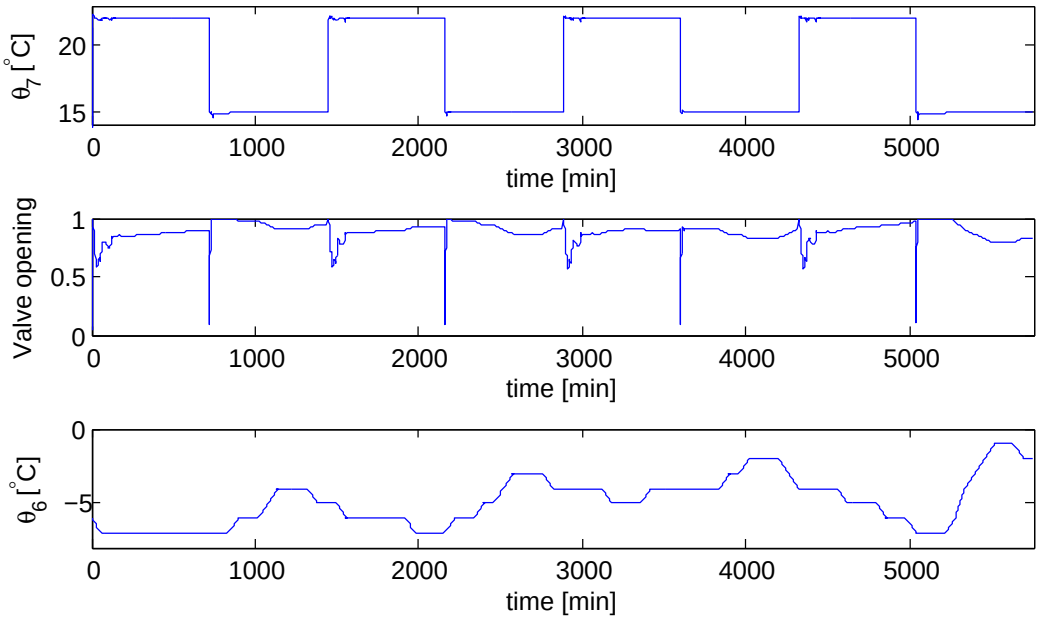

Figure B.3: Ventilation temperature (θ_7), control-valve opening, and outdoor temperature (θ_6) using the robust MPC scheme (during 4 days).

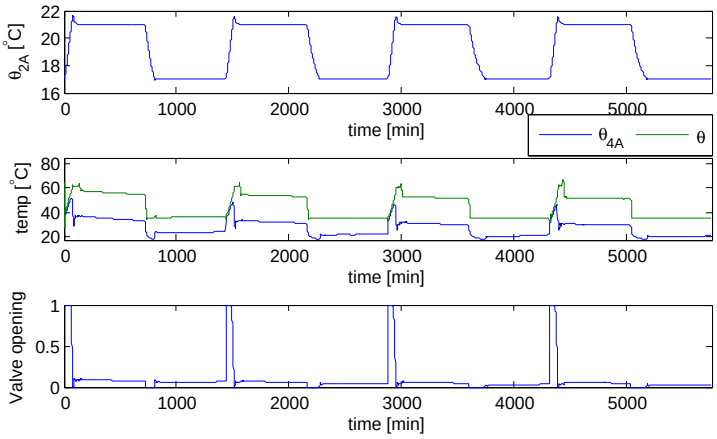

(a) Room A.

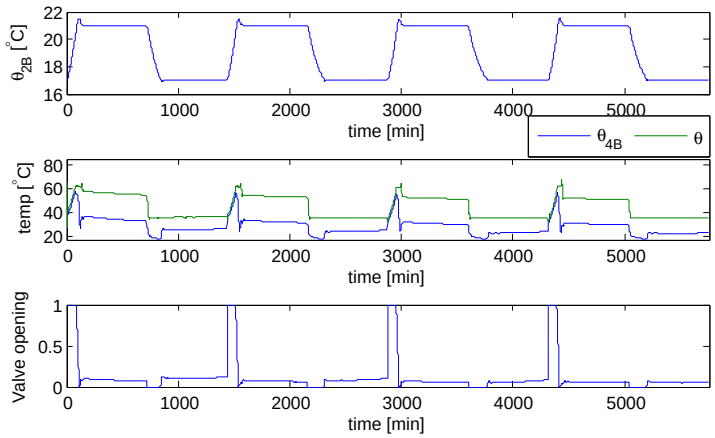

(b) Room B.

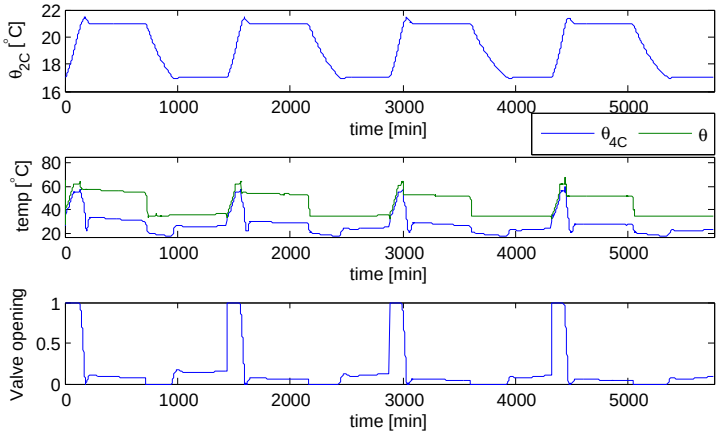

(c) Room C.

Figure B.4: Indoor temperature (θ_2), radiator temperature (θ_4), supply-water temperature (θ), and control-valve opening of the radiator using the MPC scheme with $H_p = 450$ and $H_u = 80$ (during 4 days).

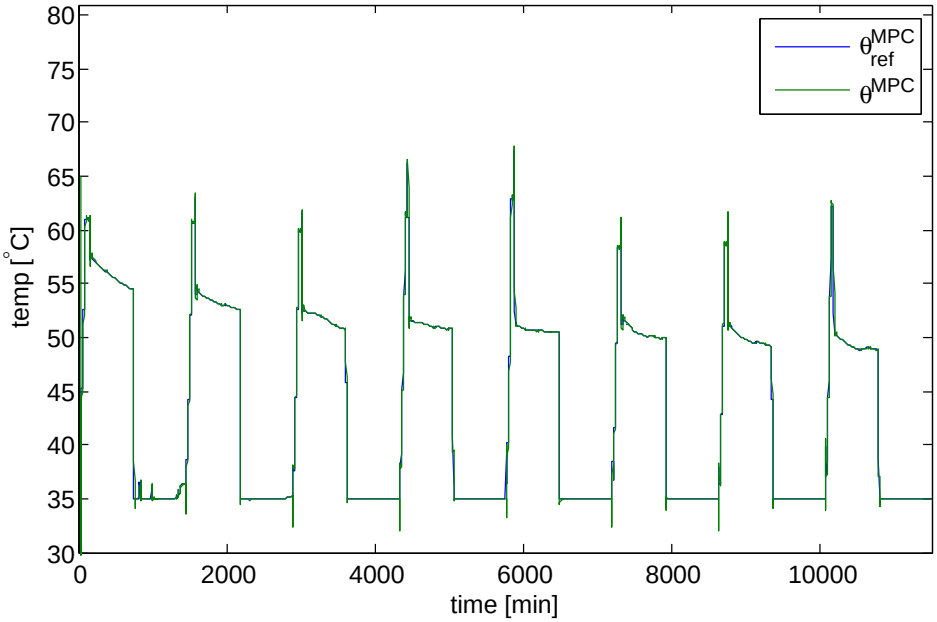

(a) Ordinary MPC scheme.

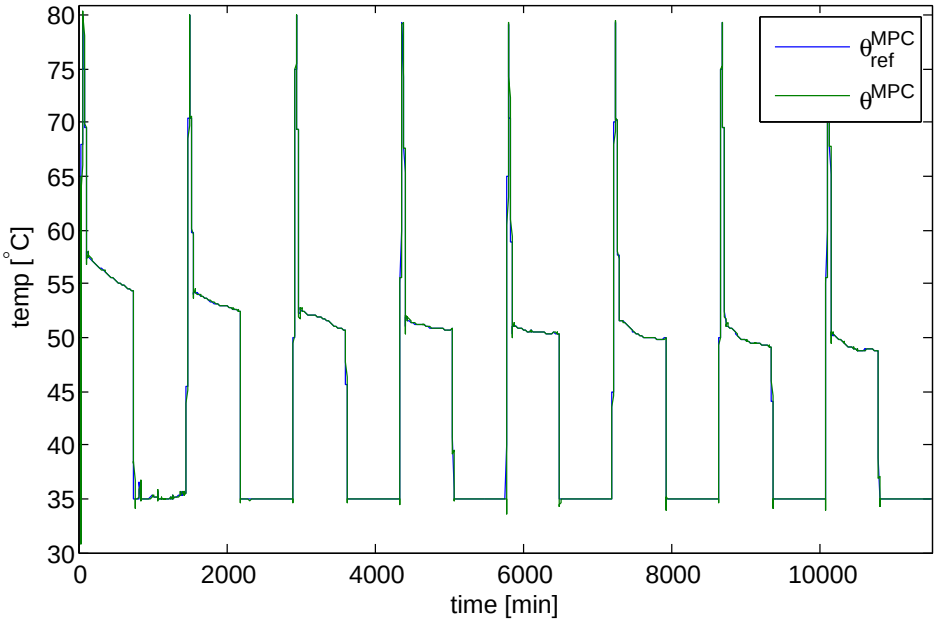

(b) Robust MPC scheme.

Figure B.5: Behavior of the MPC-generated reference (θ_{ref}^{MPC}), and the corresponding supply water temperature (θ^{MPC}) using the ordinary and the robust MPC scheme (during 8 days).

Appendix C

Simulink diagrams

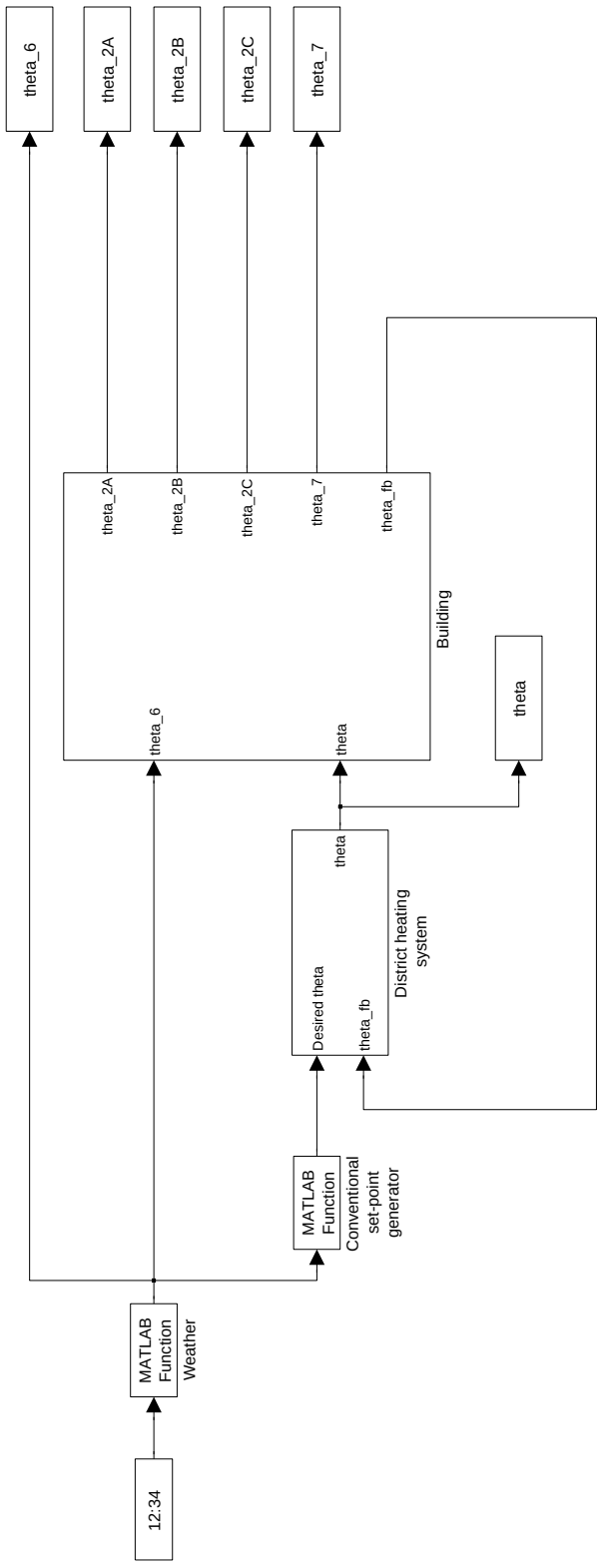

Figure C.1: The top-level Simulink diagram with a conventional control scheme.

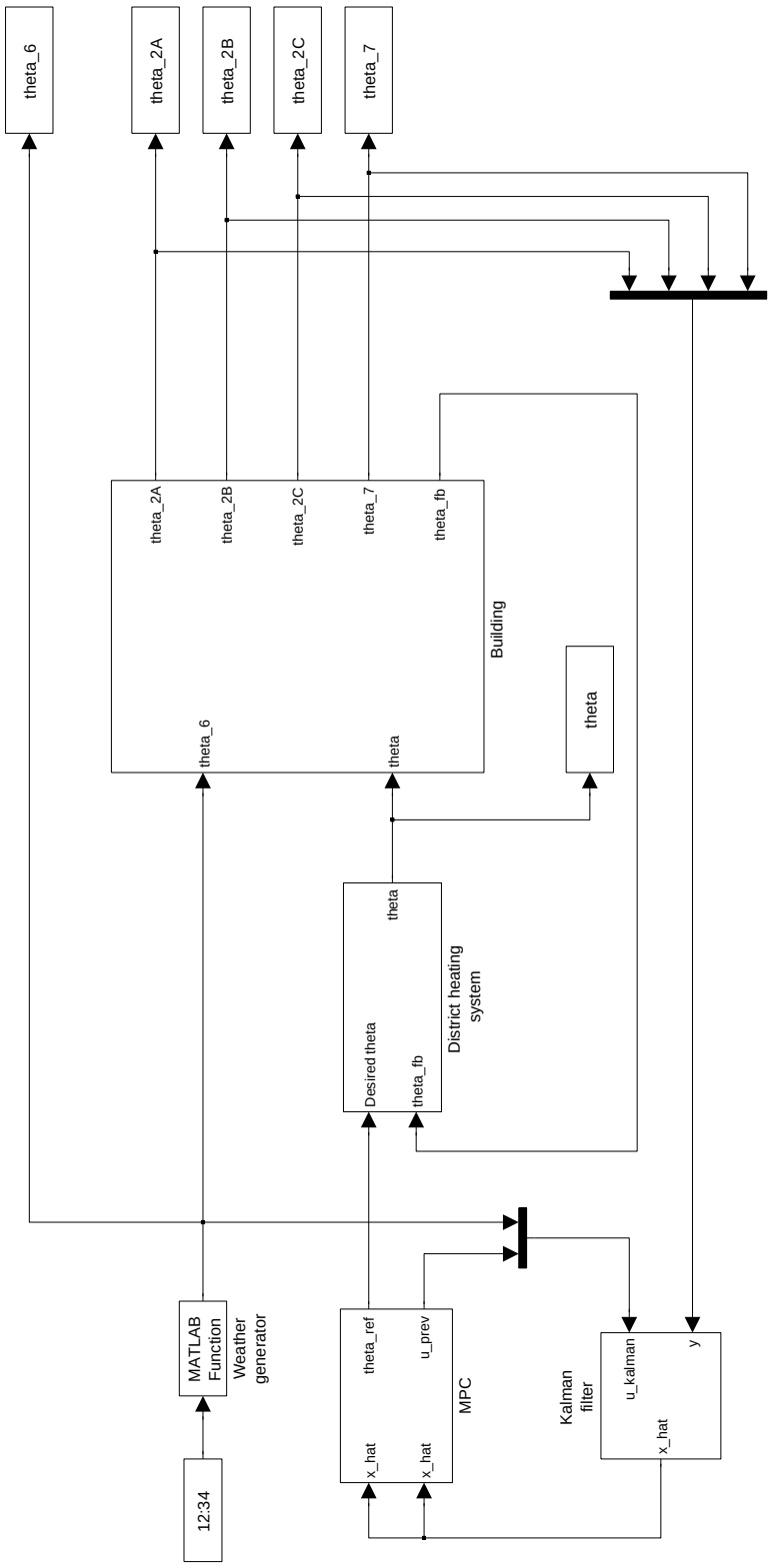

Figure C.2: The top-level Simulink diagram with an MPC control scheme.

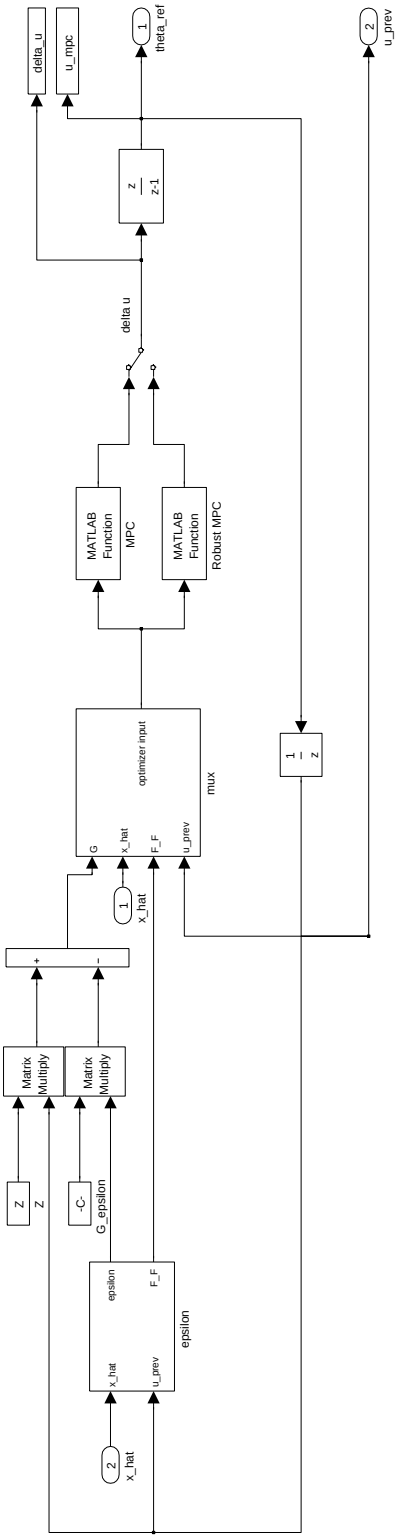

Figure C.3: Overview of the MPC controller in Simulink.

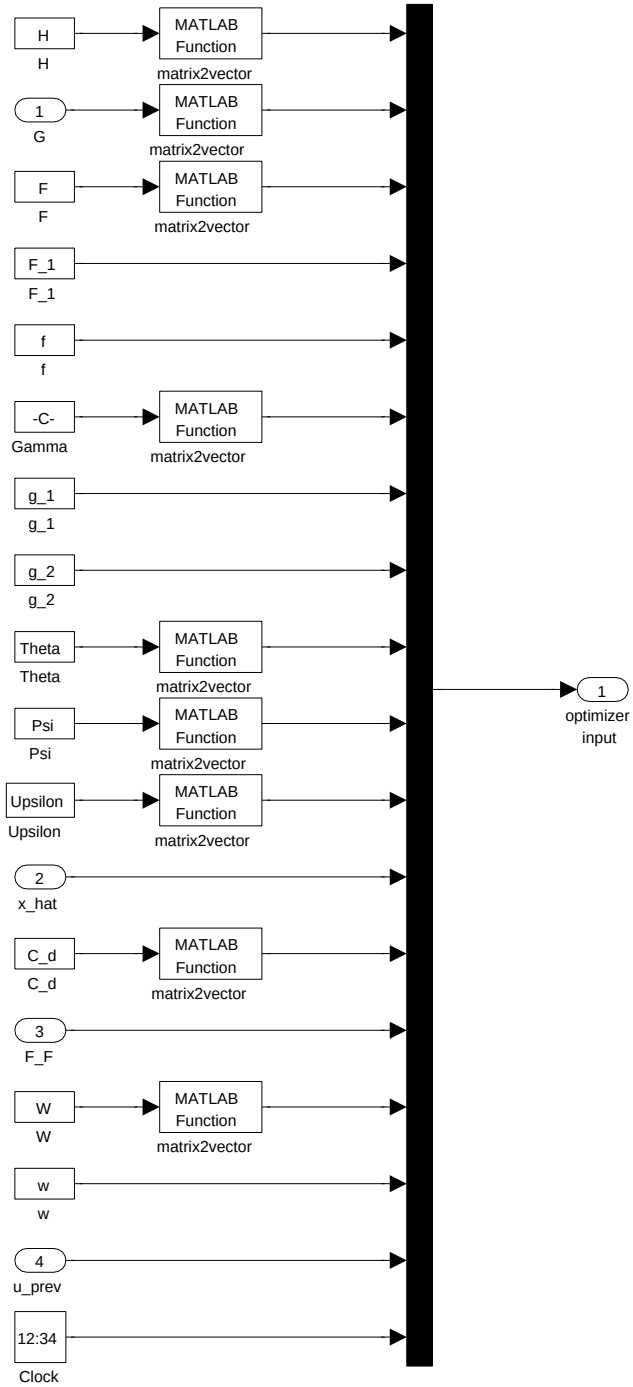

Figure C.4: A subsystem of the MPC controller in Simulink.